

Functional Characterization of N-terminal Threonine Mutations in Human Dopamine and Norepinephrine Transporters

by

Rheaclare Fraser

**A dissertation submitted in partial fulfillment
of the requirements for the degree of
Doctor of Philosophy
(Pharmacology)
in The University of Michigan
2013**

Doctoral committee:

**Professor Margaret E. Gnegy, Chair
Assistant Professor Asim Beg
Professor Stephen K. Fisher
Associate Professor Geoffrey Murphy
Professor Richard R. Neubig**

The Fraser Family Crest









Created By Mr. Brian Fraser

August 2011



Symbolism

- ~ The **cutlass** represents Grandfather George's career in agriculture and irrigation.
- ~ The **needle** represents Grandmother Edna's lustrous career as a seamstress.
- ~ Inspired by the location of the family's home in West Coast Berbice, the **grass** depicts the savannahs of Eldorado and Belladrum.
- ~ The African inspired **shield** symbolizes protection and defense of the family.
- ~ The **colors** used to bring life to the crest are loosely based on the five colors (yellow, red, green, white and black) of the Golden Arrow Head (the Guyana Flag).
- ~ Finally, the meanings of the Adinkra symbols (Ghanaian/West African) on the shield are listed below and are intended to convey wisdom, spirituality and inspiration.

			
AYA Endurance, Resourcefulness	BINKABI Peace, Harmony	DWENNIMMEN Humility and Strength	BOA ME NA ME MMOA WO Cooperation, Interdependence
			
GYE NYAME Supremacy of God	ONYANKPON ADOM NTI BIRBIARA BE YE YIE Hope, Providence, Faith	NYAME DUA God's protection and presence	BESE SAKA Affluence, Abundance, Unity

© Rheaclare Fraser
All rights reserved
2013

Dedication

This dissertation is dedicated to my entire family aka “the clan.” I am blessed to have my wonderful Mom and Dad, Robabel and Michael Fraser. Thank you for being outstanding role models and parents, for your unfaltering love, support and encouragement. To my sisters Onieka, Odonna, and Crystal I would not have completed this without all of your continuous love, laughter, and upliftment. To my brother-in-law, Adimu thank you for your advice and support over the years; and to my brother Rawle, thank you for the encouragement from overseas. To My Love Keith Spears, thank you for being my biggest cheerleader and keeping me smiling along the way. I would not have wanted to complete this journey without you by my side. I am forever grateful to grandparents and countless aunts, uncles, cousins, and family-friends of the Fraser, Wilson, Fowler, and Spears families for your love, support, and reassurance throughout the years. Finally to rising generations especially my nieces and nephews: Negus, Zerlina, Johari, Gifty, Menelik, Selassie, and Ras Khasa, may this dissertation be an inspiration towards fulfillment of your dreams and future success.

Acknowledgments

I would like to firstly acknowledge my dissertation chair, Dr. Margaret Gnegy. I tremendously appreciate your mentorship, guidance, patience, and teaching. You are a graciously wonderful advisor and person. I am grateful for the support you have provided and invaluable lessons learned throughout my scientific training. Many thanks are extended to my committee members Drs. Beg, Fisher, Murphy and Neubig. I am very appreciative of your helpful and insightful ideas and guidance to complete this work. I must also acknowledge Dr. Bipasha Guptaroy for initiating this threonine mutant project some years back, and her training and guidance during my studies. Thank you to the Rackham Graduate School, Program in Biomedical Sciences, and Pharmacology department for all their efforts in support of my success in the program, especially Tiffany Porties, Debby Mitchell, Drs. Baghdoyan, Hollenberg, Isom, Lucchesi, Osawa, Pratt, and Traynor. I would also like to acknowledge my undergraduate mentor at Spelman College, Dr. Gladys Bayse for setting me on the path to scientific research.

Graduate school would certainly have not been bearable and enjoyable without current and past lab members Bipasha, Kadee, Sarah, Chersye, Minjia, Myung; and Rong; supportive organizations AMS, AGEP, MUSES and Sister Friends; and my great friends Ashley, Alisha, Chenelle, Cheryse, Ebonie, Darius, Dan, David, Jamila, Jennifer & Max, Lauren, Leah, Miranda, Shameka, Stephanie, Suzy, and all other friends and supporters I have not mentioned by name.

TABLE OF CONTENTS

Dedication	ii
Acknowledgments.....	iii
List of Figures	vii
List of Tables	ix
Abstract	x
Chapter 1 INTRODUCTION.....	1
Dopaminergic and Noradrenergic Systems.....	1
DAT & NET Structure and Function	4
Transport model	9
Transporter conformations & gating mechanisms.....	12
Transporter associated currents.....	23
Transport measurement with the fluorescent substrate ASP ⁺	28
Thesis Summary	30
References	34
Chapter 2 SITE DIRECTED MUTATIONS NEAR TRANSMEMBRANE DOMAIN 1 (TM1) ALTER CONFORMATION AND FUNCTION OF NOREPINEPHRINE AND DOPAMINE TRANSPORTERS	53

Abstract	54
Introduction	55
Materials and Methods	57
Results	62
Discussion	83
References	90
Chapter 3 AN N-TERMINAL THREONINE MUTATION PRODUCES AN EFFLUX FAVORABLE, SODIUM-PRIMED CONFORMATION OF THE HUMAN DOPAMINE TRANSPORTER	
	96
Abstract	96
Introduction	97
Materials and Methods	100
Results	104
Affinity and Accumulation of the Fluorescent Substrate, ASP ⁺ in WT and Thr hDAT Mutant HEK Cells	104
Discussion	118
References	126
Chapter 4 DISCUSSION	131
Intracellular Gating and Reverse Transport	131
Future Directions	140

An Experimental Behavioral Model of T62D-hDAT	144
Conclusions	146
References	148

LIST OF FIGURES

Figure 1-1. Catecholamine biosynthesis from the amino acid precursor tyrosine.....	3
Figure 1-2 Amino acid sequence and transmembrane topology of (top) DAT and (bottom) NET	5
Figure 1-3 Proposed transport mechanism	11
Figure 1-4 N-terminal alignment of human (h) and rat (r) DAT, NET and SERT.....	20
Figure 1-5. Changes in the intracellular gating network of DAT.....	23
Figure 1-6 Chemical structures of ASP ⁺ (top) and MPP ⁺ (bottom).....	29
Figure 2-1. Surface expression and [³ H]DA uptake in hNET and hNET-T58 mutants.	64
Figure 2-2 Functional DA efflux properties of hNET mutants.....	67
Figure 2-3. Mutation of Thr58 (hNET) and Thr62 (hDAT) to aspartate results in enhanced substrate potency.	70
Figure 2-4. At 4°C, the accessibility of AMPH to [³ H]nisoxetine binding sites is reduced in T58D-hNET compared with binding at room temperature (RT).	77
Figure 2-5. Temperature-dependent changes in competition of AMPH for [³ H]WIN35,428 binding to hDAT mutants are reversed by addition of.....	78
Figure 2-6. Dissociation of benztropine and cocaine potencies for [³ H]DA uptake and competition for [³ H]WIN35,428 binding T62D-hDAT cells	82
Figure 2-7. Chemical structure of substrates and inhibitors	89
Figure 3-1. Affinity of the fluorescent substrate, ASP ⁺ is unaffected by the T62A or T62D hDAT mutations.....	105
Figure 3-2. Accumulation of fluorescent substrate, ASP ⁺ in T62A- and T62D-hDAT HEK cells	107

Figure 3-3. Expression of WT-, T62A-, and T62D-hDAT mutants causes similar membrane depolarization in <i>Xenopus</i> oocytes.....	109
Figure 3-4. Dopamine-induced inward currents in T62D-hDAT oocytes are partially rescued by zinc	111
Figure 3-5. Current-voltage relationships in hDAT expressing <i>Xenopus</i> oocytes.....	112
Figure 3-6. The reliance for extracellular Na ⁺ to promote DA uptake is not altered by the Thr62 hDAT mutations.	113
Figure 3-7. Initial [³ H]DA efflux in T62D-hDAT is Na ⁺ independent and resembles inducible DA efflux of WT-hDAT HEK cells.....	116
Figure 4-1 [³ H]DA uptake saturation in WT- and Y335F-hDAT HEK cells.....	133
Figure 4-2 Effects of extracellular Na ⁺ replacement on basal and AMPH-induced [³ H]DA efflux.....	134
Figure 4-3. Brandel superfusion to measure AMPH-induced DA efflux in WT- and Y335F-hDAT HEK cells preloaded with 15 μM DA for 30 min at 37°C	135
Figure 4-4 AMPH-induced DA efflux in WT- and Y335F-hDAT HEK cells preloaded with 5 μM DA for 180 min at 37°C.....	136
Figure 4-5. Schematic of transport cycle in WT-, T62D- and Y335F hDAT.....	138

LIST OF TABLES

Table 2-1. Kinetic properties of [³ H]DA uptake in hNET, hDAT, and threonine mutants	65
Table 2-2. Potency for substrates and inhibitors in inhibiting [³ H]DA uptake in hNET and hDAT mutants.	71
Table 2-3. Affinity for substrates and inhibitors in competing for [³ H]nisoxetine binding in hNET mutants.	73
Table 2-4. Affinity for substrates and inhibitors in competing for [³ H]WIN 35,428 binding in hDAT mutants.	74

ABSTRACT

The Na⁺ and Cl⁻ dependent, human dopamine (DA) and norepinephrine (NE) transporters (hDAT and hNET, respectively) control the duration of DA and NE neurotransmission by taking up extracellular neurotransmitter. Through outward and inward conformational transitions, DAT and NET work as pumps to transport substrates and ions between extracellular and intracellular environments. To study DAT and NET conformations, we mutated the threonine (Thr, T) residue within a conserved RETW sequence, which is juxtaposed to transmembrane domain 1a that is essential for ligand binding. Since the Thr residue is a putative phosphorylation site, it was mutated to alanine (Ala) (DAT, T62A; NET, T58A), or aspartate (Asp) (DAT, T62D; NET, T58D) to mimic a non-phosphorylated and phosphorylated state, respectively. Studies in heterologous HEK293 cells revealed the Thr (T) to Asp (D) mutation profoundly shifts the transporter from a predominately outward to inward orientation that exhibits reduced uptake but enhanced baseline reverse transport of substrate compared to wild type. Thr to Ala (A) mutants mostly functioned like wild type. A consequence of the predominantly inward conformation was an enhanced affinity for all substrates tested in the T to D mutants, with varying impacts of inhibitors. In further investigations, T62D-hDAT demonstrated wild type inward transport and retention of substrate when the substrate was not subject to reverse transport. These data showed that an inward-facing transporter can complete the entire transport cycle, even though it prefers an open inward-gate. Altering the transmembrane Na⁺ gradient revealed that the Thr to Asp mutation renders the mutant in a conformation mimicking that promoted by the Na⁺ gradient to elicit reverse transport. This is also the conformation elicited by amphetamine, an abused psychostimulant and transporter substrate. This suggests the T to D mutation mimics amphetamine action. My studies have contributed significantly to our knowledge of the

importance of juxtamembrane mutations to the conformation of DAT and NET, as well as knowledge of the responsiveness of transporter conformations to ligands and, crucially, to membrane gradients. This work demonstrates that the transporter, despite being a pump, can have heavily modified function at one gate without disruption of function at the other gate.

INTRODUCTION

Chapter 1

Dopaminergic and Noradrenergic Systems

Dopamine (DA) and norepinephrine (NE) are amongst the catecholamine class of neurotransmitters that have important functions within the central nervous system. In the brain, the NE projections originate from the locus ceruleus and project throughout the frontal and cerebral cortex and thalamus. Behaviors involving signaling through these neurons include anxiety, arousal, and fear. NE also has important actions in the periphery and autonomic nervous system. There are 3 main dopaminergic pathways. The *nigrostriatal* pathway projects from the substantia nigra to the striatum and is largely involved in controlling movement. Dopamine neurons within the nigrostriatal pathway are degenerated in Parkinson's disease patients.

Neurons with cell bodies originating in the ventral tegmental area project to the prefrontal cortex in the *mesocortical* system and to the nucleus accumbens in *mesolimbic* pathway. Signaling through these projections mediates effects such as cognition, emotion, and motivation (Gnegy, 2012; Meyer and Quenzer, 2005). These DA projections are a key component of drug abuse, particularly the reward and salience associated with drug taking (Robinson and Berridge, 2003).

The rate-limiting step in DA and NE synthesis is the conversion of the amino acid tyrosine to L-DOPA via tyrosine hydroxylase. DA is synthesized from the L-DOPA precursor by aromatic L-amino acid decarboxylase. Noradrenergic neurons and adrenal glands contain the enzymes necessary for production of NE and epinephrine (Figure 1-1). Newly synthesized and recycled

neurotransmitters are stored in synaptic vesicles. Neurotransmitters are taken up into vesicles via vesicular monoamine transporters (VMAT2) by a H⁺ antiport driven mechanism. Packaging of neurotransmitters into vesicles protects them from degradation by the metabolic enzymes catecholamine-O-methyl transferase (COMT) and monoamine oxidases (MAO). Several metabolites are produced from the breakdown of DA and NE by COMT and MAO. Drugs that inhibit COMT and MAO block catecholamine metabolism and have therapeutic relevance and/or contraindications with other medications (Brunton et al., 2006; Gnegy, 2012; Meyer and Quenzer, 2005).

Neuronal activation by the generation of an action potential depolarizes the membrane and stimulates vesicles to fuse with the presynaptic membrane and release neurotransmitter into the extracellular space (Rizo and Rosenmund, 2008). The concentration of neurotransmitter present in the synaptic cleft, and thus neurotransmission, is regulated by spontaneous diffusion, metabolism, and reuptake of the neurotransmitter (Giros and Caron, 1993; Leviel, 2011). The dopamine and norepinephrine transporters (DAT and NET, respectively) are presynaptic membrane proteins that have a pivotal role in decreasing the content of extracellular neurotransmitter, and thus terminating synaptic signaling.

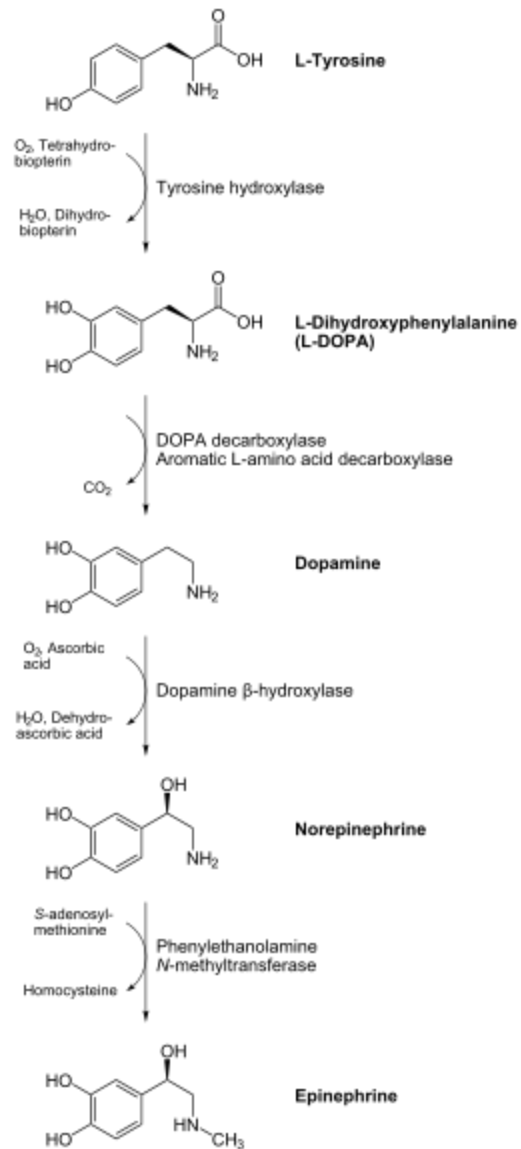


Figure 1-1. Catecholamine biosynthesis from the amino acid precursor tyrosine (Joh and Hwang, 1987).

DAT & NET Structure and Function

Structure

The monoamine transporter family includes DAT, NET and the serotonin (5-HT) transporter (SERT). These transporters belong to the *SLC6A* gene family, which includes a wide array of transporters that are expressed throughout the brain and periphery (Chen et al., 2004c; Hahn and Blakely, 2007). DAT and NET have 12 transmembrane (TM) spanning domains with alternating intra- and extracellular loops (IL, EL) and intracellular amino (N-) and carboxyl (C-) termini (Giros and Caron, 1993; Sucic and Bryan-Lluka, 2005) (Figure 1-2). These regions contain consensus sites for protein regulation such as glycosylation (EL 2), ubiquitination (N-terminus), and phosphorylation (N- and C- termini, ILs). These processes regulate a range of transporter properties that include membrane expression, distribution or trafficking (recycling and internalization), activity, and protein-protein interactions (Chen and Reith, 2000; Kristensen et al., 2011).

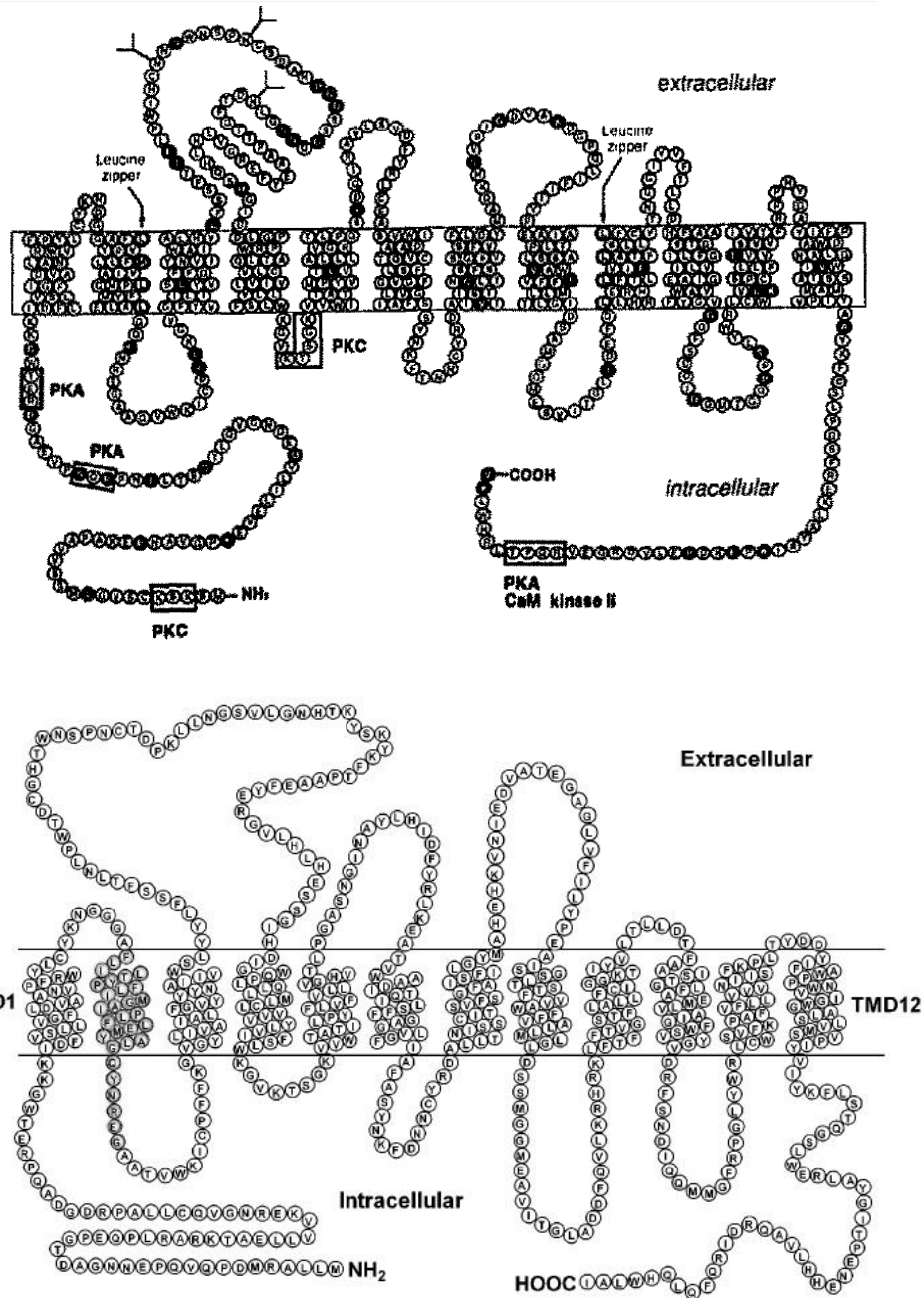


Figure 1-2. Amino acid sequence and transmembrane topology of (top) DAT and (bottom) NET, modified from (Giros and Caron, 1993; Giros et al., 1996; Susic and Bryan-Lluka, 2005).

Neurotransmitter uptake

Transporters of the *SLC6A* gene family couple substrate translocation with ion movement. The high extracellular sodium (Na^+) concentration, along with chloride (Cl^-), provides the energy for substrate transport (Hahn and Blakely, 2007). In the case of SERT, potassium is also counter-exchanged during 5-HT transport (Rudnick, 1998). The major function of transporters is to remove substrate from the extracellular space, which means that the transporter serves as a critical component to terminating synaptic signaling. DAT knockout mice demonstrate hyperlocomotor activity due to markedly increased extracellular levels of DA (Giros et al., 1996). The complexity of DAT homeostasis is exemplified by the myriad interacting proteins that influence transporter function termed as the DAT proteome (Torres, 2006). DAT interacting proteins within the proteome include, but are not limited to syntaxin 1a, Rack1, synuclein, Hic-5, and Pick-1, which bind either the N- or C-terminus of DAT (Torres, 2006). In addition, trafficking of DAT to (recycling) and from (endocytosis) the plasma membrane is regulated on a constitutive basis and by substrates themselves as well as other neurotransmitters (Furman et al., 2009; Johnson et al., 2005a; Melikian, 2004).

Monoamine transporters are targeted by a number of drugs, both therapeutic agents and drugs of abuse. Many inhibit reuptake which results in increased extracellular levels of neurotransmitter available for postsynaptic activation. For instance, inhibitors that selectively block the uptake of serotonin and norepinephrine through SERT and NET, respectively, are mainline therapies for treating depression and anxiety disorders (Meyer and Quenzer, 2005). Abused psychostimulants

like cocaine and amphetamine (AMPH) also act upon monoamine transporters to increase neurotransmitter content in the synapse. The binding site for cocaine within DAT is predicted to overlap with the site for DA (Beuming et al., 2008), resulting in competitive blockade of DA uptake. Although it shares structural similarity to amphetamines, methylphenidate (Ritalin) acts much like cocaine in that it blocks the DAT. Methylphenidate is clinically used to treat attention deficit hyperactivity disorder (ADHD) (Volkow et al., 2001). Another pharmaceutical drug, Adderall is a low dose, racemic mixture of *d*- (active) and *l*- (inactive) AMPH that is used for the treatment of ADHD and narcolepsy. However, higher doses of AMPH oversaturate the dopaminergic system, which is an important factor in the rewarding, reinforcing, and salient (wanting) properties associated with drug taking and abuse (Howell and Kimmel, 2008; Robinson and Berridge, 2003). The effects of AMPH (and the more potent methamphetamine) are substantively different from other drugs affecting the transporter because AMPH is a DAT substrate and the increased extracellular DA levels occur by a combination of actions. These include: 1) competing for neurotransmitter reuptake, 2) disrupting vesicular DA storage, and 3) stimulating reverse transport of DA (Sulzer et al., 2005).

Neurotransmitter efflux – reverse transport

AMPH is a phenylethylamine and closely related to the native structure of catecholamines; however it lacks the hydroxyl groups on the benzene ring that classify it as a catecholamine. The mechanism of AMPH action on the transporter is unique and a subject of intense study. According to the classic facilitated diffusion model, transport of AMPH into the cell is

counteracted by movement of DA out of the cell (Fischer and Cho, 1979). However, other factors have been demonstrated to be involved in AMPH-stimulated efflux. Sitte et al. (1998) demonstrated a poor correlation between substrate-induced release and transport. In comparison to DA, AMPH had a lower rate of uptake, but increased potency to stimulate release of the substrate MPP⁺ in DAT-transfected HEK 293 cells. Instead, substrate-induced release rates were in accordance with their ability to induce inward currents (Sitte et al., 1998) (see Transporter associated currents section). Transporter trafficking also influences efflux and uptake through DAT (Robertson et al., 2009). Both DA and AMPH have biphasic effects on DAT surface expression in cells or rat brain preparations from the striatum. Rapid stimulation with AMPH (< 1min) resulted in increased surface DAT and DA efflux without affecting DA influx (Furman et al., 2009; Johnson et al., 2005a). Observed unparalleled changes in the uptake and efflux properties of DAT suggest that facilitated diffusion is not the sole explanation for the mechanism of AMPH-induced DA efflux through DAT.

Another component of AMPH-stimulated DA efflux is its action on synaptic vesicles. Once inside the presynaptic terminal AMPH is taken up by vesicular monoamine transporter (VMAT)-2 and results in displacement of vesicular contents and elevation of cytosolic DA. An explanation for this is the weak base theory of AMPH action (Sulzer et al., 2005). As a weak base, AMPH would reduce the intracellular pH of vesicles, decreasing DA uptake into the vesicle while increasing the cytosolic DA available for release. A major challenge to this theory includes the ability of AMPH to stimulate efflux after vesicular depletion of neurotransmitter with reserpine, but not after the inhibition of tyrosine hydroxylase (Kalisker et al., 1975;

Weissman et al., 1966). These works underscores that AMPH requires newly synthesized DA and elevation of cytosolic DA alone is not enough to stimulate reverse transport. In fact both the exchange diffusion and vesicular depletion mechanisms are important for AMPH-induced DA release through DAT (Jones et al., 1998).

As further explained in the following section on the transport model, sodium and chloride are inwardly transported along with the catecholamine. In fact, evidence demonstrates that the increase in intracellular Na^+ provides the driving force for rebinding of DA and reversal of the transporter (Liang and Rutledge, 1982, 1983). Metabolic or pharmacological inhibition of the Na^+/K^+ ATPase results in elevated DA and NE efflux due to increased intracellular Na^+ levels (Langeloh et al., 1987; Liang and Rutledge, 1982). Although AMPH-stimulated efflux requires interaction and transport of AMPH through DAT (Jones et al., 1998), in heterologous cells it has been shown that elevation of intracellular Na^+ , independent of AMPH, is sufficient to drive DA efflux (Khoshbouei et al., 2003).

The medical availability of AMPH for its therapeutic applications contributes to its misuse and abuse. Elucidating the molecular mechanisms behind AMPH-induced DA efflux is important to understand monoamine transporters and identify potential cellular targets to reduce the abuse liability of amphetamines.

Transport model

The alternating access model posits that the transporter transitions between outward- and inward-facing orientations (Jardetzky, 1966; Krishnamurthy et al., 2009; Liang et al., 2009). In the

outward facing conformation, ligand (substrate and co-transported ions) binding is accessible from the extracellular side of the membrane. Binding of substrate and ions stimulates the transporter to assume the inward facing conformation so that ligands are released on the intracellular side of the membrane. Intricate studies over the past decade have demonstrated that although the outward and inward facing conformations are the beginning and end stages of transport, there are other intermediate interactions and movements involved in the transport process, as well.

Bacterial Sodium Symporter Homologue, LeuT

Crystallization of the *Aquifex aeolicus* bacteria leucine transporter (LeuT) (Krishnamurthy and Gouaux, 2012; Yamashita et al., 2005), in combination with molecular modeling and mutagenesis studies have revealed important structural and functional information about the Na⁺/Cl⁻ dependent transporter family. The first crystal structure of LeuT was obtained in the substrate occluded state with 2 Na⁺ and 1 Leu molecule positioned in their binding sites (Figure 1-3) (Yamashita et al., 2005).

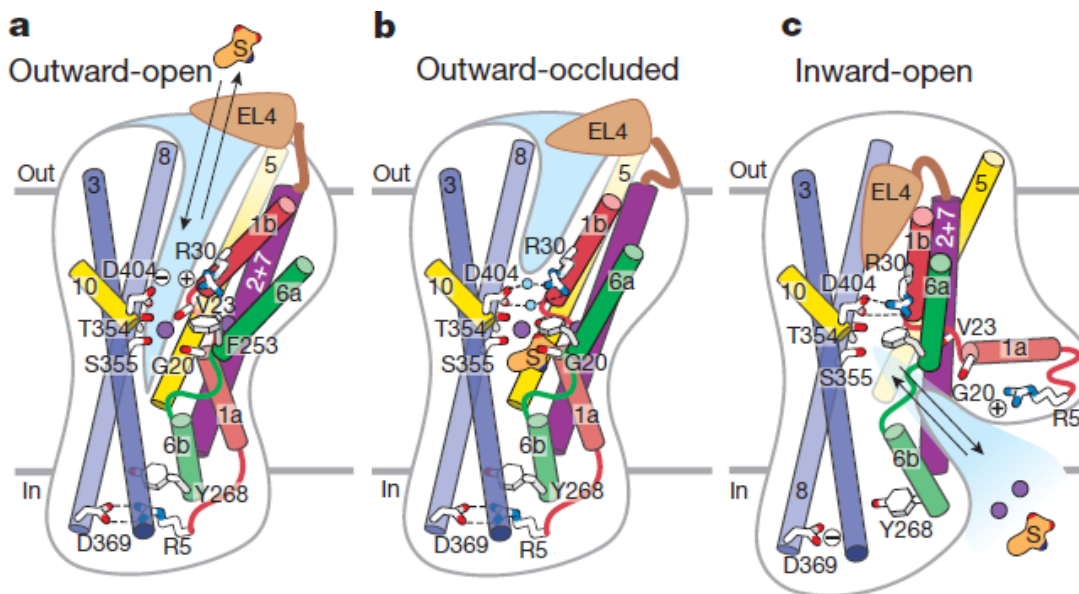
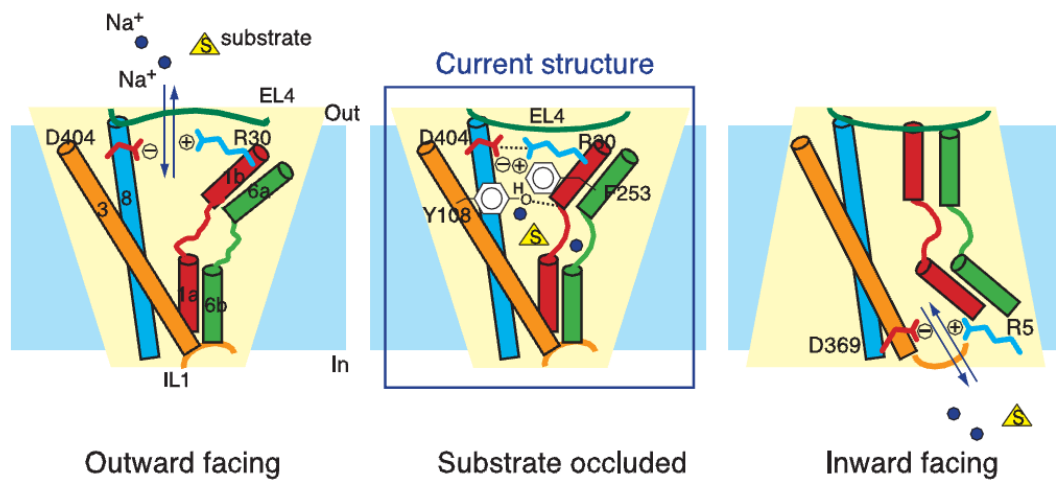


Figure 1-3. Proposed transport mechanism derived from the crystallization of LeuT in the substrate occluded state (top) (Yamashita et al., 2005). Outward-open, substrate-occluded, and inward-open crystal structures of LeuT (bottom) (Krishnamurthy and Gouaux, 2012).

Unlike eukaryotic transporters, transport via LeuT is chloride independent (Zomot et al., 2007). As a whole, the homology between LeuT and eukaryotic monoamine transporters is relatively low. However, the greatest density of conserved residues lies within TMs 1 and 6. These two TMs are positioned in an anti-parallel orientation and are separated into two segments by unwound alpha helices (TM 1a and 1b; TM 6a and 6b). The unwound regions of TM 1 and 6 along with TM 3 and 8 form the LeuT ligand binding pocket for substrate leucine and two sodium ions (Figure 1-3) (Yamashita et al., 2005). Binding of substrate and co-transported ions involves a complex network of interactions between amino acid residues of TM domains, ILs, ELs and the ligands.

Transporter conformations & gating mechanisms

Numerous studies have investigated the molecular mechanism of reuptake. Transport of substrates between the extracellular and intracellular environments is controlled by intricate gating mechanisms. The process involves a complex coordination between the substrates themselves, the domains of the transporter (TMs, EL/ILs, and N-/C- termini), ions (Na^+/Cl^-), and water molecules. To understand the gating mechanisms, it is important to also discuss the different transporter conformations in more detail. The transporter transitions between 4 main conformational states: outward-open, outward-occluded, inward-open, and inward-occluded. Although crystal structures do not yet exist for DAT and NET, the first 3 conformations have been successfully crystallized for LeuT (Krishnamurthy and Gouaux, 2012; Yamashita et al., 2005). The original substrate-occluded LeuT crystal structure showed that TM helices 1-5 and

6-10 are inverted repeats with similar structural arrangement (Yamashita et al., 2005). This finding gave rise to the rocking bundle mechanism of transport that was based upon swapping the conformations of the repeats (Forrest and Rudnick, 2009). By this model, the four-helix bundle (TMs 1, 2, 6 and 7) within the repeats would “rock” to open and close access to the binding site from the alternating orientations. Later modeling (Shan et al., 2011) and crystallization (Krishnamurthy and Gouaux, 2012) of LeuT in the inward facing state revealed that intracellular exposure of the permeation pathway relies more on a remodeling of network of interactions rather than rigid motions based on transmembrane symmetry.

The proposed transport mechanism derived from the LeuT crystal structure is paramount in our understanding of how the transport cycle operates in related monoamine transporters. The population of transporter at the presynaptic membrane could be in any given state at a particular time. However, for ease of the description here will start and end with the outward-open and inward-open states, keeping in mind the transport mechanism involves full cycling (outward-inward, inward-outward). The segments of the LeuT have been described as having 2 domains called the scaffold and core. The scaffold domain consists of TMs 3, 4, 8, 9 and 10; while the core domain is comprised of TMs 1, 2, 6 and 7. In the absence of substrate the transporter is in an outward-open state that is maintained by the high extracellular sodium concentration. The extracellular gate is comprised of TMs 1b and 6a of the core domain, which are positioned outward and away from the scaffold domain (Figure 1-5) (Krishnamurthy and Gouaux, 2012). In the absence of substrate, the permeation pathway of the transporter is closed. This is deemed the conformation of the wild-type (WT) transporter, as it is in a position to readily bind substrate

molecules from the extracellular space (Yamashita et al., 2005). Sodium binding initiates the transport cycle by increasing the entry of water, and primes the transporter for substrate binding (Shi et al., 2008). When substrate is bound, the extracellular gate closes by bridging residues in TMs 1b and 6a with residues in TM 3 and 10. These stable interactions put the transporter in the outward-occluded state where substrate is securely ‘locked’ in its binding site (Yamashita et al., 2005). As water molecules carry substrate through the permeation pathway, extracellular gating interactions are stabilized while inner networks are disrupted. The inward-open state is achieved when the intracellular gate, formed by TM segments 1a and 6b, opens to allow release of substrate and Na^+ inside the cell. Relative to other movements, the inner gate undergoes the largest structural shift during the transport cycle (Shan et al., 2011; Zhao et al., 2012). The inward-occluded state is presumed to occur during the transition of the transporter back to the outward-open state. However, there is no crystal structure of the inward-occluded state (Krishnamurthy and Gouaux, 2012), and the details of this transition are not well known.

Sodium and substrate binding sites

The requirement for sodium ion binding to transporter is well known; and presence of 2 Na^+ binding sites, termed Na1, Na2, are modeled from the LeuT crystal structure (Yamashita et al., 2005). However, a developing theory postulates the presence of two substrate binding sites termed S1 and S2, within the DAT and NET. S1 and S2 were identified from the occluded LeuT crystal structure and steered molecular dynamic (SMD) simulations studying ligand movement (Shi et al., 2008; Zhao et al., 2011). Both sodium sites are located within the core (substrate

binding pocket) of the transporter. The presence of Na⁺ in the Na1 and Na2 sites are deemed necessary to stabilize the core, unwound regions of TM 1 and TM 6, and bound substrate (Leu) molecule. The S1 site is located deep within the central binding pocket at the unwound regions of TM 1 and 6. Substrate in the S1 site directly interacts with the sodium in the Na1 site (Yamashita et al., 2005). Upon occupation of the S1 site, binding of substrate in S2 serves as an allosteric trigger for the release of Na⁺ and S1 substrate into the intracellular space (Shi et al., 2008; Zhao et al., 2011). Inhibitors like tricyclic antidepressants (TCAs) bind at the extracellular vestibule, stabilizing the extracellular gate and closed conformation to prevent transport and competitively block binding of substrate to the S2 site to inhibit transport (Singh et al., 2007; Zhao et al., 2010; Zhou et al., 2007).

The modeling studies discussed above for the proposed “substrate-driven allosteric mechanism” of the S1, S2 transport model (Shan et al., 2011) are compelling yet somewhat puzzling, given that they are inconsistent with long standing stoichiometry predictions of substrate/ion ratios of monoamine transporters. Consequently, additional studies have challenged the existence of an S2 site. Binding analyses of WT LeuT in comparison to mutants of the proposed S2 site refute the secondary site model and support a single high-affinity substrate site (Piscitelli et al., 2010). Furthermore, Krishnamurthy and Gouaux (2012) used a combination of mutagenesis and antibody based techniques to provide additional X-ray crystal structures of LeuT in the outward-open and inward-open conformational states (Krishnamurthy and Gouaux, 2012). Recall, the original LeuT crystal structure was obtained in the intermediate occluded state (also called outward-occluded) (Yamashita et al., 2005). Krishnamurthy and Gouaux (2012) provided the

structures for the LeuT orientations before binding of extracellular substrate (outward-open) and after ligand release to the intracellular space (inward-open). According to their data, as depicted in Figure 1-3, binding of substrate and sodium molecules in the core region closes off the extracellular pathway by EL 4 “packing tightly against TM 1b and TM 7 on one side and TM 3, TM 8 and EL 12 on the other side” (Krishnamurthy and Gouaux, 2012). The postulated S2 site, which include residues Ile 111 and Leu 400 would be deeply buried, thus inaccessible to bind a second substrate molecule. Instead, they postulate that the extracellular gate closes via formation of interactions between TM1b, 6a, 10, 11, and EL 4 while a disruption of interactions between TMs 1a, 6b, 8, and the N-terminus (NT) opens the intracellular gate. This triggers release of ligands to the intracellular space, instead of allosteric changes caused by substrate binding in S2 model. Transporter inhibitors block the collapse of EL 4, thus preventing the opening of the intracellular gate and arresting the transporter in the outward facing orientation (Krishnamurthy and Gouaux, 2012).

A recent molecular modeling study of SERT also disagrees with the existence of a second substrate site. According to their simulations, Koldso et al. (2011) found that substrate occupation of an S2 site did not produce transport associated conformational changes. Notably, they also modeled sodium dissociation from the Na2 site triggering intracellular substrate release, thus refuting the notion of intracellular substrate (S1) release coming from S2 substrate binding in the Shan et al. (2011) allosteric mechanism. Na2 trigger of intracellular S1 release was further supported by a significant increase in the K_m for Na^+ to stimulate serotonin uptake in a SERT Na2 site mutant, indicating more Na^+ is needed for release of 5-HT into the cell during

the uptake assay in cells without Na² compared to WT (Koldso et al., 2011). This finding is in line with the “first-in, first-out” model for hDAT function where Na⁺ binding and unbinding precedes AMPH during the outward (extracellular) to inward (intracellular) transition of DAT (Erreger et al., 2008).

Perhaps the inconsistency for the existence of the S2 site lies within variation of experimental conditions (Quick et al., 2012) and methods (high affinity binding, simulation modeling, and crystallography) utilized. Despite the discrepancy for the presence or absence of an S2 site in these models, it is agreed upon that extracellular and intracellular molecular networks are vital components that mediate the global conformational changes of the transporter. Regardless of the S2 debate, the information from LeuT structures and models has been extended towards understanding corresponding residues regulate transport within DAT and NET (for which crystal structures are not available). Various studies have combined modeling simulations and transporter mutagenesis to learn more about the specific roles of particular DAT and NET amino acids.

Dopamine transporter mutants

Residues throughout DAT have been implicated in maintaining normal transporter functions and orientation. Many studies have used site-directed mutagenesis to probe the role of various amino acid residues in transporter function. This involves using PCR to generate single or multiple point mutations and transiently or stably expressing the sequence-confirmed mutant transporter constructs in a heterologous cell line. Functions such as substrate uptake, ligand binding affinity,

and reverse transport are tested in the mutants and compared to cells containing normal, wildtype (WT) transporter. Numerous DAT mutants have been used to study the impact of particular residues on functional characteristics and/or conformational preference of the transporter. Some mutations have exhibited differential effects on inward versus outward DA transport. For instance, the S528A DAT mutant (TM 11) showed an enhanced rate of DA efflux but similar DA uptake kinetics in comparison to WT DAT (Chen and Justice, 2000). Alanine substitution of proline 572 of TM 12 displayed increased DA efflux and reduced the dependence for sodium and chloride ions to stimulate DA release (Itokawa et al., 2002). While most experimental mutagenesis studies have evaluated engineered mutations, naturally occurring DAT variants exist that also change transporter properties (Mazei-Robison and Blakely, 2005). In particular, the rare hDAT A559V variant in TM 12 was discovered in two male ADHD patients and one female patient with bipolar disorder. Analysis of this mutant in a heterologous cell based system revealed a spontaneous DA efflux attributed to an increased sensitivity for intracellular Na^+ . The A559V mutant displayed normal DAT surface expression and DA uptake in comparison to WT hDAT (Mazei-Robison et al., 2008). Experiments with transporter mutants can also provide structural insights in addition to translocation information.

Outward facing DAT mutants were created by mutating the tryptophan 84 to leucine (W84L) of TM 1 or aspartate 313 to asparagine (D313N) within TM 6. Both W84L and D313N mutations enhanced binding of the cocaine analog CFT (2b-carbomethoxy-3b-(4-fluorophenyl)tropane) (Liang et al., 2009; Lin et al., 2000). These mutants have also been used to study the Na^+ dependence and binding profile of various DAT inhibitors (Chen et al., 2004b). In contrast,

several studies have identified residues that place DAT in a predominately inward facing orientation. These include Y335A (IL 3/TM 6) (Loland et al., 2002), K264A (IL 2/TM 5), D436A (IL 4) (Loland et al., 2004), D345A (Loland et al., 2004) and D345N (IL3) (Chen et al., 2004a). Characteristics of the inward facing DAT mutants are a low capacity for DA uptake, reduced affinity for inhibitors, and enhanced substrate affinity (Chen et al., 2004a; Loland et al., 2002). Interestingly, the deficits demonstrated by Y335A and D345N mutants can be rescued by Zn^{2+} (Chen et al., 2004a; Loland et al., 2002). The extracellular face of DAT has 3 endogenous zinc binding coordination sites, H193 in EL 2 and H375 and E396, both in EL 4 (Loland et al., 1999; Norregaard et al., 1998). Zinc binding to DAT does not obstruct binding of DA, but reduces DA uptake in WT DAT. It is thought that zinc stabilizes the outward facing conformation of WT DAT and prevents the formation of other conformational states required for DA translocation (Norregaard et al., 1998). Although, Pifl et al. (2009) determined that the inhibitory or stimulatory action of Zn^{2+} depends on whether the membrane potential is below or above the reversal potential for Cl^- . Zinc effects are not observed in NET due to the lack of H193 at the equivalent NET position, but were upon mutation of the corresponding K189 residue to histidine (Norregaard et al., 1998). The studies mentioned here and many others have shed light on the importance of particular amino acid residues on transporter orientation and functions.

The conserved RETW sequence

A number of putative regulatory sites are present in the N-terminus of the transporter as highlighted in the alignment of the N-termini of DAT, NET, and SERT shown in Figure 1-4 (Vaughan, 2004).

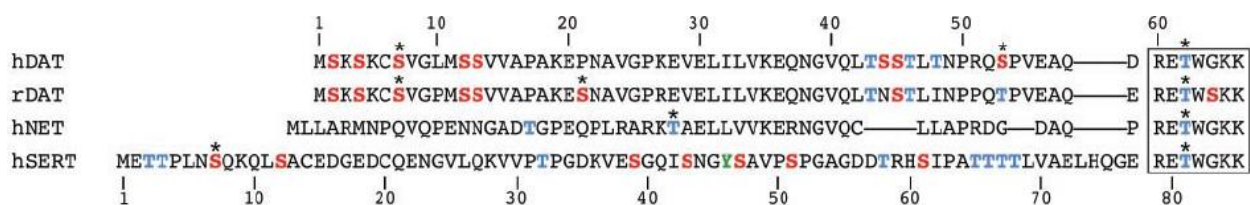


Figure 1-4. N-terminal alignment of human (h) and rat (r) DAT, NET and SERT ending before TM 1. Putative phosphorylation sites for serine (red), threonine (blue), and tyrosine (green) are highlighted (Vaughan, 2004).

Various studies have linked sites of the DAT N-terminus to modulation of transporter functions and AMPH-induced DA efflux, in particular. For instance, the N-terminal truncation of the first 22 amino acids of DAT significantly reduced AMPH-stimulated DA efflux, which was attributed to lack of phosphorylation at serine residues 7 and 12 (Khoshbouei et al., 2004). As found some years later, the first 33 amino acids of the N-terminus were required for the SNARE protein syntaxin 1A to interact with DAT, and this association increased AMPH-induced efflux in a CAMKII dependent manner (Binda et al., 2008). Interestingly, AMPH also increases the interaction of syntaxin 1A with the NET N-terminus (Dipace et al., 2007), and induces reverse transport of NET (Piffl and Singer, 1999). The NET however, lacks the serine residues

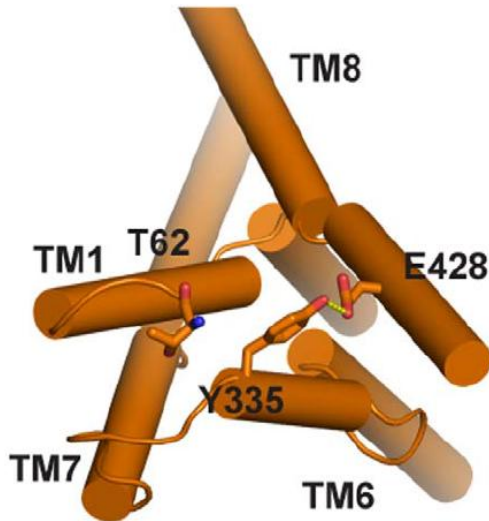
implicated in DA efflux via DAT (Figure 1-4), which points towards the involvement of additional transporter regions mediating AMPH actions.

The RETW motif at the distal end of the N-terminus is conserved amongst all monoamine transporters (Figure 1-4) (Vaughan, 2004). The short N-terminus of LeuT also contains the RE*H motif although His replaces the Thr residue (Yamashita et al., 2005). This sequence is located just before the start of TM1a, which is a critical component of the ligand binding region (Yamashita et al., 2005) and involved in the largest movements during transport (Shan et al., 2011). RETW is a canonical phosphorylation sequence for a variety of protein kinases including PKA and PKC (Giros and Caron, 1993; Vaughan, 2004). Phosphorylation is a highly investigated yet complex posttranslational modification of transporter trafficking and functional activity (Schmitt and Reith, 2010; Vaughan, 2004). Our laboratory has identified the β isoform of protein kinase C (PKC β) as a key regulator of DAT trafficking and AMPH-induced DA efflux (Chen et al., 2009; Furman et al., 2009; Johnson et al., 2005b). Due to its putative phosphorylation and high conservation amongst all monoamine transporters (Giros and Caron, 1993; Vaughan, 2004), the Thr residue within the RETW sequence was an ideal candidate to explore for additional regions involved in dopamine efflux. Alanine and aspartate mutations were made to position 62 of hDAT to mimic a non-phosphorylated (T62A) and phosphorylated (T62D) state at this site. Previous work established the T62A hDAT mutant was similar to WT. However, T62D hDAT is an inward facing mutant based upon some hallmark characteristics of an inward transporter discussed above. This conclusion was based upon reduced [3 H]DA uptake and abrogated AMPH-stimulated [3 H]DA efflux combined with elevated basal [3 H]DA efflux.

The altered characteristics of T62D hDAT were partially restored by zinc, further indicating a shift in transporter orientation in this mutant (Guptaroy et al., 2009). Work discussed in chapter 2 of this dissertation further assessed the effects of the Thr 62 DAT and corresponding Thr 58 NET mutations on substrate and inhibitor interactions with the transporter (Guptaroy et al., 2011).

The involvement of other residues within the RETW sequence on conformational changes has been made evident through a variety of mutagenesis, crystallography, and simulation modeling studies. Using computational analysis, the N-terminal Arg 60 (LeuT, R5) of the DAT RETW was shown to participate in a network of interactions with residues of IL 3, TM 6, and TM 8 that regulate intracellular access to the substrate binding site. The Arg 60 residue forms a salt bridge with Asp 436 (LeuT, D369) that is stabilized through its cationic- π interaction with residue Tyr 335 (LeuT, Y268) (Kniazeff et al., 2008). As discussed earlier, disruption of the intracellular interaction network contributes to formation of the inward-facing state (Krishnamurthy and Gouaux, 2012; Zhao et al., 2012; Zhao et al., 2010). The inward orientation is thought to occur by a change in residue binding partners during the transition from the outward-occluded to inward-open states. According to a recent simulation study, DAT Tyr 335 (TM 6) forms a hydrogen bond with Glu 428 (TM 8) when substrate is bound in the S1 site and the intracellular gate is closed. In the inward-facing state, Y335 binds to Thr 62 residue of the RETW sequence. The change in Y335 interactions is thought to facilitate the opening of the intracellular gate and inward orientation of the transporter (Figure 1-5) (Shan et al., 2011).

A. S1-DAT



B. Inward-facing

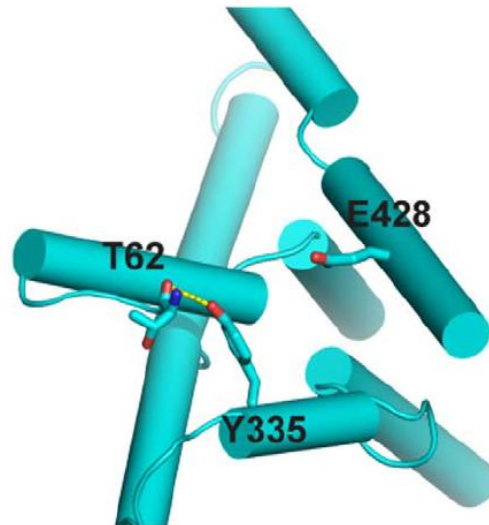


Figure 1-5. Changes in the intracellular gating network of DAT. A. View of the closed intracellular gate in outward-facing S1 bound DAT (orange); B. Inward-facing DAT (teal) with intracellular gate open (Shan et al., 2011).

Transporter associated currents

Transport through DAT and NET involves the movement of sodium, chloride, and substrate.

There is a positive net flux of charge exchange, making the transport of substrate, from outside to inside the cell, an electrogenic process. Measurable currents are therefore generated due to the exchange of ions across the plasma membrane. Electrophysiological properties and the influence of pharmacological agents are studied in transporter expression systems using voltage clamp techniques. Currents can be measured in a variety of transporter-expressing systems including neuronal cultures, heterologous cells or *Xenopus laevis* oocytes. Transporter mediated currents are related to uptake functions and transporter-mediated release.

Stoichiometry of ion flux during transport

Ionic gradients are extremely important for the movement of substrates. The ionic gradients of sodium (Na^+), chloride (Cl^-), and potassium (K^+) provide the energy to carry substrates against their concentration gradients (Hahn and Blakely, 2007). The predicted stoichiometry of ion flux varies amongst the members of the monoamine transporter family. The Na^+ : Cl^- : substrate ratio is 1:1:2 for DAT and 1:1:1 for NET and the 5-HT transporter SERT. In SERT, one K^+ ion is also transported out of the cell (Gu et al., 1994; Rudnick, 1998). Substrate-induced current measurements obtained from the transporters have been significantly greater than expected for a fixed stoichiometry (Sonders et al., 1997). Previous work has shown that substrate induced currents have a better correlation with the ability of the substrate to stimulate reverse transport (efflux) rather than uptake (influx) (Sitte et al., 1998).

Measurements of transporter currents

Two-electrode voltage clamping (TEVC) is commonly used to measure currents. This powerful technique allows the simultaneous control of membrane voltage and measurement of current to determine charge exchange. TEVC is widely used to measure large currents from ion channels. The technique can be applied to measure much smaller currents from transporter expressing systems due to their similarity to ligand-gated channels (Sonders and Amara, 1996). A voltage-recording electrode placed inside the cell measures the membrane potential. The recorded membrane voltage is compared to the command (or clamped) voltage set by the experimenter. Typically, the voltage is clamped at -60 mV, near the resting membrane potential for most

neurons. The clamp circuitry passes a current back into the cell through the second, current electrode to hold the membrane potential at the desired level. The counter current applied to the cell is measured and represents the amount of actual current or charge flowing across the cell membrane. As is the case during transport, when the inside of the cell becomes positive, a negative counter current is applied by the current electrode. This produces a downward deflecting, inward current (Sonders et al., 1997). Useful information is gained from current-voltage relationships (I-V curves), which are current measurements plotted over a range of applied voltages and usually have control currents subtracted from transporter-mediated currents. The direction of the current trace gives an indication of the net charge of ions across the membrane. The point at which the curve crosses the x-axis is the reversal potential, where there is no net ion flow. Conditions (e.g. drug treatments, mutant protein expression) that alter features of the current can serve as an indication to changes in composition of ions contributing to the current. Substrates, inhibitors and ion substitutions can be utilized to understand ligand contribution to enhancement or blockade of currents and the ions (e.g. Na^+ , Cl^- , K^+) necessary to elicit currents (Erreger et al., 2008; Sonders and Amara, 1996).

Types of transporter-mediated currents

Three types of transporter-mediated currents have been identified: substrate independent leak current, coupled substrate-induced current, and uncoupled substrate-induced current.

Measurable current is obtained in the absence of substrate that can be blocked by classic transporter inhibitors like cocaine and by substrates like DA, as well (Sonders et al., 1997). The conductance that arises from this leakiness within transporters in the absence of substrate has been termed the leak current. The relevance of this leak conductance is not well known, but has been implicated in maintenance of cell membrane potential and neuronal excitability (Sonders and Amara, 1996).

Substrate-induced inward currents that are coupled to transport have been demonstrated in neuronal cultures, cells, and oocytes systems expressing transporters, where application of endogenous (5-HT, NE, DA) substrates or AMPH stimulates inward currents that rapidly return to baseline and persist depending on the length of substrate application. Substrate-induced inward currents are also voltage dependent, as demonstrated by the declining magnitude of AMPH inward currents (Erreger et al., 2008) and a reduction in the transporter:flux ratio (DA:ion) with increased membrane depolarization (more positive potential) (Sonders and Amara, 1996). These inward currents are transporter specific as they are not observed in control cells that do not express the transporter. When measured with high temporal resolution, the substrate-induced inward current has two distinguishable components with different characteristics (Erreger et al., 2008). Substrate application induces an initial peak current that rapidly rises and

decays followed by a slow steady-state current that persists until the substrate is removed. Both currents are substrate dependent, though the steady-state current saturates at a much lower AMPH concentrations. AMPH stimulates a larger peak current than DA when the same concentrations are used; showing a unique capability of AMPH to stimulate more charge transfer across the membrane than DA (Erreger et al., 2008). Sodium also has varying effects on the currents, where the Na^+ gradient is required for the steady-state current but not the peak current, which is dependent on extracellular Na^+ (Erreger et al., 2008).

Significant components of substrate-induced currents are uncoupled from transport since the currents generated are far greater than the predicted stoichiometry for transport (Sonders et al., 1997). This added to the notion of monoamine transporters possessing channel-like properties (Carvelli et al., 2004; Kahlig et al., 2005). Kahlig and colleagues provided evidence of AMPH stimulating single-channel currents in cells expressing DAT or in dopaminergic neurons (Kahlig et al., 2005). Inhibitor-sensitive, single channel events were observed in *DAT-1* DA neurons of *Caenorhabditis elegans* that contributed to membrane depolarization (Carvelli et al., 2004). The recordings of DAT channel-like activity show rapid bursts of DA efflux that would be similar to the amount of DA released from a synaptic vesicle. These channel events are absent without DA, are blocked by DAT-specific inhibitors and require the co-substrates Na^+ and Cl^- . This channel-like activity in *Caenorhabditis elegans* is DAT-mediated as it is not detected without DAT present and still occurs when DA receptors are pharmacologically inhibited (DeFelice and Goswami, 2007). Based upon the gating mechanism proposed from the LeuT crystallization and modeling (see Transport model section), a channel-like mode induced by AMPH could be

achieved through simultaneous opening of the extra-and intracellular gates. The ‘pore’ created would allow more movement of charges through the transporter. It is not exactly clear what determines the probability of a transporter assuming a channel like mode. Recently, another hypothesis has surfaced to explain DAT currents elicited by AMPH. According to the molecular stent hypothesis, after transport, AMPH can bind internally and act as a “molecular stent that holds the transporter open” even after AMPH removal (Rodriguez-Menchaca et al., 2012). Though many important strides have been made, elucidating the mechanism of AMPH action and DAT reversal remains a continued area of investigation.

Transport measurement with the fluorescent substrate ASP⁺

Classic radioligand assays that measure binding and transport have been utilized to establish important transporter properties, like substrate and inhibitor affinity constants. Radioligand assays are beneficial due to their high sensitivity, availability of compounds and rapid detection methods. However, a major disadvantage of radioligand assays is their inability to measure real-time changes of transporter functions. Techniques like rotating disk voltammetry provide alternate methods with improved spatial resolution for measuring transport activities (Povlock and Schenk, 1997). A relatively new method utilized by Schwartz et al. (2003) demonstrated that ASP⁺ ((4-4-dimethylamino)-styryl)-N-methylpyridinium) is a viable fluorescent substrate for hNET and hDAT. ASP⁺ is a fluorescent analog of the neurotoxin MPP⁺ (Figure 1-6), which is cleaved from of MPTP. ASP⁺ has several similarities to native and previously identified substrates. ASP⁺ competes for DA and NE uptake with micromolar potencies in hDAT- and hNET-HEK cells respectively (Mason et al., 2005); its accumulation is dependent on Na⁺ and Cl⁻

and sensitive to temperature and competitive pharmacological inhibition with cocaine (DAT and NET blocker), desipramine (specific NET blocker), or high substrate concentrations (Schwartz et al., 2003).

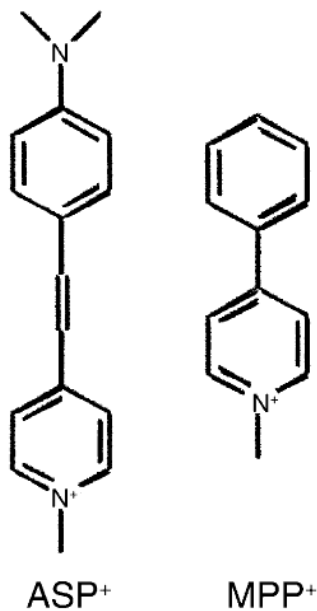


Figure 1-6. Chemical structures of ASP⁺ (left) and MPP⁺ (right) (Mason et al., 2005).

Transporter-mediated uptake of ASP⁺ has been measured in heterologous cell expression systems and native neuronal cultures (Schwartz et al., 2003). ASP⁺ is an inexpensive compound that can distinguish between substrate binding at the membrane and transport within a single cell using the same fluorescent microscopy assay.

ASP⁺ uptake activity has been well characterized and described as having two phases that are visualized by plotting the fluorescent intensity of the whole cell over a given time period after ASP⁺ application (Schwartz et al., 2003). Phase I is the rapid binding phase; and Phase II is the slower transport phase. Native substrates, like NE, are also able to reduce ASP⁺ fluorescence due to competition of the two substrates for transporter binding. ASP⁺ accumulation is detected in parental HEK293 cell lines, although the response in cells expressing transporter is significantly greater (Schwartz et al., 2003). The non-specific accumulation may be attributed to uptake through the low affinity, high capacity organic cation transporters (OCT) that can be expressed in HEK cells. Inhibitors, such as decynium 22, exists that specifically block OCTs, but have not been directly used to inhibit ASP⁺ accumulation. Due to mitochondrial sequestration ASP⁺ is not subject to efflux (Schwartz et al., 2003), and thus provides the unique experimental advantage of evaluating only the influx of substrate without the component of efflux.

Thesis Summary

Uncovering the mechanistic details governing transporter movements is a premier research focus for many laboratories. This project was initiated to understand the role of the N-terminal Thr residue within the conserved RETW sequence in the regulation of DAT and NET functions. Initial interests were in identifying additional phosphorylation sites involved in regulating reverse transport. To this end, the Thr residue of the highly conserved RETW sequence in hDAT and hNET was mutated to alanine (T→A, Ala, A) or aspartic acid (T→D, Asp, D) to mimic a non-phosphorylated and phosphorylated state, respectively. Mutant and wild type transporters

were stably expressed in human embryonic kidney (HEK) cells. The Thr 62 mutations of hDAT and hNET altered the dynamics of the transporter conformation in a way that profoundly impacted its function. The T62D-hDAT mutation showed reduced K_m and V_{max} for [3H]DA uptake and abrogated amphetamine (AMPH)-stimulated DA efflux, but had elevated basal DA efflux as compared to WT- and T62A-hDAT. These aberrant functions of the T62D mutant were partially suppressed when measured in the presence of zinc. It was concluded that T62D-hDAT is predominately inward facing, while T62A-hDAT functions more like WT-hDAT in the outward conformation (Guptaroy et al., 2009).

The work within this dissertation extends the characterization of the Thr mutations and functional properties of the transporter. As detailed in Chapter 2, the effects of the corresponding Thr mutations in hNET (T58A and T58D) on transporter surface expression, uptake of DA, and basal and AMPH-induced DA efflux were evaluated. The effects of the T58D mutation on these properties of hNET were similar to previous findings in the T62D hDAT mutant. The greater portion of Chapter 2 provides an extensive analysis of alterations to substrate and inhibitor interactions with the Thr mutant hDATs and hNETs. An array of radioligand uptake and inhibitor binding competition assays revealed an enhanced sensitivity to all substrates tested in both hDAT and hNET T \rightarrow D mutants. The actions of inhibitors differed in that their activity was not affected by the Thr mutations in hNET; however, changes were observed in T62D hDAT expressing cells that were dependent on the inhibitor structure (Guptaroy et al., 2011). These data emphasized the strong and differential influence transporter orientation has on ligand interactions.

Chapter 3 further probes the elevation of constitutive DA efflux seen in the T62D mutation of hDAT. We theorized that the inward facing conformation caused by the T→D mutation was a representation of WT hDAT in an efflux-willing orientation elicited by, for instance, exposure to AMPH. Three hypotheses were tested to support this theory and explain the increase in basal DA efflux in T62D-hDAT. They were: 1) a loss of intracellular substrate retention 2) an intrinsic membrane depolarization induced by the mutation; and 3) an enhanced dependence on intracellular sodium. My approach to these hypotheses combined various techniques: confocal microscopy with the fluorescent substrate ASP⁺, electrophysiology measurements in *Xenopus* oocytes, and radioligand assays under sodium replacement conditions. My results have led me to conclude that the T62D mutation in hDAT produces a sodium-primed transporter orientation that favors reverse transport. Surprisingly, the T62D-hDAT exhibited independence of sodium for DA efflux, not DA influx. These data strongly support the concept of T62D-hDAT mutant as an hDAT efflux model, but also the notion of separate regulation of uptake and efflux through DAT.

The final chapter provides conclusions and implications for the Thr DAT and NET mutants. A molecular interaction of T62 and Y335 has been implicated in formation of the inward facing transporter (Shan et al., 2011) that, along other molecular interactions, is disrupted by the T62D mutation (Guptaroy et al., 2009). Preliminary experiments measured the uptake and efflux properties in an hDAT cell line where the Y335 residue was mutated to a phenylalanine (Y335F) and compared to WT and Thr62 hDAT mutants. This work will demonstrate the ability of a subtle structural change to have robust impact on DAT functions. Other points for discussion

include the impact of the Thr mutations on transporter trafficking and regulation by second messenger systems, like PKC signaling; interactions with additional proteins such as the D2 DA autoreceptor and syntaxin 1A; and the potential application of the T62D-hDAT mutant mouse as a model for diseases involving excessive extracellular DA.

Taken together the data and conclusions from this dissertation add to our understanding of how monoamine transporters operate and potential changes that may occur when exposed to drugs affecting their activity and orientation.

References

Beuming, T., Kniazeff, J., Bergmann, M.L., Shi, L., Gracia, L., Raniszewska, K., Newman, A.H., Javitch, J.A., Weinstein, H., Gether, U., *et al.* (2008). The binding sites for cocaine and dopamine in the dopamine transporter overlap. *Nature neuroscience* *11*, 780-789.

Binda, F., Dipace, C., Bowton, E., Robertson, S.D., Lute, B.J., Fog, J.U., Zhang, M., Sen, N., Colbran, R.J., Gnegy, M.E., *et al.* (2008). Syntaxin 1A interaction with the dopamine transporter promotes amphetamine-induced dopamine efflux. *Molecular pharmacology* *74*, 1101-1108.

Brunton, L.L., Laso, J.S., and Parker, K., L. (2006). *Goodman & Gilman's the pharmacological basis of therapeutics* 11 edn (McGraw-Hill Companies, Inc.) pp. 164, 237-296, 299, 429-460.

Carvelli, L., McDonald, P.W., Blakely, R.D., and Defelice, L.J. (2004). Dopamine transporters depolarize neurons by a channel mechanism. *Proceedings of the National Academy of Sciences of the United States of America* *101*, 16046-16051.

Chen, N., and Justice, J.B. (2000). Differential effect of structural modification of human dopamine transporter on the inward and outward transport of dopamine. *Brain research. Molecular brain research* *75*, 208-215.

Chen, N., and Reith, M.E. (2000). Structure and function of the dopamine transporter. *European journal of pharmacology* *405*, 329-339.

Chen, N., Rickey, J., Berfield, J.L., and Reith, M.E. (2004a). Aspartate 345 of the dopamine transporter is critical for conformational changes in substrate translocation and cocaine binding. *The Journal of biological chemistry* *279*, 5508-5519.

Chen, N., Zhen, J., and Reith, M.E. (2004b). Mutation of Trp84 and Asp313 of the dopamine transporter reveals similar mode of binding interaction for GBR12909 and bztropine as opposed to cocaine. *Journal of neurochemistry* *89*, 853-864.

Chen, N.H., Reith, M.E., and Quick, M.W. (2004c). Synaptic uptake and beyond: the sodium- and chloride-dependent neurotransmitter transporter family SLC6. *Pflugers Archiv : European journal of physiology* *447*, 519-531.

Chen, R., Furman, C.A., Zhang, M., Kim, M.N., Gereau, R.W.t., Leitges, M., and Gnegy, M.E. (2009). Protein kinase C beta is a critical regulator of dopamine transporter trafficking and regulates the behavioral response to amphetamine in mice. *The Journal of pharmacology and experimental therapeutics* 328, 912-920.

DeFelice, L.J., and Goswami, T. (2007). Transporters as channels. *Annual review of physiology* 69, 87-112.

Dipace, C., Sung, U., Binda, F., Blakely, R.D., and Galli, A. (2007). Amphetamine induces a calcium/calmodulin-dependent protein kinase II-dependent reduction in norepinephrine transporter surface expression linked to changes in syntaxin 1A/transporter complexes. *Molecular pharmacology* 71, 230-239.

Erreger, K., Grewer, C., Javitch, J.A., and Galli, A. (2008). Currents in response to rapid concentration jumps of amphetamine uncover novel aspects of human dopamine transporter function. *J Neurosci* 28, 976-989.

Fischer, J.F., and Cho, A.K. (1979). Chemical release of dopamine from striatal homogenates: evidence for an exchange diffusion model. *The Journal of pharmacology and experimental therapeutics* 208, 203-209.

Forrest, L.R., and Rudnick, G. (2009). The rocking bundle: a mechanism for ion-coupled solute flux by symmetrical transporters. *Physiology* 24, 377-386.

Furman, C.A., Chen, R., Guptaroy, B., Zhang, M., Holz, R.W., and Gnegy, M. (2009). Dopamine and amphetamine rapidly increase dopamine transporter trafficking to the surface: live-cell imaging using total internal reflection fluorescence microscopy. *J Neurosci* 29, 3328-3336.

Giros, B., and Caron, M.G. (1993). Molecular characterization of the dopamine transporter. *Trends in pharmacological sciences* 14, 43-49.

Giros, B., Jaber, M., Jones, S.R., Wightman, R.M., and Caron, M.G. (1996). Hyperlocomotion and indifference to cocaine and amphetamine in mice lacking the dopamine transporter. *Nature* 379, 606-612.

Gnegy, M.E. (2012). Catecholamines. In *Basic Neurochemistry* (Elsevier Inc.), pp. 280-296.

Gu, H., Wall, S.C., and Rudnick, G. (1994). Stable expression of biogenic amine transporters reveals differences in inhibitor sensitivity, kinetics, and ion dependence. *The Journal of biological chemistry* 269, 7124-7130.

Guptaroy, B., Fraser, R., Desai, A., Zhang, M., and Gnegy, M.E. (2011). Site-Directed Mutations near Transmembrane Domain 1 Alter Conformation and Function of Norepinephrine and Dopamine Transporters. *Molecular pharmacology* 79, 520-532.

Guptaroy, B., Zhang, M., Bowton, E., Binda, F., Shi, L., Weinstein, H., Galli, A., Javitch, J.A., Neubig, R.R., and Gnegy, M.E. (2009). A juxtamembrane mutation in the N terminus of the dopamine transporter induces preference for an inward-facing conformation. *Molecular pharmacology* 75, 514-524.

Hahn, M.K., and Blakely, R.D. (2007). The functional impact of SLC6 transporter genetic variation. *Annual review of pharmacology and toxicology* 47, 401-441.

Howell, L.L., and Kimmel, H.L. (2008). Monoamine transporters and psychostimulant addiction. *Biochem Pharmacol* 75, 196-217.

Itokawa, M., Lin, Z., and Uhl, G.R. (2002). Dopamine efflux via wild-type and mutant dopamine transporters: alanine substitution for proline-572 enhances efflux and reduces dependence on extracellular dopamine, sodium and chloride concentrations. *Brain research. Molecular brain research* 108, 71-80.

Jardetzky, O. (1966). Simple allosteric model for membrane pumps. *Nature* 211, 969-970.

Joh, T.H., and Hwang, O. (1987). Dopamine beta-hydroxylase: biochemistry and molecular biology. *Ann N Y Acad Sci* 493, 342-350.

Johnson, L.A., Furman, C.A., Zhang, M., Guptaroy, B., and Gnegy, M.E. (2005a). Rapid delivery of the dopamine transporter to the plasmalemmal membrane upon amphetamine stimulation. *Neuropharmacology* 49, 750-758.

Johnson, L.A., Guptaroy, B., Lund, D., Shamban, S., and Gnegy, M.E. (2005b). Regulation of amphetamine-stimulated dopamine efflux by protein kinase C beta. *The Journal of biological chemistry* 280, 10914-10919.

Jones, S.R., Gainetdinov, R.R., Wightman, R.M., and Caron, M.G. (1998). Mechanisms of amphetamine action revealed in mice lacking the dopamine transporter. *J Neurosci* 18, 1979-1986.

Kahlig, K.M., Binda, F., Khoshbouei, H., Blakely, R.D., McMahon, D.G., Javitch, J.A., and Galli, A. (2005). Amphetamine induces dopamine efflux through a dopamine transporter channel. *Proceedings of the National Academy of Sciences of the United States of America* 102, 3495-3500.

Kalisker, A., Waymire, J.C., and Rutledge, C.O. (1975). Effects of 6-hydroxydopamine and reserpine on amphetamine-induced release of norepinephrine in rat cerebral cortex. *The Journal of pharmacology and experimental therapeutics* 193, 64-72.

Khoshbouei, H., Sen, N., Guptaroy, B., Johnson, L., Lund, D., Gnegy, M.E., Galli, A., and Javitch, J.A. (2004). N-terminal phosphorylation of the dopamine transporter is required for amphetamine-induced efflux. *PLoS Biol* 2, E78.

Khoshbouei, H., Wang, H., Lechleiter, J.D., Javitch, J.A., and Galli, A. (2003). Amphetamine-induced dopamine efflux. A voltage-sensitive and intracellular Na⁺-dependent mechanism. *The Journal of biological chemistry* 278, 12070-12077.

Kniazeff, J., Shi, L., Loland, C.J., Javitch, J.A., Weinstein, H., and Gether, U. (2008). An intracellular interaction network regulates conformational transitions in the dopamine transporter. *The Journal of biological chemistry* 283, 17691-17701.

Koldso, H., Noer, P., Grouleff, J., Autzen, H.E., Sinning, S., and Schiott, B. (2011). Unbiased simulations reveal the inward-facing conformation of the human serotonin transporter and Na⁽⁺⁾ ion release. *PLoS computational biology* 7, e1002246.

Krishnamurthy, H., and Gouaux, E. (2012). X-ray structures of LeuT in substrate-free outward-open and apo inward-open states. *Nature* 481, 469-474.

Krishnamurthy, H., Piscitelli, C.L., and Gouaux, E. (2009). Unlocking the molecular secrets of sodium-coupled transporters. *Nature* 459, 347-355.

Kristensen, A.S., Andersen, J., Jorgensen, T.N., Sorensen, L., Eriksen, J., Loland, C.J., Stromgaard, K., and Gether, U. (2011). SLC6 neurotransmitter transporters: structure, function, and regulation. *Pharmacological reviews* 63, 585-640.

Langeloh, A., Bonisch, H., and Trendelenburg, U. (1987). The mechanism of the 3H-noradrenaline releasing effect of various substrates of uptake1: multifactorial induction of outward transport. *Naunyn-Schmiedeberg's archives of pharmacology* 336, 602-610.

Leviel, V. (2011). Dopamine release mediated by the dopamine transporter, facts and consequences. *Journal of neurochemistry* 118, 475-489.

Liang, N.Y., and Rutledge, C.O. (1982). Evidence for carrier-mediated efflux of dopamine from corpus striatum. *Biochem Pharmacol* 31, 2479-2484.

Liang, N.Y., and Rutledge, C.O. (1983). Calcium-independent release of [3H]dopamine by veratridine in pargyline- and reserpine-treated corpus striatum. *European journal of pharmacology* 89, 153-155.

Liang, Y.J., Zhen, J., Chen, N., and Reith, M.E. (2009). Interaction of catechol and non-catechol substrates with externally or internally facing dopamine transporters. *Journal of neurochemistry* 109, 981-994.

Lin, Z., Wang, W., and Uhl, G.R. (2000). Dopamine transporter tryptophan mutants highlight candidate dopamine- and cocaine-selective domains. *Molecular pharmacology* 58, 1581-1592.

Loland, C.J., Granas, C., Javitch, J.A., and Gether, U. (2004). Identification of intracellular residues in the dopamine transporter critical for regulation of transporter conformation and cocaine binding. *The Journal of biological chemistry* 279, 3228-3238.

Loland, C.J., Norregaard, L., and Gether, U. (1999). Defining proximity relationships in the tertiary structure of the dopamine transporter. Identification of a conserved glutamic acid as a

third coordinate in the endogenous Zn(2+)-binding site. *The Journal of biological chemistry* 274, 36928-36934.

Loland, C.J., Norregaard, L., Litman, T., and Gether, U. (2002). Generation of an activating Zn(2+) switch in the dopamine transporter: mutation of an intracellular tyrosine constitutively alters the conformational equilibrium of the transport cycle. *Proceedings of the National Academy of Sciences of the United States of America* 99, 1683-1688.

Mason, J.N., Farmer, H., Tomlinson, I.D., Schwartz, J.W., Savchenko, V., DeFelice, L.J., Rosenthal, S.J., and Blakely, R.D. (2005). Novel fluorescence-based approaches for the study of biogenic amine transporter localization, activity, and regulation. *Journal of neuroscience methods* 143, 3-25.

Mazei-Robison, M.S., and Blakely, R.D. (2005). Expression studies of naturally occurring human dopamine transporter variants identifies a novel state of transporter inactivation associated with Val382Ala. *Neuropharmacology* 49, 737-749.

Mazei-Robison, M.S., Bowton, E., Holy, M., Schmudermaier, M., Freissmuth, M., Sitte, H.H., Galli, A., and Blakely, R.D. (2008). Anomalous dopamine release associated with a human dopamine transporter coding variant. *J Neurosci* 28, 7040-7046.

Melikian, H.E. (2004). Neurotransmitter transporter trafficking: endocytosis, recycling, and regulation. *Pharmacol Ther* 104, 17-27.

Meyer, J.S., and Quenzer, L.F. (2005). *Psychopharmacology: drugs, the brain, and behavior* (Sunderland, MA U.S.A: Sinauer Associates, Inc.), pp. 118-137.

Norregaard, L., Frederiksen, D., Nielsen, E.O., and Gether, U. (1998). Delineation of an endogenous zinc-binding site in the human dopamine transporter. *The EMBO journal* 17, 4266-4273.

Pifl, C., and Singer, E.A. (1999). Ion dependence of carrier-mediated release in dopamine or norepinephrine transporter-transfected cells questions the hypothesis of facilitated exchange diffusion. *Molecular pharmacology* 56, 1047-1054.

Pifl, C., Wolf, A., Rebernik, P., Reither, H., and Berger, M.L. (2009). Zinc regulates the dopamine transporter in a membrane potential and chloride dependent manner. *Neuropharmacology* 56, 531-540.

Piscitelli, C.L., Krishnamurthy, H., and Gouaux, E. (2010). Neurotransmitter/sodium symporter orthologue LeuT has a single high-affinity substrate site. *Nature* 468, 1129-1132.

Povlock, S.L., and Schenk, J.O. (1997). A multisubstrate kinetic mechanism of dopamine transport in the nucleus accumbens and its inhibition by cocaine. *Journal of neurochemistry* 69, 1093-1105.

Quick, M., Shi, L., Zehnpfennig, B., Weinstein, H., and Javitch, J.A. (2012). Experimental conditions can obscure the second high-affinity site in LeuT. *Nature structural & molecular biology* 19, 207-211.

Rizo, J., and Rosenmund, C. (2008). Synaptic vesicle fusion. *Nature structural & molecular biology* 15, 665-674.

Robertson, S.D., Matthies, H.J., and Galli, A. (2009). A Closer Look at Amphetamine-Induced Reverse Transport and Trafficking of the Dopamine and Norepinephrine Transporters. *Mol Neurobiol*.

Robinson, T.E., and Berridge, K.C. (2003). Addiction. *Annual review of psychology* 54, 25-53.

Rodriguez-Menchaca, A.A., Solis, E., Jr., Cameron, K., and De Felice, L.J. (2012). S(+)-amphetamine induces a persistent leak in the human dopamine transporter: molecular stent hypothesis. *British journal of pharmacology* 165, 2749-2757.

Rudnick, G. (1998). Ion-coupled neurotransmitter transport: thermodynamic vs. kinetic determinations of stoichiometry. *Methods in enzymology* 296, 233-247.

Schmitt, K.C., and Reith, M.E. (2010). Regulation of the dopamine transporter: aspects relevant to psychostimulant drugs of abuse. *Ann N Y Acad Sci* 1187, 316-340.

Schwartz, J.W., Blakely, R.D., and DeFelice, L.J. (2003). Binding and transport in norepinephrine transporters. Real-time, spatially resolved analysis in single cells using a fluorescent substrate. *The Journal of biological chemistry* 278, 9768-9777.

Shan, J., Javitch, J.A., Shi, L., and Weinstein, H. (2011). The substrate-driven transition to an inward-facing conformation in the functional mechanism of the dopamine transporter. *PloS one* 6, e16350.

Shi, L., Quick, M., Zhao, Y., Weinstein, H., and Javitch, J.A. (2008). The mechanism of a neurotransmitter:sodium symporter--inward release of Na⁺ and substrate is triggered by substrate in a second binding site. *Molecular cell* 30, 667-677.

Singh, S.K., Yamashita, A., and Gouaux, E. (2007). Antidepressant binding site in a bacterial homologue of neurotransmitter transporters. *Nature* 448, 952-956.

Sitte, H.H., Huck, S., Reither, H., Boehm, S., Singer, E.A., and Piffl, C. (1998). Carrier-mediated release, transport rates, and charge transfer induced by amphetamine, tyramine, and dopamine in mammalian cells transfected with the human dopamine transporter. *Journal of neurochemistry* 71, 1289-1297.

Sonders, M.S., and Amara, S.G. (1996). Channels in transporters. *Current opinion in neurobiology* 6, 294-302.

Sonders, M.S., Zhu, S.J., Zahniser, N.R., Kavanaugh, M.P., and Amara, S.G. (1997). Multiple ionic conductances of the human dopamine transporter: the actions of dopamine and psychostimulants. *J Neurosci* 17, 960-974.

Sucic, S., and Bryan-Lluka, L.J. (2005). Roles of transmembrane domain 2 and the first intracellular loop in human noradrenaline transporter function: pharmacological and SCAM analysis. *Journal of neurochemistry* 94, 1620-1630.

Sulzer, D., Sonders, M.S., Poulsen, N.W., and Galli, A. (2005). Mechanisms of neurotransmitter release by amphetamines: a review. *Prog Neurobiol* 75, 406-433.

Torres, G.E. (2006). The dopamine transporter proteome. *Journal of neurochemistry* 97 *Suppl 1*, 3-10.

Vaughan, R.A. (2004). Phosphorylation and regulation of psychostimulant-sensitive neurotransmitter transporters. *The Journal of pharmacology and experimental therapeutics* 310, 1-7.

Volkow, N.D., Wang, G., Fowler, J.S., Logan, J., Gerasimov, M., Maynard, L., Ding, Y., Gatley, S.J., Gifford, A., and Franceschi, D. (2001). Therapeutic doses of oral methylphenidate significantly increase extracellular dopamine in the human brain. *J Neurosci* 21, RC121.

Weissman, A., Koe, B.K., and Tenen, S.S. (1966). Antiamphetamine effects following inhibition of tyrosine hydroxylase. *The Journal of pharmacology and experimental therapeutics* 151, 339-352.

Yamashita, A., Singh, S.K., Kawate, T., Jin, Y., and Gouaux, E. (2005). Crystal structure of a bacterial homologue of Na⁺/Cl⁻-dependent neurotransmitter transporters. *Nature* 437, 215-223.

Zhao, C., Stolzenberg, S., Gracia, L., Weinstein, H., Noskov, S., and Shi, L. (2012). Ion-controlled conformational dynamics in the outward-open transition from an occluded state of LeuT. *Biophysical journal* 103, 878-888.

Zhao, Y., Terry, D., Shi, L., Weinstein, H., Blanchard, S.C., and Javitch, J.A. (2010). Single-molecule dynamics of gating in a neurotransmitter transporter homologue. *Nature* 465, 188-193.

Zhao, Y., Terry, D.S., Shi, L., Quick, M., Weinstein, H., Blanchard, S.C., and Javitch, J.A. (2011). Substrate-modulated gating dynamics in a Na⁺-coupled neurotransmitter transporter homologue. *Nature* 474, 109-113.

Zhou, Z., Zhen, J., Karpowich, N.K., Goetz, R.M., Law, C.J., Reith, M.E., and Wang, D.N. (2007). LeuT-desipramine structure reveals how antidepressants block neurotransmitter reuptake. *Science (New York, N.Y.)* 317, 1390-1393.

Zomot, E., Bendahan, A., Quick, M., Zhao, Y., Javitch, J.A., and Kanner, B.I. (2007). Mechanism of chloride interaction with neurotransmitter:sodium symporters. *Nature* 449, 726-730.

Beuming, T., Kniazeff, J., Bergmann, M.L., Shi, L., Gracia, L., Raniszewska, K., Newman, A.H., Javitch, J.A., Weinstein, H., Gether, U., *et al.* (2008). The binding sites for cocaine and dopamine in the dopamine transporter overlap. *Nature neuroscience* 11, 780-789.

Binda, F., Dipace, C., Bowton, E., Robertson, S.D., Lute, B.J., Fog, J.U., Zhang, M., Sen, N., Colbran, R.J., Gnegy, M.E., *et al.* (2008). Syntaxin 1A interaction with the dopamine transporter promotes amphetamine-induced dopamine efflux. *Molecular pharmacology* 74, 1101-1108.

Brunton, L.L., Laso, J.S., and Parker, K., L. (2006). *Goodman & Gilman's the pharmacological basis of therapeutics* 11 edn (McGraw-Hill Companies, Inc.).

Carvelli, L., McDonald, P.W., Blakely, R.D., and Defelice, L.J. (2004). Dopamine transporters depolarize neurons by a channel mechanism. *Proceedings of the National Academy of Sciences of the United States of America* 101, 16046-16051.

Chen, N., and Justice, J.B. (2000). Differential effect of structural modification of human dopamine transporter on the inward and outward transport of dopamine. *Brain research. Molecular brain research* 75, 208-215.

Chen, N., and Reith, M.E. (2000). Structure and function of the dopamine transporter. *European journal of pharmacology* 405, 329-339.

Chen, N., Rickey, J., Berfield, J.L., and Reith, M.E. (2004a). Aspartate 345 of the dopamine transporter is critical for conformational changes in substrate translocation and cocaine binding. *The Journal of biological chemistry* 279, 5508-5519.

Chen, N., Zhen, J., and Reith, M.E. (2004b). Mutation of Trp84 and Asp313 of the dopamine transporter reveals similar mode of binding interaction for GBR12909 and benztropine as opposed to cocaine. *Journal of neurochemistry* 89, 853-864.

Chen, N.H., Reith, M.E., and Quick, M.W. (2004c). Synaptic uptake and beyond: the sodium- and chloride-dependent neurotransmitter transporter family SLC6. *Pflugers Archiv : European journal of physiology* 447, 519-531.

Chen, R., Furman, C.A., Zhang, M., Kim, M.N., Gereau, R.W., Leitges, M., and Gnegy, M.E. (2008). Protein kinase C β is a critical regulator of dopamine transporter trafficking and regulates the behavioral response to amphetamine in mice. *The Journal of pharmacology and experimental therapeutics*.

DeFelice, L.J., and Goswami, T. (2007). Transporters as channels. *Annual review of physiology* 69, 87-112.

Dipace, C., Sung, U., Binda, F., Blakely, R.D., and Galli, A. (2007). Amphetamine induces a calcium/calmodulin-dependent protein kinase II-dependent reduction in norepinephrine transporter surface expression linked to changes in syntaxin 1A/transporter complexes. *Molecular pharmacology* 71, 230-239.

Erreger, K., Grewer, C., Javitch, J.A., and Galli, A. (2008). Currents in response to rapid concentration jumps of amphetamine uncover novel aspects of human dopamine transporter function. *J Neurosci* 28, 976-989.

Fischer, J.F., and Cho, A.K. (1979). Chemical release of dopamine from striatal homogenates: evidence for an exchange diffusion model. *The Journal of pharmacology and experimental therapeutics* 208, 203-209.

Forrest, L.R., and Rudnick, G. (2009). The rocking bundle: a mechanism for ion-coupled solute flux by symmetrical transporters. *Physiology* 24, 377-386.

Furman, C.A., Chen, R., Guptaroy, B., Zhang, M., Holz, R.W., and Gnegy, M. (2009). Dopamine and amphetamine rapidly increase dopamine transporter trafficking to the surface:

live-cell imaging using total internal reflection fluorescence microscopy. *J Neurosci* 29, 3328-3336.

Giros, B., and Caron, M.G. (1993). Molecular characterization of the dopamine transporter. *Trends in pharmacological sciences* 14, 43-49.

Giros, B., Jaber, M., Jones, S.R., Wightman, R.M., and Caron, M.G. (1996). Hyperlocomotion and indifference to cocaine and amphetamine in mice lacking the dopamine transporter. *Nature* 379, 606-612.

Gnegy, M.E. (2012). Catecholamines. In *Basic Neurochemistry* (Elsevier Inc.), pp. 280-296.

Gu, H., Wall, S.C., and Rudnick, G. (1994). Stable expression of biogenic amine transporters reveals differences in inhibitor sensitivity, kinetics, and ion dependence. *The Journal of biological chemistry* 269, 7124-7130.

Guptaroy, B., Fraser, R., Desai, A., Zhang, M., and Gnegy, M.E. (2011). Site-Directed Mutations near Transmembrane Domain 1 Alter Conformation and Function of Norepinephrine and Dopamine Transporters. *Molecular pharmacology* 79, 520-532.

Guptaroy, B., Zhang, M., Bowton, E., Binda, F., Shi, L., Weinstein, H., Galli, A., Javitch, J.A., Neubig, R.R., and Gnegy, M.E. (2009). A juxtamembrane mutation in the N terminus of the dopamine transporter induces preference for an inward-facing conformation. *Molecular pharmacology* 75, 514-524.

Hahn, M.K., and Blakely, R.D. (2007). The functional impact of SLC6 transporter genetic variation. *Annual review of pharmacology and toxicology* 47, 401-441.

Howell, L.L., and Kimmel, H.L. (2008). Monoamine transporters and psychostimulant addiction. *Biochem Pharmacol* 75, 196-217.

Itokawa, M., Lin, Z., and Uhl, G.R. (2002). Dopamine efflux via wild-type and mutant dopamine transporters: alanine substitution for proline-572 enhances efflux and reduces dependence on extracellular dopamine, sodium and chloride concentrations. *Brain research. Molecular brain research* 108, 71-80.

Jardetzky, O. (1966). Simple allosteric model for membrane pumps. *Nature* 211, 969-970.

Joh, T.H., and Hwang, O. (1987). Dopamine beta-hydroxylase: biochemistry and molecular biology. *Ann N Y Acad Sci* 493, 342-350.

Johnson, L.A., Furman, C.A., Zhang, M., Guptaroy, B., and Gnegy, M.E. (2005a). Rapid delivery of the dopamine transporter to the plasmalemmal membrane upon amphetamine stimulation. *Neuropharmacology* 49, 750-758.

Johnson, L.A., Guptaroy, B., Lund, D., Shamban, S., and Gnegy, M.E. (2005b). Regulation of amphetamine-stimulated dopamine efflux by protein kinase C beta. *The Journal of biological chemistry* 280, 10914-10919.

Jones, S.R., Gainetdinov, R.R., Wightman, R.M., and Caron, M.G. (1998). Mechanisms of amphetamine action revealed in mice lacking the dopamine transporter. *J Neurosci* 18, 1979-1986.

Kahlig, K.M., Binda, F., Khoshbouei, H., Blakely, R.D., McMahon, D.G., Javitch, J.A., and Galli, A. (2005). Amphetamine induces dopamine efflux through a dopamine transporter channel. *Proceedings of the National Academy of Sciences of the United States of America* 102, 3495-3500.

Kalisker, A., Waymire, J.C., and Rutledge, C.O. (1975). Effects of 6-hydroxydopamine and reserpine on amphetamine-induced release of norepinephrine in rat cerebral cortex. *The Journal of pharmacology and experimental therapeutics* 193, 64-72.

Khoshbouei, H., Sen, N., Guptaroy, B., Johnson, L., Lund, D., Gnegy, M.E., Galli, A., and Javitch, J.A. (2004). N-terminal phosphorylation of the dopamine transporter is required for amphetamine-induced efflux. *PLoS Biol* 2, E78.

Khoshbouei, H., Wang, H., Lechleiter, J.D., Javitch, J.A., and Galli, A. (2003). Amphetamine-induced dopamine efflux. A voltage-sensitive and intracellular Na⁺-dependent mechanism. *The Journal of biological chemistry* 278, 12070-12077.

Kniazeff, J., Shi, L., Loland, C.J., Javitch, J.A., Weinstein, H., and Gether, U. (2008). An intracellular interaction network regulates conformational transitions in the dopamine transporter. *The Journal of biological chemistry* 283, 17691-17701.

Koldso, H., Noer, P., Grouleff, J., Autzen, H.E., Sinning, S., and Schiott, B. (2011). Unbiased simulations reveal the inward-facing conformation of the human serotonin transporter and Na(+) ion release. *PLoS computational biology* 7, e1002246.

Krishnamurthy, H., and Gouaux, E. (2012). X-ray structures of LeuT in substrate-free outward-open and apo inward-open states. *Nature* 481, 469-474.

Krishnamurthy, H., Piscitelli, C.L., and Gouaux, E. (2009). Unlocking the molecular secrets of sodium-coupled transporters. *Nature* 459, 347-355.

Kristensen, A.S., Andersen, J., Jorgensen, T.N., Sorensen, L., Eriksen, J., Loland, C.J., Stromgaard, K., and Gether, U. (2011). SLC6 neurotransmitter transporters: structure, function, and regulation. *Pharmacological reviews* 63, 585-640.

Langeloh, A., Bonisch, H., and Trendelenburg, U. (1987). The mechanism of the 3H-noradrenaline releasing effect of various substrates of uptake1: multifactorial induction of outward transport. *Naunyn-Schmiedeberg's archives of pharmacology* 336, 602-610.

Leviel, V. (2011). Dopamine release mediated by the dopamine transporter, facts and consequences. *Journal of neurochemistry* 118, 475-489.

Liang, N.Y., and Rutledge, C.O. (1982). Evidence for carrier-mediated efflux of dopamine from corpus striatum. *Biochem Pharmacol* 31, 2479-2484.

Liang, N.Y., and Rutledge, C.O. (1983). Calcium-independent release of [3H]dopamine by veratridine in pargyline- and reserpine-treated corpus striatum. *European journal of pharmacology* 89, 153-155.

Liang, Y.J., Zhen, J., Chen, N., and Reith, M.E. (2009). Interaction of catechol and non-catechol substrates with externally or internally facing dopamine transporters. *Journal of neurochemistry* 109, 981-994.

Lin, Z., Wang, W., and Uhl, G.R. (2000). Dopamine transporter tryptophan mutants highlight candidate dopamine- and cocaine-selective domains. *Molecular pharmacology* 58, 1581-1592.

Loland, C.J., Granas, C., Javitch, J.A., and Gether, U. (2004). Identification of intracellular residues in the dopamine transporter critical for regulation of transporter conformation and cocaine binding. *The Journal of biological chemistry* 279, 3228-3238.

Loland, C.J., Norregaard, L., and Gether, U. (1999). Defining proximity relationships in the tertiary structure of the dopamine transporter. Identification of a conserved glutamic acid as a third coordinate in the endogenous Zn(2+)-binding site. *The Journal of biological chemistry* 274, 36928-36934.

Loland, C.J., Norregaard, L., Litman, T., and Gether, U. (2002). Generation of an activating Zn(2+) switch in the dopamine transporter: mutation of an intracellular tyrosine constitutively alters the conformational equilibrium of the transport cycle. *Proceedings of the National Academy of Sciences of the United States of America* 99, 1683-1688.

Mason, J.N., Farmer, H., Tomlinson, I.D., Schwartz, J.W., Savchenko, V., DeFelice, L.J., Rosenthal, S.J., and Blakely, R.D. (2005). Novel fluorescence-based approaches for the study of biogenic amine transporter localization, activity, and regulation. *Journal of neuroscience methods* 143, 3-25.

Mazei-Robison, M.S., and Blakely, R.D. (2005). Expression studies of naturally occurring human dopamine transporter variants identifies a novel state of transporter inactivation associated with Val382Ala. *Neuropharmacology* 49, 737-749.

Mazei-Robison, M.S., Bowton, E., Holy, M., Schmudermaier, M., Freissmuth, M., Sitte, H.H., Galli, A., and Blakely, R.D. (2008). Anomalous dopamine release associated with a human dopamine transporter coding variant. *J Neurosci* 28, 7040-7046.

Melikian, H.E. (2004). Neurotransmitter transporter trafficking: endocytosis, recycling, and regulation. *Pharmacol Ther* 104, 17-27.

Meyer, J.S., and Quenzer, L.F. (2005). *Psychopharmacology: drugs, the brain, and behavior* (Sunderland, MA U.S.A: Sinauer Associates, Inc.).

Miller, L.D., Lee, K.C., Mochly-Rosen, D., and Cartwright, C.A. (2004). RACK1 regulates Src-mediated Sam68 and p190RhoGAP signaling. *Oncogene* 23, 5682-5686.

Norregaard, L., Frederiksen, D., Nielsen, E.O., and Gether, U. (1998). Delineation of an endogenous zinc-binding site in the human dopamine transporter. *The EMBO journal* 17, 4266-4273.

Pifl, C., and Singer, E.A. (1999). Ion dependence of carrier-mediated release in dopamine or norepinephrine transporter-transfected cells questions the hypothesis of facilitated exchange diffusion. *Molecular pharmacology* 56, 1047-1054.

Pifl, C., Wolf, A., Rebernik, P., Reither, H., and Berger, M.L. (2009). Zinc regulates the dopamine transporter in a membrane potential and chloride dependent manner. *Neuropharmacology* 56, 531-540.

Piscitelli, C.L., Krishnamurthy, H., and Gouaux, E. (2010). Neurotransmitter/sodium symporter orthologue LeuT has a single high-affinity substrate site. *Nature* 468, 1129-1132.

Povlock, S.L., and Schenk, J.O. (1997). A multisubstrate kinetic mechanism of dopamine transport in the nucleus accumbens and its inhibition by cocaine. *Journal of neurochemistry* 69, 1093-1105.

Quick, M., Shi, L., Zehnpfennig, B., Weinstein, H., and Javitch, J.A. (2012). Experimental conditions can obscure the second high-affinity site in LeuT. *Nature structural & molecular biology* 19, 207-211.

Rizo, J., and Rosenmund, C. (2008). Synaptic vesicle fusion. *Nature structural & molecular biology* 15, 665-674.

Robertson, S.D., Matthies, H.J., and Galli, A. (2009). A Closer Look at Amphetamine-Induced Reverse Transport and Trafficking of the Dopamine and Norepinephrine Transporters. *Mol Neurobiol*.

Robinson, T.E., and Berridge, K.C. (2003). Addiction. *Annual review of psychology* 54, 25-53.

Rodriguez-Menchaca, A.A., Solis, E., Jr., Cameron, K., and De Felice, L.J. (2012). S(+)-amphetamine induces a persistent leak in the human dopamine transporter: molecular stent hypothesis. *British journal of pharmacology* *165*, 2749-2757.

Rudnick, G. (1998). Ion-coupled neurotransmitter transport: thermodynamic vs. kinetic determinations of stoichiometry. *Methods in enzymology* *296*, 233-247.

Schmitt, K.C., and Reith, M.E. (2010). Regulation of the dopamine transporter: aspects relevant to psychostimulant drugs of abuse. *Ann N Y Acad Sci* *1187*, 316-340.

Schwartz, J.W., Blakely, R.D., and DeFelice, L.J. (2003). Binding and transport in norepinephrine transporters. Real-time, spatially resolved analysis in single cells using a fluorescent substrate. *The Journal of biological chemistry* *278*, 9768-9777.

Shan, J., Javitch, J.A., Shi, L., and Weinstein, H. (2011). The substrate-driven transition to an inward-facing conformation in the functional mechanism of the dopamine transporter. *PloS one* *6*, e16350.

Shi, L., Quick, M., Zhao, Y., Weinstein, H., and Javitch, J.A. (2008). The mechanism of a neurotransmitter:sodium symporter--inward release of Na⁺ and substrate is triggered by substrate in a second binding site. *Molecular cell* *30*, 667-677.

Singh, S.K., Yamashita, A., and Gouaux, E. (2007). Antidepressant binding site in a bacterial homologue of neurotransmitter transporters. *Nature* *448*, 952-956.

Sitte, H.H., Huck, S., Reither, H., Boehm, S., Singer, E.A., and Piffl, C. (1998). Carrier-mediated release, transport rates, and charge transfer induced by amphetamine, tyramine, and dopamine in mammalian cells transfected with the human dopamine transporter. *Journal of neurochemistry* *71*, 1289-1297.

Sonders, M.S., and Amara, S.G. (1996). Channels in transporters. *Current opinion in neurobiology* *6*, 294-302.

Sonders, M.S., Zhu, S.J., Zahniser, N.R., Kavanaugh, M.P., and Amara, S.G. (1997). Multiple ionic conductances of the human dopamine transporter: the actions of dopamine and psychostimulants. *J Neurosci* *17*, 960-974.

Sucic, S., and Bryan-Lluka, L.J. (2005). Roles of transmembrane domain 2 and the first intracellular loop in human noradrenaline transporter function: pharmacological and SCAM analysis. *Journal of neurochemistry* *94*, 1620-1630.

Sulzer, D., Sonders, M.S., Poulsen, N.W., and Galli, A. (2005). Mechanisms of neurotransmitter release by amphetamines: a review. *Prog Neurobiol* *75*, 406-433.

Torres, G.E. (2006). The dopamine transporter proteome. *Journal of neurochemistry* *97 Suppl 1*, 3-10.

Vaughan, R.A. (2004). Phosphorylation and regulation of psychostimulant-sensitive neurotransmitter transporters. *The Journal of pharmacology and experimental therapeutics* *310*, 1-7.

Volkow, N.D., Wang, G., Fowler, J.S., Logan, J., Gerasimov, M., Maynard, L., Ding, Y., Gatley, S.J., Gifford, A., and Franceschi, D. (2001). Therapeutic doses of oral methylphenidate significantly increase extracellular dopamine in the human brain. *J Neurosci* *21*, RC121.

Weissman, A., Koe, B.K., and Tenen, S.S. (1966). Antiamphetamine effects following inhibition of tyrosine hydroxylase. *The Journal of pharmacology and experimental therapeutics* *151*, 339-352.

Yamashita, A., Singh, S.K., Kawate, T., Jin, Y., and Gouaux, E. (2005). Crystal structure of a bacterial homologue of Na⁺/Cl⁻-dependent neurotransmitter transporters. *Nature* *437*, 215-223.

Zhao, C., Stolzenberg, S., Gracia, L., Weinstein, H., Noskov, S., and Shi, L. (2012). Ion-controlled conformational dynamics in the outward-open transition from an occluded state of LeuT. *Biophysical journal* *103*, 878-888.

Zhao, Y., Terry, D., Shi, L., Weinstein, H., Blanchard, S.C., and Javitch, J.A. (2010). Single-molecule dynamics of gating in a neurotransmitter transporter homologue. *Nature* *465*, 188-193.

Zhao, Y., Terry, D.S., Shi, L., Quick, M., Weinstein, H., Blanchard, S.C., and Javitch, J.A. (2011). Substrate-modulated gating dynamics in a Na⁺-coupled neurotransmitter transporter homologue. *Nature* 474, 109-113.

Zhou, Z., Zhen, J., Karpowich, N.K., Goetz, R.M., Law, C.J., Reith, M.E., and Wang, D.N. (2007). LeuT-desipramine structure reveals how antidepressants block neurotransmitter reuptake. *Science* (New York, N.Y.) 317, 1390-1393.

Zomot, E., Bendahan, A., Quick, M., Zhao, Y., Javitch, J.A., and Kanner, B.I. (2007). Mechanism of chloride interaction with neurotransmitter:sodium symporters. *Nature* 449, 726-730.

SITE DIRECTED MUTATIONS NEAR TRANSMEMBRANE DOMAIN 1 (TM1)

Chapter 2

ALTER CONFORMATION AND FUNCTION OF NOREPINEPHRINE AND

DOPAMINE TRANSPORTERS

Reprinted with permission of the American Society of Pharmacology and Experimental Therapeutics. All rights reserved.

Copyright © 2011 The American Society for Pharmacology and Experimental Therapeutics
Mol Pharmacol 79:520–532, 2011 *Printed in U.S.A.*

Bipasha Guptaroy, Rheaclare Fraser, Aalisha Desai, Minjia Zhang and Margaret E. Gnegy
Department of Pharmacology, 1150 W. Medical Center Drive, University of Michigan, Ann
Arbor, Michigan 48109 (B.G., R.F., M.Z., A.D. and M.E.G.)

Abbreviations: AMPH, amphetamine; DA, dopamine; hDAT, human dopamine transporter;
hNET, human norepinephrine transporter; HEK, human embryonic kidney cells; KRH, Krebs-
Ringer Hepes buffer; PKC, protein kinase C; PKA, cAMP dependent protein kinase; TM,
transmembrane domain; GBR12935, 1-[2-(diphenylmethoxy)ethyl]-4-(3-phenylpropyl)-
piperazine; IL, intracellular loop; ANOVA, analysis of variance

Abstract

The human dopamine and norepinephrine transporters (hDAT and hNET, respectively) control neurotransmitter levels within the synaptic cleft and are the site of action for amphetamine (AMPH) and cocaine. We investigated the role of a threonine residue within the highly conserved and putative phosphorylation sequence RETW, located just before transmembrane domain 1, in regulating hNET and hDAT function. The Thr residue was mutated to either alanine or aspartate. Similar to the inward facing T62D-hDAT, T58D-hNET demonstrated reduced [³H]DA uptake but enhanced basal DA efflux as compared to hNET with no further effect of AMPH. The mutations had profound effects on substrate function and binding. The potency of substrates to inhibit [³H]DA uptake and compete with radioligand binding was increased in T→A and/or T→D mutants. Substrates, but not inhibitors, demonstrated temperature-sensitive effects of binding. Neither the functional potency nor binding affinity for hNET blockers was altered from wild type in hNET mutants. There was, however, a significant reduction in potency for cocaine and benztropine to inhibit [³H]DA uptake in T62D-hDAT as compared with hDAT. The potency of these drugs to inhibit [³H](–)-2-β-carbomethoxy-3-β-(4-fluorophenyl)tropane-1,5-naphthalenedisulfonate (WIN 35,428) binding was not increased, demonstrating a discordance between functional and binding site effects. Taken together, these results concur with the notion that the T→D mutation in RETW alters the preferred conformation of both hNET and hDAT to favor one that is more inward facing. Although substrate activity and binding are primarily altered in this conformation, the function of inhibitors with distinct structural characteristics may also be affected.

Introduction

The availability of the monoamine neurotransmitters dopamine (DA) and norepinephrine (NE) around the synaptic cleft is regulated by DA and NE transporters (DAT and NET, respectively), which mediate the reuptake of released neurotransmitter into the presynaptic terminal (Amara and Kuhar, 1993; Blakely and Bauman, 2000; Giros and Caron, 1993). Transporter-mediated reuptake terminates the presence of neurotransmitter at the synaptic cleft.

Both DAT and NET are members of the SLC6 Na⁺/Cl⁻ dependent transporter family (Torres et al., 2003). Substrate transport through these proteins is coupled to the concomitant transport of Na⁺ and Cl⁻ ions (Chen and Reith, 2000; Norregaard and Gether, 2001). An alternating access model was proposed to explain the functioning of these transporters, in which the transporter would oscillate between two primary conformations, an “outward-facing” mode accessible to the extracellular medium and an “inward-facing” mode that is open to the intracellular milieu (Rudnick, 1997). According to this model, both substrate and inhibitors bind the transporter when it assumes an outward-facing conformation. Substrates, however, elicit a conformational change that promotes an inward-facing conformation resulting in translocation of substrate along with Na⁺ and Cl⁻ ions.

Monoamine transporters contain 12 transmembrane domains (TM), connecting intracellular and extracellular loops and intracellular amino and carboxyl termini (Torres et al., 2003). The elucidation of the crystal structure of the bacterial leucine transporter (LeuT_{Aa}), a homolog of monoamine transporters, provided insight into the three-dimensional structure of these

transporters (Yamashita et al., 2005). The structure revealed a substrate-occluded state possibly representing a state between the outward- and inward-facing conformations and suggested the existence of important ionic interactions amongst residues in the N-terminus (Arg5), TM8 (Asp369) and TM6 (Tyr206) as part of a network of ionic interactions that could constitute an intracellular “gate” (Singh, 2008; Yamashita et al., 2005). Mutagenesis studies demonstrate similar interactions between corresponding residues in DAT (Arg60 in the N terminus, Asp436 at the end of TM8 and Tyr335 in intracellular loop 3 close to TM6) (Kniazeff et al., 2008). These studies establish that the N-terminal Arg60 (DAT) residue, which is highly conserved in monoamine transporters, plays a critical role in transporter function. Mutations of Tyr335 and Asp436 also have profound impact on DAT conformation and function; specifically, mutation of all of these residues (Arg60, Asp436, and Tyr335) of DAT to Ala appear to promote a conformation (presumably inward-facing) of the transporter in which DA uptake is significantly compromised (Kniazeff et al., 2008; Loland et al., 2004; Loland et al., 2002).

The RETW motif is conserved in all monoamine transporters (residues 60-63 in DAT and 56-59 in NET), and mutations within this motif have robust effects on hDAT function. Mutation of both Arg and Trp, but not Glu, within this motif in hDAT profoundly affects DA uptake (Chen et al., 2001; Kniazeff et al., 2008). In the corresponding sequence (RDTW) in GAT-1, deletion of either Arg44, Thr46, or Trp47 render the transporter totally inactive (Bennett et al., 2000), and only certain substitutions are tolerated. We have demonstrated that mutation of the Thr residue within the RETW motif similarly has profound effect on DAT conformation and function (Guptaroy et al., 2009). Mutation of Thr62 to Asp in DAT resulted in a transporter that favors an

inward-facing conformation, which promotes constitutive efflux of DA from cells and prevents accumulation of internal DA. We now present evidence for a similar, although not identical, effect of the same mutations in the corresponding Thr residue (Thr58) in hNET. These studies further establish the importance of the highly conserved N-terminal residues proximal to TM1 in maintaining monoamine transporter conformations that sustain normal transporter function.

Monoamine transporters are also the target for both therapeutic and abused drugs such as antidepressants, AMPH, and cocaine (Norregaard and Gether, 2001). Mutants of DAT with altered conformational equilibrium are useful tools in binding studies and provide invaluable information about the affinity of structurally diverse transporter inhibitors (Liang et al., 2009; Schmitt et al., 2008). These studies demonstrate that the transporter and ligand conformation determines the interaction between them. In the present study, we used the N-terminal threonine mutants of hDAT (Thr62) and hNET (Thr58) to investigate the effect of various substrates and inhibitors on transport and binding characteristics. We find that in Thr to Asp mutants, which favor an inward-facing conformation, the affinity for both catechol and non-catechol substrates is enhanced and that substrate binding is temperature-dependent. Conversely, these mutations have no appreciable effect on the interaction of the transporters with most inhibitors, with the exception of benztropine and cocaine in hDAT.

Materials and Methods

Mutagenesis and Generation of Stable Cell Lines. The hDAT mutants and cell lines were generated as described previously (Guptaroy et al., 2009). The hNET mutants were generated by

polymerase chain reaction using sense and antisense oligonucleotides and pfu polymerase (Stratagene, La Jolla, CA). After digestion of parental DNA with Dpn I (Promega Corporation, Madison, WI), competent DH5 α cells were transformed with mutagenic DNA. Mutations were confirmed by DNA sequencing and the cDNAs were used to transfect human embryonic kidney 293 cells using Lipofectamine (Invitrogen, Carlsbad, CA). A stable pool of G418-resistant cells was selected and maintained in the presence of 100 μ g/ml G418 in Dulbecco's modified Eagle's medium supplemented with 10% fetal bovine serum, 1% penicillin/streptomycin at 37°C and 5% CO₂.

Surface Biotinylation and Immunoblotting. To label cell surface transporters, cells were treated with sulfosuccinimidyl-2-(biotinamido) ethyl-1, 3-dithiopropionate (sulfo-NHS-SS biotin) (Pierce, Rockford, IL) at 4°C as described previously (Johnson et al., 2005). The reaction was quenched for 15 min with 100 mM glycine at 4°C. Cells were lysed in solubilization buffer (25 mM Tris, 150 mM NaCl, 1 mM EDTA, 5 mM N-ethylmaleimide, 100 μ M phenylmethylsulfonyl fluoride, and 1% Triton X-100) containing protease inhibitors (Roche, Indianapolis, IN) and centrifuged at 20,000g to remove cell debris. Biotinylated proteins in cell lysates containing 800 μ g of protein were bound to 50 μ l streptavidin beads (Pierce) by incubating for 1 hr at room temperature. The beads were washed with solubilization buffer and eluted in 25 μ l SDS-polyacrylamide gel electrophoresis sample buffer containing 100 mM dithiothreitol and resolved by electrophoresis on a 10% Tris-glycine gel along with samples of the lysate. Proteins were transferred to a nitrocellulose membrane (GE Healthcare Chalfont St. Giles, Buckinghamshire, UK) and blocked for 1 hr in 5% milk in 10 mM Tris, pH 7.4, 150 mM

NaCl, and 0.1% Tween 20. hNET was detected using anti-NET (Alpha Diagnostics, San Antonio, TX) and horse radish peroxidase-conjugated secondary antibody (Santa Cruz Biotechnologies Inc, Santa Cruz, CA) by enhanced chemiluminescence reagent (Pierce). Quantification of bands was done by densitometry using Scion Image software (Scion Corporation, Frederick, MD).

[³H]DA Uptake and Competition Assays. Cells were plated on 24-well plates at a density of 100,000 cells per well one day prior to performing the assays. [³H]DA uptake was measured in KRH (25 mM HEPES, pH 7.4, 125 mM NaCl, 4.8 mM KCl, 1.2 mM KH₂PO₄, 1.3 mM CaCl₂, 1.2 mM MgSO₄, and 5.6 mM glucose containing 50 μM pargyline, 1 mM tropolone and 50 μM ascorbic acid) in the absence or presence of 10 μM GBR12935 (Sigma, St. Louis, MO) or 100 μM cocaine. The initial rate of uptake was analyzed using 30 nM to 3 μM [³H]DA (specific activity 59.3 Ci/mmol; PerkinElmer Life and Analytical Sciences, Waltham, MA) for 2 min at room temperature in a final volume of 250 μl. The reaction was stopped by rapidly washing three times with 1 ml of ice cold phosphate-buffered saline. Cells were solubilized in 1% SDS and radioactivity was measured using Scintverse (Thermo Fisher Scientific, Waltham, MA) in a liquid scintillation counter (LS 5801; Beckman Coulter, Fullerton, CA). For competition assays, cells were incubated with [³H]DA for 3 min in the presence of increasing concentrations of competing substrates or inhibitors (Sigma-Aldrich). Cells were preincubated with inhibitors for 10 min before initiating [³H]DA uptake and substrates were added simultaneously with [³H]DA. Non-specific binding was determined in the presence of transporter inhibitors (DAT, 5-10 μM GBR12935 or 100 μM cocaine; NET, 1-3 μM desipramine or 100 μM cocaine). The IC₅₀ values

for uptake inhibition by substrates will represent the K_m for the substrate. In case of inhibitors, the IC_{50} values are close to the K_i values, because 30 nM [3H]DA is far below the K_m for DA.

[3H]DA Efflux. Basal efflux of [3H]DA was measured in cells plated on 12 well plates at a density of 1.5×10^5 cells per well. Cells were loaded for 20 min at room temperature with 1 μM [3H]DA in KRH. After loading, cells were washed rapidly with KRH three times. KRH (500 μl) was added and removed after 5 min for scintillation counting and this was repeated at 10- and 15-min time points. After 15 min, cells were lysed in 1% SDS and counted to determine the amount of [3H]DA remaining in the cells. Cells from a separate well were lysed immediately after loading with [3H]DA to obtain an estimate of the total amount of [3H]DA in the cells at the start of the experiment.

AMPH-stimulated DA Efflux. Confluent 100 mm plates of cells were washed twice with KRH and incubated at 37°C with 15 μM DA for 30 min. Cells were washed with KRH, harvested, and resuspended in 200 μl KRH and 150 μl of the cells were placed on a Whatman GF/B filter (Whatman, Clifton, NJ) in a chamber of a Brandel superfusion apparatus (SF-12; Brandel, Gaithersburg, MD). Superfusion chambers were maintained at room temperature and KRH was perfused at a rate of 400 $\mu l/min$. Samples were collected every 2 min. Following a 45 min wash to reduce baseline, cells received a 2-min bolus of 10 μM *d*-AMPH. Fractions were collected for the next 50 min. Samples were collected into vials containing 25 μl of an internal standard solution (0.05 M $HClO_4$, 4.55 mM dihydrobenzylamine, 1M metabisulfate and 0.1 M EDTA) as described previously (Kantor et al., 2001). Samples were stored at $-80^\circ C$ and DA content was

measured by high pressure liquid chromatography with electrochemical detection. DA efflux was quantified as the peak DA in the eluent.

Binding Assays. Cells were plated on 24-well plates at a density of 10^5 cells per well one day before the experiment. Cells were rinsed with KRH and binding of 4 nM [^3H]-(-)-2- β -carbomethoxy-3- β -(4-fluorophenyl)tropane-1,5-naphthalenedisulfonate (WIN 35,428) (specific activity, 85 Ci/mmol; Life and Analytical Sciences) (hDAT) or 3 nM [^3H]nisoxetine (specific activity 87.2 Ci/mmol; Perkin Elmer, Life and Analytical Sciences) (hNET) was measured in the absence or presence of transporter inhibitors (DAT: 5-10 μM GBR-12935 or 100 μM cocaine; NET: 1-3 μM desipramine or 100 μM cocaine). All assays were performed at the peak time for saturation binding determined previously (30 min for [^3H]WIN 35,428 and 90 min for [^3H]nisoxetine). Reactions were incubated for 30 min or 90 min at room temperature or on ice as indicated. Binding was attenuated by rapidly washing three times with ice-cold phosphate-buffered saline. Cells were solubilized in 1% SDS and counted in a Beckman scintillation counter using Scintverse. In competition assays, the indicated concentrations of substrates or inhibitors were used during incubations. For K_d determination, cells were incubated with increasing concentrations of [^3H]WIN 35,428 (1-100 nM) for hDAT and [^3H]nisoxetine (1-30 nM) for hNET and processed as described above. K_i values reported in the legends of Tables 2-3 and 2-4 were determined from the Cheng-Prusoff correction in GraphPad Prism using the IC_{50} values (listed in tables) and radioligand K_d values (given in the Results text).

Statistical Analysis. Kinetic constants, including K_m , V_{max} and IC_{50} values for the transporter constructs were determined by nonlinear regression analysis of the mean values for each mutant using GraphPad Prism version 5 (GraphPad Software, San Diego, CA). Statistical significance was determined using GraphPad Prism version 5 either by comparison to wild type using a 2-way ANOVA with posttest Bonferroni analysis or with an *F*-test by comparing fits in which selected values were constrained to be equal or were allowed to differ. The null hypothesis was that the best fit parameter for the value did not differ. A conclusion of statistical significance represents a rejection of the null hypothesis and indicates a difference between designated values. Values plus the 95% confidence levels are reported. In most cases, the *F*-distributions are reported in the tables and figure legends to maintain flow in the text.

Results

Surface Expression and DA Uptake in hNET and Mutant Transporters. Both T58A-hNET and T58D-hNET express in the cell at levels equivalent to hNET, but traffic less efficiently to the cell surface as compared to hNET. As shown in Figure 2-1A, total transporter levels in the lysate on a protein basis were the same for all three transporters but the amount of surface transporter was reduced in T58A-hNET and T58D-hNET (Figure 2-1A). A quantitative representation of the amount of surface transporter as fold of hNET demonstrated that T58A-hNET is expressed on the surface at 60% and T58D-hDAT at 50% of the level of hNET (Figure 2-1B, $n = 7$).

Inward transport through the hNET mutants was determined by measuring [³H]DA uptake. Using [³H]DA is valid because the NET can transport both NE and DA. In fact, NET has greater affinity for DA than NE and greater V_{\max} values for DA uptake as compared to NE (Eshleman et al., 1999; Gu et al., 1994). In view of this preference of NET for DA we used [³H]DA transport to understand the properties of substrate transport in the hNET constructs. Other mutants of NET have been characterized based on their DA transport properties (Danek Burgess and Justice, 1999).

[³H]DA uptake velocities for the hNET constructs were determined from the initial rates calculated from time course curves at varying concentrations of [³H]DA. Values were normalized to surface expression of hNET. The data in Figure 2-1C show that T58D-hNET cells had a dramatically reduced V_{\max} as compared with hNET ($p < 0.05$). There was a similar significant reduction of the V_{\max} for [³H]DA uptake in T62D-hDAT as compared to hDAT (Table 2-1) (Guptaroy et al., 2009). On the contrary, there was a significant increase in the normalized (corrected for surface expression) V_{\max} value for [³H]DA uptake in T58A-hNET (1.3 pmol per 10^5 cells per min) as compared to hNET (0.76 pmol per 10^5 cells per min, $p < 0.0003$). This is in contrast to the corresponding hDAT mutant T62A-hDAT (Guptaroy et al., 2009), in which the V_{\max} value was significantly lower than that of hDAT (Table 2-1). In hNET, therefore, the mutation of Thr58 to Ala or to Asp has opposing effects on [³H]DA uptake. These results demonstrate that although the Asp mutation of the corresponding threonine residues in hDAT and hNET similarly affects DA uptake, the Ala mutation has a differential effect on [³H]DA uptake properties of hDAT and hNET. There was no significant difference in the K_m

values for [³H]DA uptake amongst hNET, T58A-hNET and T58D-hNET (Table 2-1). In keeping with previous reports (Gu et al., 1994) we also observe a greater affinity for [³H]DA in hNET (K_m , 0.23 μ M) compared to hDAT (K_m , 2.2 μ M) ($p < 0.002$). The difference between K_m values for [³H]DA uptake between T62A-hDAT and T58A-hNET or between T62D-hDAT and T58D-hNET were reduced or negated, demonstrating that mutation of the threonine counteracted structural differences between hDAT and hNET in affinity for [³H]DA. The V_{max} for T58A-hNET, however, was more than 3 times that for T62A-hDAT ($p < 0.0001$).

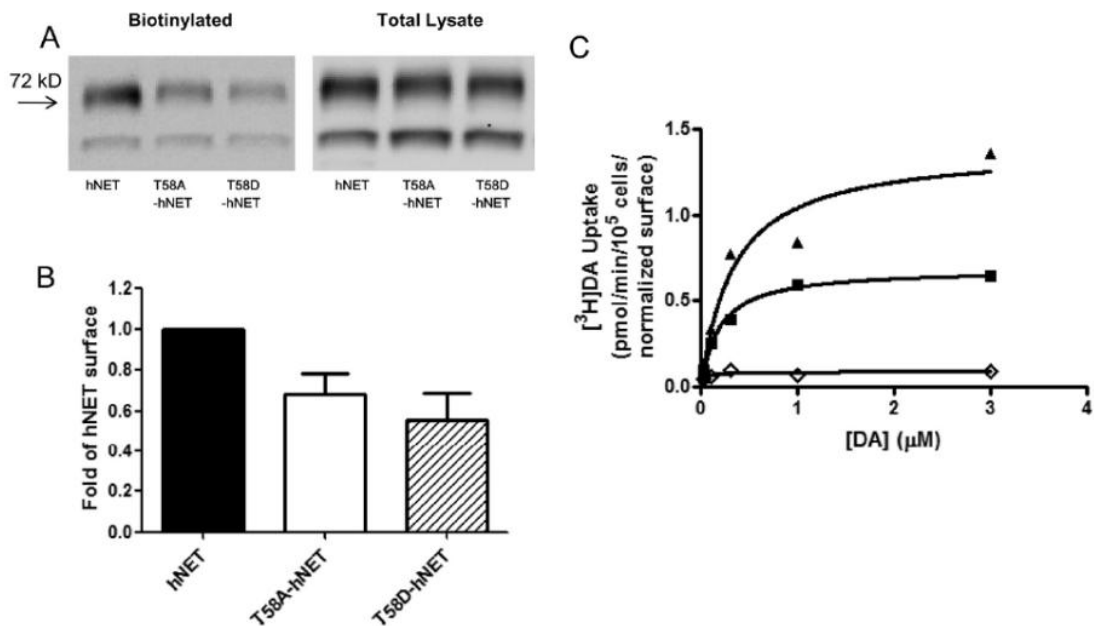


Figure 2-1. Surface expression and [³H]DA uptake in hNET and hNET-T58 mutants. Cell surface expression of hNET, T58A-hNET, or T58D-hNET was analyzed by biotinylation as described under *Materials and Methods*. A representative Western blot (A) and quantitation of surface transporter compared with hNET (B) are shown. Data represent mean \pm S.E.M, $n = 7$. C, [³H]DA uptake ($n = 3$) was calculated in hNET (■), T58A-hNET (▲), and T58D-hNET (◇) by measuring initial rates at increasing concentrations of [³H]DA as described under *Materials and Methods*.

Table 2-1. Kinetic properties of [³H]DA uptake in hNET, hDAT, and threonine mutants K_m and V_{max} values were determined by nonlinear regression using Prism.

The V_{max} values from this analysis were normalized to wild-type surface expression and are shown as mean \pm S.E.M. Statistical significance was determined using Prism F test by comparing fits in which selected values were constrained to be equal or were allowed to differ. The null hypothesis was that the best-fit parameter for the value did not differ. A conclusion of statistical significance represents a rejection of the null hypothesis and indicates a difference between designated values. Comparison of V_{max} values within hNET: hNET vs. T58A-hNET, $P < 0.001$, $F_{1,26} = 17.21$; hNET vs. T58D-hNET, $P < 0.05$, $F_{1,26} = 5.347$. Comparison of V_{max} values within hDAT: hDAT vs. T62A-hDAT, $P < 0.01$, $F_{1,57} = 7.097$; hDAT vs. T62D-hDAT, $P < 0.05$, $F_{1,64} = 4.920$.

	V_{max}	K_m
	<i>pmol / 10⁵ cells / min</i>	μM
hNET	0.76 (0.68–0.86)	0.23 (0.14–0.32)
T58A-hNET	1.3 (1.1–1.6)***	0.32 (0.10–0.53)
T58D-hNET	0.13 (0.07–0.19)*	0.12 (0.0–0.36)
hDAT ^a	0.82 (0.40–1.24)	2.2 (0.08–4.2)
T62A-hDAT ^a	0.38 (0.31–0.46)**	0.8 (0.35–1.25)
T62D-hDAT ^a	0.07 (0.052–0.094)*	0.17 (0.0–0.38)

^a Data from Guptaroy et al. (2009).

* $P < 0.05$.

** $P < 0.01$.

*** $P < 0.001$.

Basal Efflux Is Elevated in the T58D-hNET Mutant. Because the transporter basically functions as a pump in forward and reverse transport modes, a reduction in substrate uptake (as seen in T58D-hNET) could be due to an increase in DA efflux. In order to evaluate this possibility for the T58D-hNET mutant, cells were loaded with [³H]DA for 20 min at room temperature and rapidly washed. Efflux of [³H]DA was measured every 5 min for 15 min as described under *Materials and Methods*. In Figure 2-2A, basal efflux of [³H]DA is expressed as percentage of the total amount of [³H]DA present in the cells after the 20 min DA loading period. This representation of the data is independent of the variable surface expression because both the uptake and the efflux in each cell type depend on the number of surface transporters. The initial

DA content in the cells after the loading period in units of counts per minute per 10^5 cells was: $21,649 \pm 809$ for hNET, $19,062 \pm 486$ for T58A-hNET and $6,364 \pm 726$ for T58A-hDAT ($n = 3$). The basal efflux of [^3H]DA in the 5-min fraction in T58D-hNET was significantly greater than in either hNET or T58A-hNET cells (two-way ANOVA, $p < 0.001$). This efflux reached a level comparable to hNET and T58A-hNET by 10 min. These results suggest that the greatly reduced V_{max} of DA uptake in T58D-hNET cells is due to an increase in basal DA efflux that prevents the accumulation of intracellular DA, similar to our results reported with T62D-hDAT (Guptaroy et al., 2009). For T62D-hDAT this property was attributed to a preference for a more inward-facing conformation. In view of the similarity in characteristics of [^3H]DA uptake and basal [^3H]DA efflux between T62D-hDAT and T58D-hNET, it is reasonable to postulate that the underlying mechanism leading to this phenotype is the same in both these mutant transporters, supporting the conclusion that T58D-hNET, like T62D-hDAT, is predominantly inward-facing.

AMPH-Stimulated DA Efflux Is Reduced in T58A-hNET. AMPH-stimulated DA efflux was measured in T58A-hNET and hNET at a single AMPH concentration ($10 \mu\text{M}$) using a superfusion protocol. Following loading with unlabeled DA, cells were placed in a superfusion apparatus, and DA efflux in response to $10 \mu\text{M}$ AMPH was measured. To eliminate variability due to uneven loading, data were calculated as fractional DA efflux, which is the amount of DA in the effluent as a percentage of the total amount of DA originally present in the cells. As shown in Figure 2-2B, in T58A-hNET cells there was significantly less AMPH-stimulated DA efflux as compared to hNET. The fact that DA influx was enhanced but the responsiveness to AMPH was reduced in T58A-hNET as compared to hNET, suggests that mutation of T58 to Ala may elicit a

conformation that is slow to transition back to outward-facing. On the contrary, the T58D-hNET mutant was completely unresponsive to AMPH (data not shown). As demonstrated in the data in Figure 2-2A, the baseline efflux was elevated in T58D-hNET compared with hNET and T58A-hNET, but there was no response to AMPH.

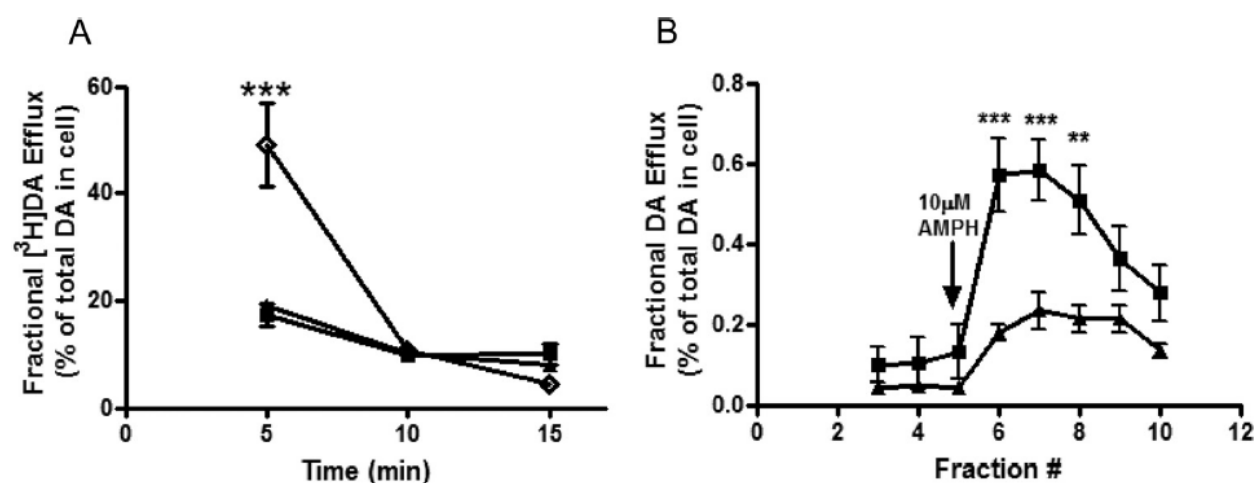


Figure 2-2. Functional DA efflux properties of hNET mutants. **A**, cells were loaded with 5 μM [^3H]DA for 20 min at room temperature and washed with KRH. Basal efflux was measured in hNET (■), T58A-hNET (▲), and T58D-hNET (◇) as described under Materials and Methods. Efflux is expressed as the percentage of total [^3H]DA present in the cell at the start of the experiment ($n = 3$). In a two-way ANOVA considering time and mutants, $p < 0.001$ for time, $p < 0.01$ for mutants, and $p < 0.001$ for interaction between time and mutants. In Bonferroni post-test, ***, $p < 0.001$ for hNET or T58A-hNET compared with T58D-hNET. **B**, AMPH-stimulated DA efflux was assessed by superfusion of the cells as described under *Materials and Methods*. Cells were loaded with DA, washed with KRH for 30 min, and then challenged with AMPH for 2 min. Fractions (800 μl) were collected, and DA content was analyzed by high-performance liquid chromatography and electrochemical detection. Data are expressed as DA concentration in each fraction as a percentage of total amount of DA taken up in the cells ($n = 4$). In a two-way ANOVA comparing time with mutants, $p < 0.0001$ for time, $p < 0.01$ for mutants, and $p < 0.001$ for interaction between time and mutants. In Bonferroni post-test, ***, $p < 0.001$; **, $p < 0.01$.

The IC_{50} for Inhibition of [^3H]DA uptake by Substrates Is Decreased in Thr mutants.

Mutants with altered conformational equilibrium interact differentially with substrates and inhibitors (Chen et al., 2001; Chen et al., 2004b; Liang et al., 2009; Loland et al., 2008; Loland et

al., 2002; Schmitt et al., 2008). We examined the effect of the mutations on the potency for substrates and inhibitors to functionally inhibit [³H]DA uptake. As shown in Figure 2-3, mutation of Thr-58 in hNET to Asp increases the affinity for both catechol (Figure 2-3A, DA, and Figure 2-3B, NE) and non-catechol substrates (Figure 2-3C, AMPH), as demonstrated by a leftward shift of the competition curve. Accordingly, the IC₅₀ values were significantly lower for DA, NE, and AMPH in T58D-hNET as compared to hNET. The IC₅₀ values, 95% confidence intervals (CI), and F-distribution showing significant differences are given in Table 2-2. Mutation of Thr58 to Ala in hNET similarly increased the potency of DA and AMPH in inhibiting [³H]DA uptake but not to the same extent as for the T→D mutation (T58A-hNET versus T58D-hNET for DA, *p* < 0.0001; for AMPH, *p* < 0.0001). A similar increase in affinity for all three substrates was observed in T62D-hDAT (Figure 2-3C & D and Table 2-2) compared with hDAT. As with Thr58 in hNET, mutation of Thr62 in hDAT to Ala increased the potency for DA and AMPH but not to same degree as the T→D mutation (T62A-hDAT versus T62D-hDAT for DA, *p* < 0.05; for AMPH, *p* < 0.0001). Furthermore, the preference for AMPH over DA is lost in the T58D-hNET mutants and greatly reduced in the T62D-hDAT mutants as compared with wild type. The potency of NE, however, was not significantly changed by a Thr-to-Ala mutation in either hNET or hDAT.

In contrast to the change in IC₅₀ values for DA uptake, the mutations have no effect on the sensitivity of inhibitors to block [³H]DA transport in hNET mutants. IC₅₀ values for cocaine, benztropine, nisoxetine, and desipramine did not significantly differ amongst hNET, T58A-hNET and T58D-hNET (Table 2-2). On the contrary, the potency of cocaine and benztropine to

inhibit [³H]DA uptake was reduced in T62D-hDAT compared with hDAT. Both drugs are more selective for hDAT than for hNET. The potencies of cocaine and benztropine were reduced in T62D-hDAT as compared with wild type, but they were able to completely block the [³H]DA uptake. The potency of GBR12935, a highly selective DAT inhibitor of a different structural class, was unaltered by mutation of Thr62 to Asp. A Thr to Ala mutation did not change potency for any inhibitor in either hNET or hDAT. Therefore, mutation of Thr to Asp or Thr to Ala within the RETW sequence of hDAT or hNET disrupted the functional activity of the transporter substrates much more than the transporter inhibitors.

The IC₅₀ values of the inhibitors for hNET reported here are higher than some reported values (Eshleman et al., 1999; Han and Gu, 2006; Owens et al., 1997) but similar to others (Mortensen and Amara, 2006). This could be attributed to differences in assay conditions and cell lines (Han and Gu, 2006). Passage number and expression level in transfected cells caused variability in the inhibition potency of cocaine for DA uptake (Chen and Reith, 2007; Ukairo et al., 2007). The use of [³H]DA as opposed to [³H]NE as substrate might have affected the IC₅₀ values. In contrast, the IC₅₀ for inhibition of binding (Table 2-3, Table 2-4) were comparable with values reported previously (Reith et al., 2005), possibly because of the similarity of the assay condition and reagents used.

NET

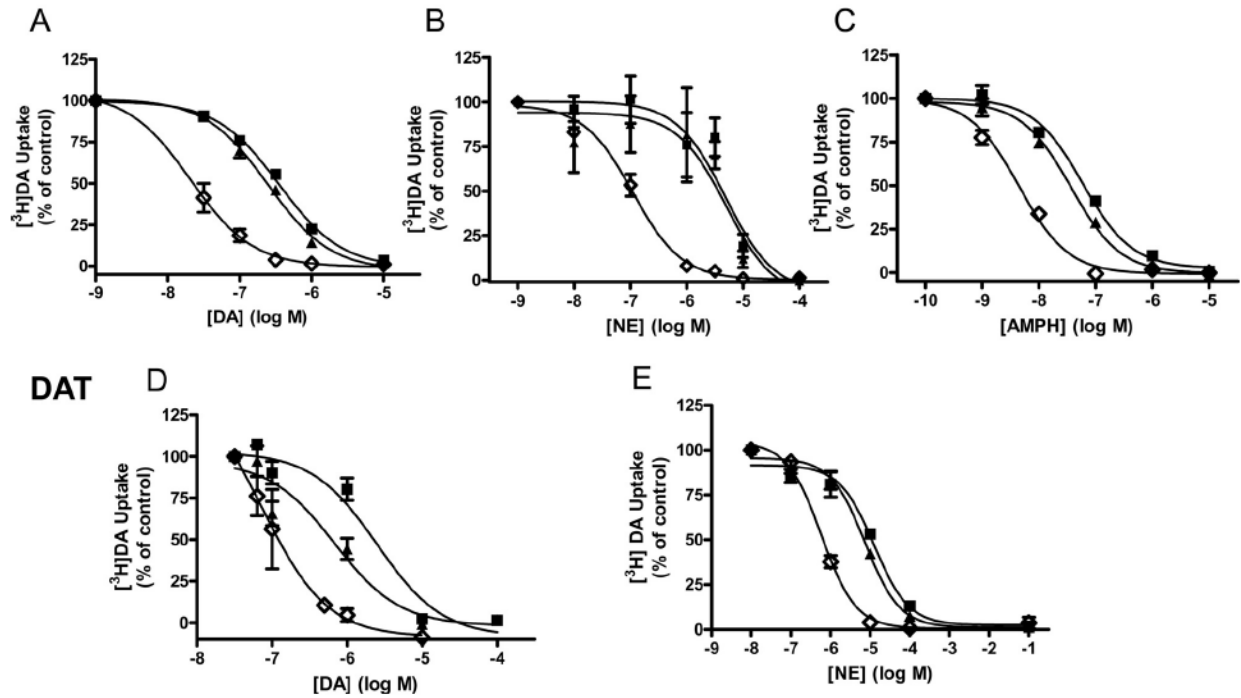


Figure 2-3. Mutation of Thr88 (hNET) and Thr62 (hDAT) to aspartate results in enhanced substrate potency. DA transport was measured in hNET (■), T58A-hNET (▲), and T58D-hNET (◇) cells in the presence of increasing concentration of DA (A), NE (B), and AMPH (C) and in hDAT (■), T62A-hDAT (▲), and T62D-hDAT (◇) cells in the presence of increasing concentrations of DA (D) and NE (E). Cells were incubated with 30 nM [³H]DA and indicated concentrations of competing substrate for 3 min at room temperature and processed as described under *Materials and Methods*. Data are expressed as percentage of [³H]DA uptake in the absence of any added substrate (control). IC₅₀ values, 95% confidence intervals, and statistical analysis of the results are given in Table 2-2.

Table 2-2. Potency for substrates and inhibitors in inhibiting [³H]DA uptake in hNET and hDAT mutants.

Data were calculated as a percentage of uptake in the absence of competing substrate or inhibitor and analyzed by nonlinear regression. Data displayed in the table are IC₅₀ values with confidence intervals (CI) given in parentheses (n = 3–6). Statistical significance was determined by an *F* test by comparing fits in which selected values were constrained to be equal or were allowed to differ. The null hypothesis was that the best-fit parameter for the value did not differ. A conclusion of statistical significance represents a rejection of the null hypothesis and indicates a difference between designated values

	hNET	T58A-hNET	T58D-hNET	hDAT	T62A-hDAT	T62D-hDAT
	<i>nM</i>					
Substrates						
DA (n = 3)	340 (280–410)	230* (180–300) <i>F</i> _{1,30} = 4.694	6*** (2–20) <i>F</i> _{1,30} = 206.6	2510 (1250–5000)	680* (270–1700) <i>F</i> _{1,29} = 6.544	54*** (18–160) <i>F</i> _{1,29} = 50.77
NE (n = 3)	550 (350–850)	370 (140–900)	70*** (50–90) <i>F</i> _{1,30} = 63.95	12,600 (7900–20,000)	7500 (5500–10,000)	590*** (460–760) <i>F</i> _{1,30} = 128.1
AMPH (hNET, n = 3; hDAT, n = 6)	59 (43–82)	37* (28–48) <i>F</i> _{1,30} = 4.80	5*** (3.4–5.9) <i>F</i> _{1,30} = 140.4	310 (270–350)	130** (120–150) <i>F</i> _{1,30} = 11.93	12*** (9–17) <i>F</i> _{1,30} = 62.33
Inhibitors						
Cocaine (hNET, n = 3; hDAT, n = 6)	3970 (2000–7900)	3180 (1470–6880)	6240 (3500–11,300)	260 (130–510)	300 (180–510)	1130** (540–2400) <i>F</i> _{1,64} = 9.261
Benztropine (hNET, n = 3; hDAT, n = 6)	3730 (2060–6750)	4760 (2250–10,000)	9250 (3600–23,300)	140 (65–310)	170 (120–250)	1240*** (540–2800) <i>F</i> _{1,64} = 19.86
Nisoxetine (n = 3)	32 (20–50)	30 (13–73)	16 (6–40)	N.D.	N.D.	N.D.
Desipramine (n = 3)	19 (12–30)	15 (8–29)	12 (8–17)	N.D.	N.D.	N.D.
GBR12935 (n = 6)	N.D.	N.D.	N.D.	105 (81–135)	109 (51–231)	191 (90–388)

* *P* < 0.05 compared with wild-type value.

** *P* < 0.01 compared with wild-type value.

*** *P* < 0.001 compared with wild-type value.

The Affinity of Substrates, but Not Inhibitors, for Binding to hNET or hDAT Is Increased

in Thr mutants. To determine if Thr58 contributes to the binding of substrates and inhibitors, we tested substrate and inhibitor competition of whole cell [³H]nisoxetine binding to NET and its mutants. When the binding assays were performed at room temperature, as were the [³H]DA uptake assays, the pattern of change in affinity of substrates mirrored that of the [³H]DA uptake studies. There was no change in *K*_d for [³H]nisoxetine among the three mutants. The *K*_d values for hNET (n = 3), T58A-hNET (n = 5), and T58D-hNET (n = 5) were 3.3 ± 1, 4.6 ± 0.6, and 7.0 ± 1 nM (± S.E.M), respectively. As shown in Table 2-3, the affinities of DA (*p* < 0.01) and

AMPH ($p < 0.02$) for T58D-hNET were significantly greater than that for hNET. There was no change in affinity for NE in T58D-hNET, but there was a reduction in the fraction of [^3H]nisoxetine binding sites that the catecholamine could access. In hNET, 18% (95% CI, 7.9-27) of the total [^3H]nisoxetine binding sites were inaccessible to maximal concentrations of NE as compared to 45% (95% CI, 34-55) of the total binding sites in T58D-hNET ($p < 0.005$, $F_{1,30} = 15.16$). There was no significant change in affinity for DA or AMPH at T58A-hNET as compared with hNET. As shown in the lower panels of Table 2-3, there was no change in potency for any inhibitor measured, including desipramine, for T58A-hNET or T58D-hNET as compared to hNET.

A similar result was seen with the Thr-62 mutations in hDAT (Table 2-4). The affinity for both DA ($p < 0.0001$) and AMPH ($p < 0.001$) to compete for [^3H]WIN 35,428 binding was greatly increased in T62D-hDAT as compared with hDAT. Moreover, the potency of DA ($p < 0.01$) and AMPH ($p < 0.002$) was significantly increased in T62A-hDAT as compared to hDAT. These data mirror the effects of the hDAT mutations on inhibitory potency for [^3H]DA uptake, signaling that the substrate binding site is close to, if not identical, with the substrate transport site. As shown in Table 2-4, there was no change in affinity of GBR12935 or benztropine to compete for [^3H]WIN 35,428 binding to hDAT, T62A-hDAT or T62D-hDAT. The K_d for hDAT, T62A-hDAT, and T62D-hDAT are 16 ± 2 , 10 ± 1 , and 7 ± 1 nM (\pm S.E.M), respectively ($n = 3$). There was, however, an increase in affinity for binding of cocaine to T62D-hDAT ($p < 0.02$), in contrast to the reduction in potency for cocaine to block [^3H]DA uptake.

Table 2-3. Affinity for substrates and inhibitors in competing for [³H]nisoxetine binding in hNET mutants.

Data were calculated as a percent of total [³H]nisoxetine binding in the absence of competing substrate or inhibitor and analyzed by nonlinear regression. Data displayed in the table are IC₅₀ values with confidence intervals (CI) given within parenthesis. The number of experiments (n) is given under the ligand. Statistical significance was determined by an *F* test by comparing fits in which selected values were constrained to be equal or were allowed to differ. The null hypothesis was that the best fit parameter for the value did not differ. A conclusion of statistical significance represents a rejection of the null hypothesis and indicates a difference between designated values. *F* test values and degrees of freedom are given only in cases of statistical differences.

The Ki (nM) values (with CI) at RT for WT-, T58A-, and T58D-hNET are as follows: DA – 275 (105-719), 237 (68-851), and 25 (20-302); NE – 161 (73-357), 451 (319-636), and 99 (20-488); AMPH – 95 (31-296), 62 (23-163), and 11 (3.7-33); cocaine – 588 (201-1718), 1017 (480-2154), and 940 (291-3040); desipramine – 5.4 (3.1-9.4), 7.4 (3.9-13.9), and 4.0 (0.82-19); bntropine – 1726 (1195-2492), 2474 (1589-3852), and 3494 (1294-9435).

The Ki (nM) values (with CI) at 4°C for WT-, T58A-, and T58D-hNET are as follows: DA – 238 (108-526), 64 (37-111), and 30 (2.2-417); NE – 327 (113-945), 306 (127-739), and N.S.; AMPH – 0.9 (0.53-1.8), 2.6 (1.9-3.7), and 2.9 (1.1-7.9); cocaine – 532 (420-674), 866 (355-2110), and 809 (137-4765); desipramine – 11.4 (8.8-14.7), 8.8 (6.6-11.8), and 20.7 (5.9-73.2).

Ligands	IC ₅₀ (95% CI)					
	Room Temperature			4°C		
	hNET	T58A-hNET	T58D-hNET	hNET	T58A-hNET	T58D-hNET
	<i>nM</i>					
Substrates						
DA (n = 3)	490 (230–1000)	370 (140–1000)	35* (3–430) <i>F</i> _{1,23} = 7.474*	384 (170–850)	89*† (52–160) <i>F</i> _{1,30} = 6.845* <i>F</i> _{1,26} = 4.958†	44* (3–60) <i>F</i> _{1,20} = 4.814**
NE (RT, n = 3) (4°C, n = 6)	308 (139–681)	745* (527–1051) <i>F</i> _{1,30} = 5.287*	141 (28–697)	527 (182–1524)	427 (177–1031)	N.S.
AMPH (RT, n = 3) (4°C, n = 6)	182 (58–565)	102 (39–270)	16* (5.2–47) <i>F</i> _{1,30} = 6.703*	2.7††† (1.5–4.7) <i>F</i> _{1,63} = 31.64†††	4.6††† (3.4–6.3) <i>F</i> _{1,63} = 39.03†††	5.3 (2.2–12)
Inhibitors						
Cocaine	1122 (383–3280)	1680 (793–3960)	1340 (416–4340)	858 (678–1080)	1208 (496–2943)	1171 (200–6900)
Desipramine	10 (5.9–18)	12 (6.2–23)	6 (1.2–27)	18 (14–23)	12 (9–16)	18 (5–67)
Bntropine	3290 (2280–4760)	4088 (2626–6365)	4990 (1848–13,480)	N.D.	N.D.	N.D.

N.S., no significant binding.

* *P* < 0.05 compared with wild-type value.

** *P* < 0.01 compared with wild-type value.

*** *P* < 0.001 compared with wild-type value.

† *P* < 0.05 compared with values at RT.

†† *P* < 0.01 compared with values at RT.

††† *P* < 0.001 compared with values at RT.

Table 2-4. Affinity for substrates and inhibitors in competing for [³H]WIN 35,428 binding in hDAT mutants.

Data were calculated as a percent of total [³H]WIN 35,428 binding in the absence of competing substrate or inhibitor and analyzed by nonlinear regression. Data displayed in the table are IC₅₀ values with confidence intervals (CI) given within parenthesis. The number of experiments (n) is given under the ligand. Statistical significance was determined by an *F*-test by comparing fits in which selected values were constrained to be equal or were allowed to differ. The null hypothesis was that the best fit parameter for the value did not differ. A conclusion of statistical significance represents a rejection of the null hypothesis and indicates a difference between designated values. *F*-test values and degrees of freedom are given only in cases of statistical differences.

The Ki (nM) values (with CI) at RT for WT-, T62A-, and T62D-hNET are as follows: DA – 1064 (598-1892), 332 (201-547), and 6.8 (1.9-246); AMPH – 311 (161-601), 44 (23-85), and 5.2 (2.8-9.6); cocaine – ambiguous fit for all cell types; benztropine – 50 (31-83), 71 (28-181), and 104 (52-207); GBR12935 – ambiguous fit for all cell types.

The Ki (nM) values (with CI) at 4°C for WT-, T62A-, and T62D-hNET are as follows: DA – 61 (20-185), 13 (6.5-25), and 6.7 (1.4-31); AMPH – 94 (49-183), 12 (4.8-29), and 71 (1.9-2630); AMPH + Zn²⁺ – 412 (216-784), 46 (32-66), and 8 (2.2-29).

Ligands	IC ₅₀ (95% CI)					
	Room Temperature			4°C		
	hDAT	T62A-hDAT	T62D-hDAT	hDAT	T62A-hDAT	T62D-hDAT
	<i>nM</i>					
Substrates						
DA (n = 3)	1300 (75–2370)	460** (280–760) <i>F</i> _{1,30} = 8.176**	11*** (3.2–43) <i>F</i> _{1,30} = 37.92***	73 ^{††} (24–220) <i>F</i> _{1,30} = 15.21 ^{††}	17 ^{†††} (9–34) <i>F</i> _{1,30} = 43.45 ^{†††}	10 (2.2–49)
AMPH (RT, n = 3)	390 (200–750)	62** (32–120) <i>F</i> _{1,30} = 11.93**	8*** (4–15) <i>F</i> _{1,30} = 63.33***	113 [†] (60–220) <i>F</i> _{1,30} = 5.380 [†]	16 [†] (6–38) <i>F</i> _{1,30} = 5.513 [†]	110 (4.9–4100)
AMPH + 100 μM Zn ²⁺ (n = 3)				494 [‡] (260–940) <i>F</i> _{1,30} = 7.108 [‡]	61 ^{‡‡} (43–88) <i>F</i> _{1,30} = 8.476 ^{‡‡}	13 (3–45)
Inhibitors						
Cocaine (n = 3)	222 (120–410)	205 (98–430)	46* (16–130) <i>F</i> _{1,30} = 6.127*	N.D.	N.D.	N.D.
Benztropine (n = 3)	63 (38–100)	99 (39–253)	160 (100–486)	N.D.	N.D.	N.D.
GBR12935 (n = 3)	50 (20–130)	125 (56–280)	113 (45–290)	N.D.	N.D.	N.D.

N.D., not determined.

* *P* < 0.05 compared with wild-type value.

** *P* < 0.01 compared with wild-type value.

*** *P* < 0.001 compared with wild-type value.

† *P* < 0.05 compared with values at RT.

†† *P* < 0.01 compared with values at RT.

††† *P* < 0.001 compared with values at RT.

‡ *P* < 0.05 compared with values at 4°C.

‡‡ *P* < 0.01 compared with values at 4°C.

The Affinity and Extent of Substrate Binding in T58D-hNET is Sensitive to Temperature.

In some experiments, we performed [³H]nisoxetine binding assays on ice as described (Distelmaier et al., 2004) and found notable differences in binding characteristics when the assays were conducted at 4° versus room temperature. The K_d values for [³H]nisoxetine binding in hNET, T58A-hNET, and T58D-hNET at 4° were 4.9 ± 1 , 7.6 ± 0.7 , and 6.7 ± 1 nM (\pm S.E.M), respectively. These values were not different from each other and were not different from those measured at room temperature. The IC_{50} s for DA and NE in hNET were comparable and unchanged when measured at the two temperatures (Table 2-3), but the apparent affinity for AMPH was over 60-fold greater when assayed at 4°C (3 nM) as compared to room temperature (182 nM). The 95% confidence intervals and *F*-distributions for all IC_{50} values are given in Table 2-3. In the T58A-hNET cells, the IC_{50} values for DA and AMPH were significantly reduced at 4°C as compared with RT, but there was no change in potency for NE. IC_{50} values for DA and AMPH competition of [³H]nisoxetine binding in T58A-hNET cells at RT vs 4°C were for DA, 370 versus 89 nM, respectively, $p < 0.05$; for AMPH, 100 versus 5 nM, respectively, $p < 0.0001$. Striking changes in competition for [³H]nisoxetine binding to T58D-hNET were noted for all substrates between the two temperatures. The affinity for DA in T58D-hNET at 4°C was not significantly changed from that measured at RT, but there was a striking change in the accessibility of the [³H]nisoxetine sites for which DA could compete. Access of all three substrates to all of the sites labeled with [³H]nisoxetine in T58D-hNET cells was restricted (shown for AMPH in Figure 2-4). DA could compete for only 30% of the [³H]nisoxetine binding sites at 4°C as compared with RT and AMPH competed for only 41%. In

T58D-hNET cells, the percent unbound for DA in competing for [³H]nisoxetine sites is 43% (95% CI, 25-61) at RT versus 70% at 4°C (96% CI, 65-75) ($p < 0.002$, $F_{1,24} = 12.03$). The percentage unbound for AMPH at RT is 35% (95% CI, 26-42) versus 59% (95% CI, 54-64) at 4°C ($p < 0.0001$, $F_{1,63} = 23.73$). In hNET and T58A-hNET, AMPH competed for more than 80% of the [³H]nisoxetine binding sites at 4°C, demonstrating that T58D-hNET was most severely compromised at the low temperature (Figure 2-4). NE was unable to compete for [³H]nisoxetine binding sites in T58D-hNET at any concentration (Table 2-3). In contrast to the sensitivity of substrate competition for temperature, there was no change in either potency or extent of competition for [³H]nisoxetine binding for the inhibitors desipramine or cocaine, at RT versus 4°C.

We examined whether substrate competition for [³H]WIN 35,428 binding in hDAT was similarly temperature sensitive. The K_d values for [³H]WIN 35,428 binding in the hDAT mutants at 4°C were not different from one another and were not different from those measured at room temperature. The K_d values for [³H]WIN 35,428 binding in hDAT, T62A-hDAT, and T62D-hDAT at 4° were 20 ± 3 , 12 ± 4 , and 7 ± 4 nM (\pm S.E.M), respectively. As shown in Table 2-4 and Figure 2-5, the affinity for DA and AMPH was increased in both hDAT and T62A-hDAT when [³H]WIN 35,428 binding was measured at 4°C as compared with RT. The IC_{50} value for DA competition for [³H]WIN 35,428 binding in hDAT was 1.3 μ M at RT versus 73 nM at 4°C ($p < 0.0005$) and in T62A-hDAT was 460 nM versus 17 nM at 4°C ($p < 0.05$). The IC_{50} value for AMPH competition for [³H]WIN 35,428 binding in hDAT was 390 nM at RT versus 113 nM at 4°C ($p < 0.05$). The binding curves are shown in Figure 2-5, and the 95% confidence limits

and *F*-distributions for these values are given in Table 2-4. The affinity of DA for [³H]WIN 35,428 binding in T62D-hDAT was already very high and was not changed at 4°C. The affinity of AMPH for T62D-hDAT at 4°C is compromised by the sharply reduced accessibility of AMPH, similar to that seen with hNET. DA accessed 84% [16% unbound (95% CI, 4.7-28)] of the [³H]WIN 35,428 binding sites in T62D-hDAT at RT but accessed only 53% [47% unbound (95% CI, 39-55)] of the sites at 4°C (*p* < 0.0001 *F*_{1,29} = 22.48). Likewise, AMPH accessed 73% [27% unbound (95% CI, 21-33)] of the total [³H]WIN 35,428 binding sites in T62D-hDAT at RT but could access only 29% (95% CI, 58-84)) of [³H]WIN35,428 binding sites at 4°C (*p* < 0.05 *F*_{1,45} = 5.158). These data suggest that at 4°C the transporter favors a conformation that can readily accommodate binding of inhibitors, but not substrates.

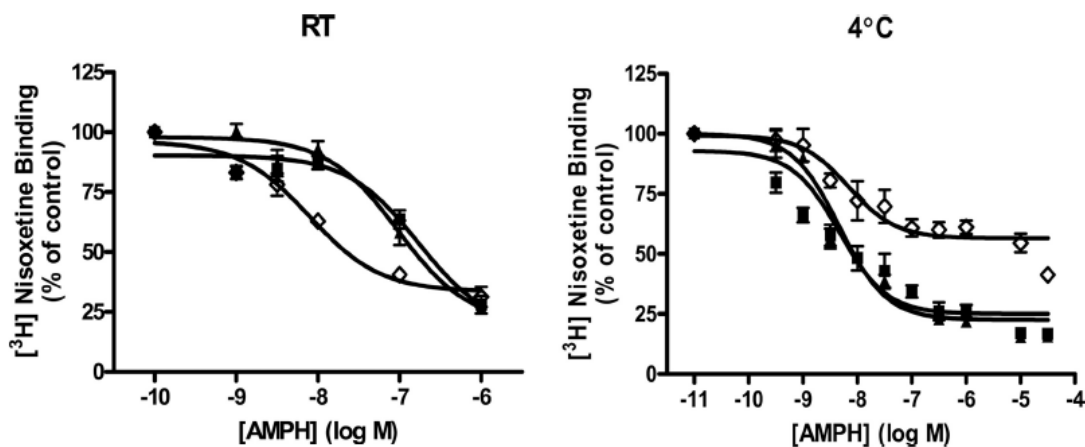


Figure 2-4. At 4°C, the accessibility of AMPH to [³H]nisoxetine binding sites is reduced in T58D-hNET compared with binding at room temperature (RT). hNET (■), T58A-hNET (▲), and T58D-hNET (◇) cells were incubated with 3 nM [³H]nisoxetine and indicated concentrations of AMPH (0–30 μM) for 90 min at ambient temperature (RT) or 30 min at 4°C. Data (n = 3–9) are calculated as [³H]nisoxetine binding in the presence of different concentrations of AMPH and expressed as a percentage of binding in the absence of AMPH (control). IC₅₀ values and statistical values are given in Table 2-3 and text.

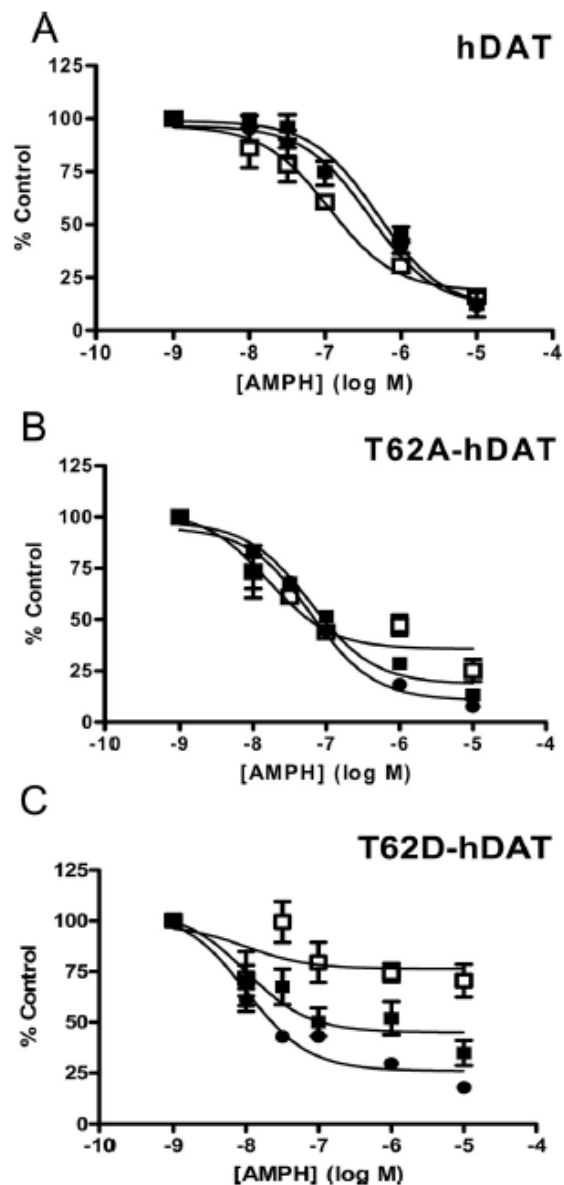


Figure 2-5. Temperature-dependent changes in competition of AMPH for $[^3\text{H}]$ WIN 35,428 binding to hDAT mutants are reversed by addition of Zn^{2+} . The hDAT (A) T62A-hDAT (B), and T62D-hDAT (C) cells were incubated with 4 nM $[^3\text{H}]$ WIN 35,428 at room temperature (●), on ice (□), or on ice in the presence of 100 μM Zn^{2+} (■). Data ($n = 3-9$) are shown as a percentage of $[^3\text{H}]$ WIN 35,428 bound in the absence of any AMPH (control) at the given concentrations of AMPH (0–10 μM). IC_{50} values, bottom-of-curve values, and statistical analyses are given in Table 2-3 and text.

Zn²⁺ Rescues Substrate Binding at Low Temperature in T62D-hDAT. The effect of conformation on transporter activity can be examined in DAT due to its sensitivity to the ion, Zn²⁺. DAT, as opposed to NET, contains three residues in its extracellular loops that coordinately bind Zn²⁺ (Norregaard et al., 1998). Upon binding to DAT, Zn²⁺ potentiates an uncoupled Cl⁻ conductance in DAT, which modulates the membrane potential such that DA uptake is restricted and DA efflux is enhanced (Meinild et al., 2004). In the presence of Zn²⁺, the equilibria of mutant transporters that appear predominantly inward-facing, in which DA uptake is compromised, are shifted toward a more outward-facing conformation, resulting in enhanced DA uptake (Chen et al., 2004a; Guptaroy et al., 2009; Loland et al., 2002). We examined whether Zn²⁺ would shift the equilibrium of substrate binding at 4°C to more resemble the potency and availability for substrates to bind at RT. As shown in Figure 2-5 and Table 2-4, the potency of AMPH for [³H]WIN 35,428 binding to hDAT was increased 3-fold when assayed on ice, but when 100 μM Zn²⁺ was present at 4°C, the curve was identical to that assayed at RT. The IC₅₀ for AMPH at 4°C + Zn²⁺ was 494 nM (95% CI, 26-94) as compared to 113 nM (95% CI, 6-22) at 4°C (p < 0.02). When the T62A-hDAT mutant was measured at 4°C, there was a significant reduction in the IC₅₀ for AMPH but also a significant reduction in the percentage of binding sites accessed (11% unbound at RT (95% CI, 0.8-20) versus 36% unbound at 4°C (95% CI, 31-47), p < 0.0004 F_{1,29} = 15.74). As seen in Figure 2-5B, addition of Zn²⁺ at 4°C restored the potency of AMPH in T62A-hDAT cells to RT levels [IC₅₀ at 4°C + Zn²⁺, 61 nM (95% CI, 43-88); p < 0.01 compared to 4°C] and enhanced the accessibility of AMPH to [³H]WIN 35,428 binding sites [percentage unbound at 4°C + Zn²⁺, 19% (95% CI, 13-23); p < 0.002, F_{1,29} = 11.95

as compared to 4°C]. As shown in Figure 2-5C, the dramatic reduction in the ability of AMPH to access [³H]WIN 35,428 in T62D-hDAT cells was corrected when 100 μM Zn²⁺ was included at 4°C. Inclusion of 100 μM Zn²⁺ in the assay significantly restored the accessibility of AMPH to [³H]WIN 35,428 sites (4°C + Zn²⁺, 44% unbound; p < 0.05, F_{1,46} = 4.233). Zn²⁺ also appeared to restore the potency of AMPH to match that attained at RT but the difference in IC₅₀ values between 4°C and 4°C + Zn²⁺ [IC₅₀, 13 nM (95% CI 3-45)] was not statistically significant due to the variability in binding at 4°C.

Benztropine and Cocaine Interact Differentially with T62D-hDAT. Examination of the data in Table 2-2 and Table 2-3 reveal that, for assays conducted at RT, there is a strong concordance in IC₅₀ values for inhibition of [³H]DA uptake with the IC₅₀ values obtained for competition of radioligand binding. This is true for substrates and generally true for inhibitors with the exception of the effects of cocaine and benztropine at T62D-hDAT. The IC₅₀ values for cocaine and benztropine in inhibiting [³H]DA uptake at T62D-hDAT was increased, showing a reduction in potency as compared to hDAT (Table 2-2). On the other hand, this reduction in potency as compared to hDAT was not exhibited when cocaine and benztropine competed for [³H]WIN 35,428 binding. For these drugs there is discordance between their effectiveness in inhibiting DA uptake and their ability to bind to T62D-hDAT. This is seen clearly in Figure 2-6, in which the dose response curves for inhibition of [³H]DA uptake in hDAT and T62D-hDAT are compared for those for competition with [³H]WIN 35,428 binding. The IC₅₀ for benztropine inhibition of [³H]DA in hDAT (126 nM; 95% CI, 58-271) does not differ from that of the IC₅₀ for [³H]WIN 35,428 binding competition (65 nM; 95% CI, 35-107). On the contrary, in T62D-

hDAT cells the IC₅₀ for benztropine in inhibiting [³H]DA uptake (851 nM; 95% CI 514-1411) is significantly greater than that for competition of [³H]WIN 35,428 binding (163 nM; 95% CI 81-325, p < 0.002). Likewise, in hDAT cells, the IC₅₀ for blockade of [³H]DA uptake by cocaine (253 nM; 95% CI 127-505) is the same as that for competition for [³H]WIN35,428 binding (223 nM; 95% CI 121-411). In T62D-hDAT cells, the difference between inhibitory potency and binding potency for cocaine is greater than that for benztropine, primarily due to an enhancement in binding potency for cocaine as compared to wild type. The IC₅₀ for cocaine in inhibiting [³H]DA uptake in T62D-hDAT cells (1130 nM (95% CI 536-2380)) is significantly greater than the IC₅₀ for competing with [³H]WIN 35,428 (48 nM, (95% CI, 17-133), p < 0.0001).

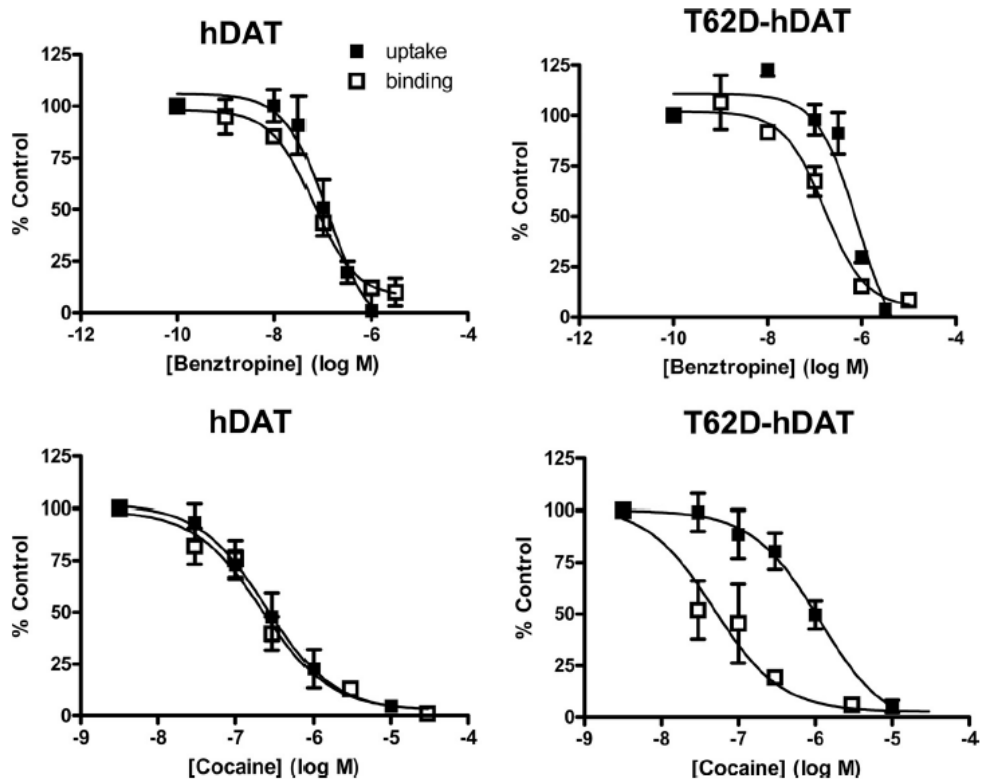


Figure 2-6. Dissociation of benztropine and cocaine potencies for [³H]DA uptake and competition for [³H]WIN 35,428 binding T62D-hDAT cells. Dose-response curves representing potency of benztropine (top) and cocaine (bottom) for inhibition of [³H]DA uptake (■) and competition for [³H]WIN35,428 binding (□) binding in hDAT (left) and T62D-hDAT cells (right). The assays were conducted as described under *Materials and Methods*. Data (n = 3–12) are shown as percentage of value in the absence of benztropine or cocaine (control). IC₅₀ values are given in Table 2-2 and Table 2-3. Statistical comparisons of IC₅₀ values for inhibition of DA uptake versus [³H]WIN 35,428 competition in T62D-hDAT: for benztropine, p < 0.002, F_{1,52} = 11.65; for cocaine, p < 0.0001, F_{1,47} = 18.33. For both cocaine and benztropine in hDAT, p > 0.3.

Discussion

The bidirectional transport of substrates through monoamine transporters and their interaction with therapeutic and abused psychostimulant drugs is conformation-dependent. Emerging evidence indicates that interactions between specific transporter residues are critically important for maintaining relevant conformations and, when disrupted by mutations, impact transporter function. Here we show that mutations in a conserved N-terminal threonine residue of DAT and NET, alters transporter conformation and function.

The juxtamembrane threonine residue (T62 in DAT, T58 in NET) resides in the RETW motif which is a putative phosphorylation site for protein kinase C/A/G, although phosphorylation at this site has not yet been shown. We demonstrated that mutations that mimic the phosphorylation state of this threonine residue have profound effects on the conformation and function of DAT (Guptaroy et al., 2009). This intracellular threonine residue is not part of the substrate-binding site and presumably affects the permeation pathway indirectly through its effect on the interaction of critical residues. An elegant study exploring the nature of the conformational changes associated with substrate transport in LeuT_{Aa} demonstrated that movement of the amino acid residue at position 7 of the N-terminal is associated with opening and closing of the inward gate (Zhao et al., 2010). In LeuT_{Aa} the histidine residue at position 7 in the REHW motif corresponds to the threonine residue in RETW of DAT and NET and could potentially be critical in intracellular gating in monoamine transporters. In addition, these residues are adjacent to those involved in a conserved interaction network at the intracellular gate, which in DAT includes Val259 and Tyr335 (Kniazeff et al., 2008). Using molecular dynamic simulation, we

demonstrated that a mutation at Thr62 in hDAT disrupts its interaction with Lys260, which is adjacent to Val259, and consequently affects the interaction between Val259 and Tyr335 (Guptaroy et al., 2009). The greater structural disruption of the aspartate mutant as compared with the alanine mutant was reflected in their functional activities. The data suggested that T62D-hDAT preferred an inward-facing conformation. We now demonstrate that corresponding mutations in NET result in similar but not identical phenotypes, although the overall conformational changes are probably similar. Differences could be due the inherent dissimilarities between the two structures. It is suggested that both alanine and aspartate mutants of the homologous threonine residue in the serotonin, DA, and NE transporters promote an inward facing conformation and lack AMPH-stimulated efflux (Sucic et al., 2010). Though our data for the aspartate mutants in DAT and NET agree with these findings, we have consistently detected AMPH-stimulated DA efflux in the alanine mutants, although to a lesser extent than in the wild-type transporter. The reduced efflux in T58A-hDAT could be due to a slow outward transition rate, resulting in a conformation that could be more inward-facing than that of hNET. However, the overall nature of interaction of substrates and inhibitors with the alanine mutants remained similar to the wild type transporter, leading us to conclude that the conformation of the alanine mutants of hDAT and hNET retains similarity to the wild-type transporter.

DA influx activity diverges between DAT and NET in the alanine mutants, although efflux properties are similar. In T62A-hDAT, both influx and AMPH-stimulated efflux of DA were reduced, and this was attributed to a slowing of the transition between the inward and outward states of the transporter (Guptaroy et al., 2009). In contrast, in T58A-hNET we see opposing

effects on DA influx (increased) and efflux (reduced). The rate of inward and outward transition might also be affected in T58A-hNET. The N-terminal domains of DAT and NET have low homology and are of dissimilar lengths, which could contribute to differences between the uptake characteristics of T62A-hDAT and T58A-hNET. The alanine mutation may affect the interaction of diverse proteins with hDAT and hNET or differentially affect the interaction with the same protein.

In both hNET and hDAT, the aspartate mutation increased the potency for DA and AMPH to inhibit [³H]DA uptake and compete for radioligand binding. The alanine mutation behaved similarly, except for substrate binding in hNET. The general concordance of potency in function and binding suggests that the conformation elicited by either the Ala or Asp mutations increases the affinity for substrates at their binding site. An increase in accessibility of the substrates is unlikely because the substrate potency for transporter binding was enhanced at 4°C, but accessibility to the binding sites was often reduced. Nor is it likely that there is a defect in reorientation of the DA-transporter complex to an outward-facing form, which would kinetically result in an increased potency for substrates (Chen et al., 2004a), because basal efflux of [³H]DA was enhanced in both T58D-hNET (Figure 2-2A) and T62D-hDAT (Guptaroy et al., 2009). The apparent affinity for substrates was also increased in Y335A-hDAT and D345N-hDAT, which are postulated to prefer a predominantly inward-facing conformation (Chen et al., 2004a; Chen et al., 2001; Loland et al., 2002). Increases in functional and binding potencies were most notable for AMPH. Potency for NE was only enhanced for inhibition of [³H]DA uptake in the aspartate mutants compared to wild-type transporter. Some of these disparities could result from structural

variations of the substrates. Because of the benzene-diol and the α -hydroxy side chain group, NE would have more points of attachment within the binding pocket than would AMPH (Indarte et al., 2008). Fewer required attachment points for the non-catechol AMPH may permit the substrate to more easily attain an energetically favorable ligand pose within the binding pocket.

The effect of conformational restriction on substrate binding was further demonstrated by measurement of radioligand binding at 4°C. At 4°C, the conformation of hNET or hDAT was restricted into one resembling an inward-facing conformation, because the potency of substrates, especially AMPH, was significantly increased as compared with RT values. The mobility of the aspartate mutants was severely compromised such that substrates could not access all [³H]radioligand binding sites, but inhibitor binding was unaffected. The restoration of AMPH's access to [³H]WIN 35,428 binding sites in hDAT as well as the reduction of AMPH's binding potency to RT values by Zn²⁺ strongly indicates a limited mobility of an inward-facing conformation of hDAT at 4°C. Indeed in D345N-hDAT, Zn²⁺ stimulated [³H]WIN 35,428 binding by countering the defect in outward reorientation of the transporter (Chen et al., 2004a). However, a reduced potency for DA was observed at 4°C by Bonnet et al. (1990), but this study was performed in rat striatal membranes. No temperature-dependent difference was observed in the K_i for DA binding in hDAT-transfected human embryonic kidney 293 cells (Chen et al., 2001) but we saw no difference in the K_i for hNET. The reason for the increased potency for substrates at 4°C is unclear but is under investigation.

The threonine mutations affected substrates more strongly than tested inhibitors (Figure 2-7), with the exception of cocaine and benztropine effects on hDAT. In particular, there was no effect of the mutations on the function or binding of desipramine or nisoxetine in hNET or on GBR12935 in hDAT. The structure of LeuT_{Aa} suggests a separation in substrate and some inhibitor binding in transporter proteins (Singh, 2008). Within LeuT_{Aa}, a secondary binding site located extracellularly to the substrate binding site (Shi et al., 2008) serves as a vestibule for binding antidepressants (Singh et al., 2007; Zhou et al., 2007). On the basis of these results, homology-based molecular modeling identified two putative binding pockets in NET and DAT: one which binds cocaine and corresponds to the leucine binding site and another similar to the clomipramine binding site in LeuT_{Aa} (Ravna et al., 2009). Interaction between residues further into the lipid bilayer in TM1 are predicted to be altered in the interaction with tricyclic antidepressants including desipramine (Henry et al., 2007) and may not be as severely affected by these threonine mutations.

The modification of the substrate binding site in the threonine mutants may account for the altered activity of benztropine and cocaine in the aspartate mutants. Molecular modeling of DAT suggests that the binding sites of DA, AMPH, cocaine, and benztropine-like drugs overlap and correspond to the substrate binding site in LeuT_{Aa} that is distinct from the antidepressant binding pocket (Beuming et al., 2008). These drugs are weak inhibitors at hNET, so their binding to hNET may not have been affected by the aspartate mutation. The impaired ability of cocaine and other inhibitors to inhibit DA uptake in Y335A-DAT was attributed to its shift to an inward-facing conformation (Loland et al., 2002) and the prevailing notion that cocaine binds to

and stabilizes transporters in their outward-facing conformation (Chen and Justice, 1998; Loland et al., 2004). Other inward-facing mutants of hDAT (D345N, D436A, and K264A) show similar but less dramatic decreases in the inhibitory potency of cocaine (Chen et al., 2004a; Loland et al., 2004). Our data suggest that cocaine and benztropine bind normally to T62D-hDAT but have a reduced potency in inhibiting DA uptake. There is, therefore, discordance between inhibitor radioligand binding and function. A lack of correlation has been observed previously in cocaine potency for inhibition of uptake and binding in wild-type DAT (Wang et al., 2003). It cannot be excluded that disruption of the normal translocation cycle in mutant transporters causes uptake and binding affinities to diverge. These results support the notion that the DAT conformation responsible for inhibitor high-affinity binding is less responsible for DA uptake (Wang et al., 2003). In some DAT mutants, cocaine and benztropine interactions differ (Chen et al., 2004b; Loland et al., 2008; Schmitt et al., 2008; Ukairo et al., 2005). Because both cocaine and benztropine compounds contain tropane rings, the altered conformation of T62D-hDAT may affect side-chain associations with this ring structure. It is unclear why the binding potency of cocaine is increased in T62D-hDAT. It could be that T62D-hDAT rapidly oscillates between inward and outward states—a condition supported by its enhanced basal efflux, which is contingent upon the transporter more readily assuming an outward conformation.

The above evidence strongly argues for a critical role of the highly conserved threonine residue in the juxtamembrane N-terminal domain of monoamine transporters in determining transporter conformation and functions such as substrate binding, permeation, reverse transport, and drug interactions.

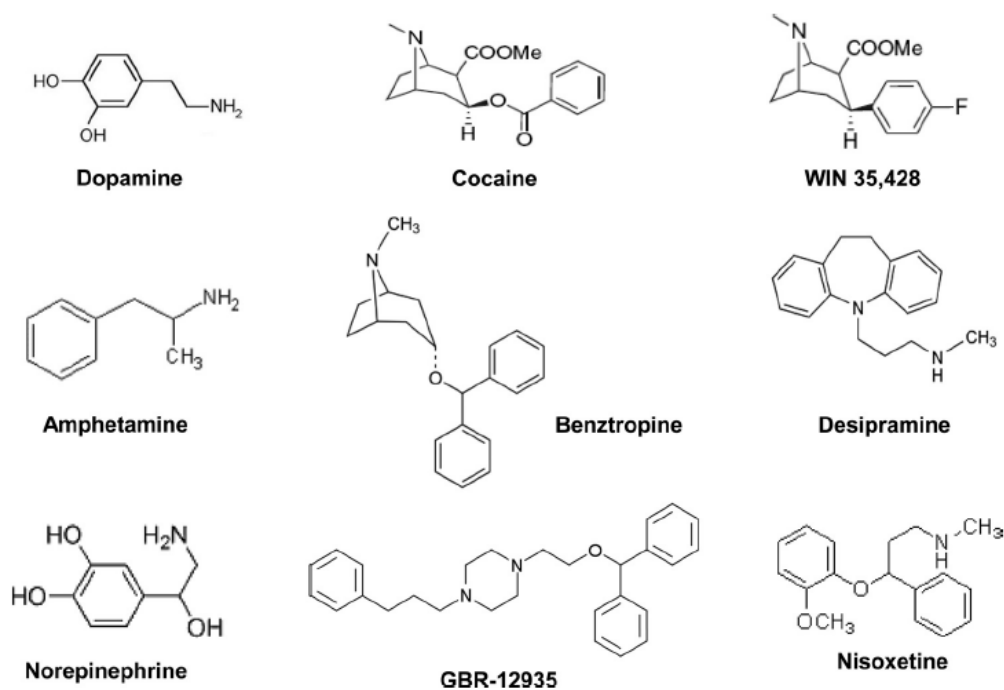


Figure 2-7. Chemical structure of substrates and inhibitors. These include substrates dopamine, norepinephrine, and amphetamine and inhibitors cocaine and the cocaine analog WIN 35,428, benztropine, GBR-12935, desipramine, and nisoxetine.

Acknowledgements

We thank Dr. Randy D. Blakely for providing us with hNET cDNA and Dr. Jonathan A. Javitch for the FLAG-hDAT cDNA. Benztropine was generously provided by Dr. A. K. Dutta, Department of Pharmaceutical Sciences, Wayne State University. We thank Hobart Ng Ng Tsai for technical assistance.

References

Amara, S.G., and Kuhar, M.J. (1993). Neurotransmitter transporters: recent progress. *Annu Rev Neurosci* *16*, 73-93.

Bennett, E.R., Su, H., and Kanner, B.I. (2000). Mutation of arginine 44 of GAT-1, a (Na⁺) + Cl⁻)-coupled gamma-aminobutyric acid transporter from rat brain, impairs net flux but not exchange. *The Journal of biological chemistry* *275*, 34106-34113.

Beuming, T., Kniazeff, J., Bergmann, M.L., Shi, L., Gracia, L., Raniszewska, K., Newman, A.H., Javitch, J.A., Weinstein, H., Gether, U., *et al.* (2008). The binding sites for cocaine and dopamine in the dopamine transporter overlap. *Nature neuroscience* *11*, 780-789.

Blakely, R.D., and Bauman, A.L. (2000). Biogenic amine transporters: regulation in flux. *Current opinion in neurobiology* *10*, 328-336.

Bonnet, J.J., Benmansour, S., Costentin, J., Parker, E.M., and Cubeddu, L.X. (1990). Thermodynamic analyses of the binding of substrates and uptake inhibitors on the neuronal carrier of dopamine labeled with [3H]GBR 12783 or [3H]mazindol. *The Journal of pharmacology and experimental therapeutics* *253*, 1206-1214.

Chen, N., and Justice, J.B., Jr. (1998). Cocaine acts as an apparent competitive inhibitor at the outward-facing conformation of the human norepinephrine transporter: kinetic analysis of inward and outward transport. *J Neurosci* *18*, 10257-10268.

Chen, N., and Reith, M.E. (2000). Structure and function of the dopamine transporter. *European journal of pharmacology* *405*, 329-339.

Chen, N., and Reith, M.E. (2007). Substrates and inhibitors display different sensitivity to expression level of the dopamine transporter in heterologously expressing cells. *Journal of neurochemistry* *101*, 377-388.

Chen, N., Rickey, J., Berfield, J.L., and Reith, M.E. (2004a). Aspartate 345 of the dopamine transporter is critical for conformational changes in substrate translocation and cocaine binding. *The Journal of biological chemistry* *279*, 5508-5519.

Chen, N., Vaughan, R.A., and Reith, M.E. (2001). The role of conserved tryptophan and acidic residues in the human dopamine transporter as characterized by site-directed mutagenesis. *Journal of neurochemistry* 77, 1116-1127.

Chen, N., Zhen, J., and Reith, M.E. (2004b). Mutation of Trp84 and Asp313 of the dopamine transporter reveals similar mode of binding interaction for GBR12909 and benztropine as opposed to cocaine. *Journal of neurochemistry* 89, 853-864.

Danek Burgess, K.S., and Justice, J.B., Jr. (1999). Effects of serine mutations in transmembrane domain 7 of the human norepinephrine transporter on substrate binding and transport. *Journal of neurochemistry* 73, 656-664.

Distelmaier, F., Wiedemann, P., Bruss, M., and Bonisch, H. (2004). Functional importance of the C-terminus of the human norepinephrine transporter. *Journal of neurochemistry* 91, 537-546.

Eshleman, A.J., Carmolli, M., Cumbay, M., Martens, C.R., Neve, K.A., and Janowsky, A. (1999). Characteristics of drug interactions with recombinant biogenic amine transporters expressed in the same cell type. *The Journal of pharmacology and experimental therapeutics* 289, 877-885.

Giros, B., and Caron, M.G. (1993). Molecular characterization of the dopamine transporter. *Trends in pharmacological sciences* 14, 43-49.

Gu, H., Wall, S.C., and Rudnick, G. (1994). Stable expression of biogenic amine transporters reveals differences in inhibitor sensitivity, kinetics, and ion dependence. *The Journal of biological chemistry* 269, 7124-7130.

Guptaroy, B., Zhang, M., Bowton, E., Binda, F., Shi, L., Weinstein, H., Galli, A., Javitch, J.A., Neubig, R.R., and Gnegy, M.E. (2009). A juxtamembrane mutation in the N terminus of the dopamine transporter induces preference for an inward-facing conformation. *Molecular pharmacology* 75, 514-524.

Han, D.D., and Gu, H.H. (2006). Comparison of the monoamine transporters from human and mouse in their sensitivities to psychostimulant drugs. *BMC pharmacology* 6, 6.

Henry, L.K., Meiler, J., and Blakely, R.D. (2007). Bound to be different: neurotransmitter transporters meet their bacterial cousins. *Mol Interv* 7, 306-309.

Indarte, M., Madura, J.D., and Surratt, C.K. (2008). Dopamine transporter comparative molecular modeling and binding site prediction using the LeuT(Aa) leucine transporter as a template. *Proteins* 70, 1033-1046.

Johnson, L.A., Furman, C.A., Zhang, M., Guptaroy, B., and Gnegy, M.E. (2005). Rapid delivery of the dopamine transporter to the plasmalemmal membrane upon amphetamine stimulation. *Neuropharmacology* 49, 750-758.

Kantor, L., Hewlett, G.H., Park, Y.H., Richardson-Burns, S.M., Mellon, M.J., and Gnegy, M.E. (2001). Protein kinase C and intracellular calcium are required for amphetamine-mediated dopamine release via the norepinephrine transporter in undifferentiated PC12 cells. *The Journal of pharmacology and experimental therapeutics* 297, 1016-1024.

Kniazeff, J., Shi, L., Loland, C.J., Javitch, J.A., Weinstein, H., and Gether, U. (2008). An intracellular interaction network regulates conformational transitions in the dopamine transporter. *The Journal of biological chemistry* 283, 17691-17701.

Liang, Y.J., Zhen, J., Chen, N., and Reith, M.E. (2009). Interaction of catechol and non-catechol substrates with externally or internally facing dopamine transporters. *Journal of neurochemistry* 109, 981-994.

Loland, C.J., Desai, R.I., Zou, M.F., Cao, J., Grundt, P., Gerstbrein, K., Sitte, H.H., Newman, A.H., Katz, J.L., and Gether, U. (2008). Relationship between conformational changes in the dopamine transporter and cocaine-like subjective effects of uptake inhibitors. *Molecular pharmacology* 73, 813-823.

Loland, C.J., Granas, C., Javitch, J.A., and Gether, U. (2004). Identification of intracellular residues in the dopamine transporter critical for regulation of transporter conformation and cocaine binding. *The Journal of biological chemistry* 279, 3228-3238.

Loland, C.J., Norregaard, L., Litman, T., and Gether, U. (2002). Generation of an activating Zn(2+) switch in the dopamine transporter: mutation of an intracellular tyrosine constitutively

alters the conformational equilibrium of the transport cycle. *Proceedings of the National Academy of Sciences of the United States of America* 99, 1683-1688.

Meinild, A.K., Sitte, H.H., and Gether, U. (2004). Zinc potentiates an uncoupled anion conductance associated with the dopamine transporter. *The Journal of biological chemistry* 279, 49671-49679.

Mortensen, O.V., and Amara, S.G. (2006). Gain of function mutants reveal sites important for the interaction of the atypical inhibitors benztropine and bupropion with monoamine transporters. *Journal of neurochemistry* 98, 1531-1540.

Norregaard, L., Frederiksen, D., Nielsen, E.O., and Gether, U. (1998). Delineation of an endogenous zinc-binding site in the human dopamine transporter. *The EMBO journal* 17, 4266-4273.

Norregaard, L., and Gether, U. (2001). The monoamine neurotransmitter transporters: structure, conformational changes and molecular gating. *Curr Opin Drug Discov Devel* 4, 591-601.

Owens, M.J., Morgan, W.N., Plott, S.J., and Nemeroff, C.B. (1997). Neurotransmitter receptor and transporter binding profile of antidepressants and their metabolites. *The Journal of pharmacology and experimental therapeutics* 283, 1305-1322.

Ravna, A.W., Sylte, I., and Dahl, S.G. (2009). Structure and localisation of drug binding sites on neurotransmitter transporters. *J Mol Model* 15, 1155-1164.

Reith, M.E., Wang, L.C., and Dutta, A.K. (2005). Pharmacological profile of radioligand binding to the norepinephrine transporter: instances of poor indication of functional activity. *Journal of neuroscience methods* 143, 87-94.

Rudnick, G. (1997). Mechanism of biogenic amine neurotransmitter transporters. In *Neurotransmitter Transporters: Structure, Function and Regulation*, M.E. Reith, ed. (New Jersey).

Schmitt, K.C., Zhen, J., Kharkar, P., Mishra, M., Chen, N., Dutta, A.K., and Reith, M.E. (2008). Interaction of cocaine-, benztropine-, and GBR12909-like compounds with wild-type and mutant

human dopamine transporters: molecular features that differentially determine antagonist-binding properties. *Journal of neurochemistry* 107, 928-940.

Shi, L., Quick, M., Zhao, Y., Weinstein, H., and Javitch, J.A. (2008). The mechanism of a neurotransmitter:sodium symporter--inward release of Na⁺ and substrate is triggered by substrate in a second binding site. *Molecular cell* 30, 667-677.

Singh, S.K. (2008). LeuT: A prokaryotic stepping stone on the way to a eukaryotic neurotransmitter transporter structure. *Channels (Austin)* 2.

Singh, S.K., Yamashita, A., and Gouaux, E. (2007). Antidepressant binding site in a bacterial homologue of neurotransmitter transporters. *Nature* 448, 952-956.

Sucic, S., Dallinger, S., Zdrzil, B., Weissensteiner, R., Jorgensen, T.N., Holy, M., Kudlacek, O., Seidel, S., Cha, J.H., Gether, U., *et al.* (2010). The N terminus of monoamine transporters is a lever required for the action of amphetamines. *The Journal of biological chemistry* 285, 10924-10938.

Torres, G.E., Gainetdinov, R.R., and Caron, M.G. (2003). Plasma membrane monoamine transporters: structure, regulation and function. *Nat Rev Neurosci* 4, 13-25.

Ukairo, O.T., Bondi, C.D., Newman, A.H., Kulkarni, S.S., Kozikowski, A.P., Pan, S., and Surratt, C.K. (2005). Recognition of benztrapine by the dopamine transporter (DAT) differs from that of the classical dopamine uptake inhibitors cocaine, methylphenidate, and mazindol as a function of a DAT transmembrane 1 aspartic acid residue. *The Journal of pharmacology and experimental therapeutics* 314, 575-583.

Ukairo, O.T., Ramanujapuram, S., and Surratt, C.K. (2007). Fluctuation of the dopamine uptake inhibition potency of cocaine, but not amphetamine, at mammalian cells expressing the dopamine transporter. *Brain research* 1131, 68-76.

Wang, W., Sonders, M.S., Ukairo, O.T., Scott, H., Kloetzel, M.K., and Surratt, C.K. (2003). Dissociation of high-affinity cocaine analog binding and dopamine uptake inhibition at the dopamine transporter. *Molecular pharmacology* 64, 430-439.

Yamashita, A., Singh, S.K., Kawate, T., Jin, Y., and Gouaux, E. (2005). Crystal structure of a bacterial homologue of Na⁺/Cl⁻-dependent neurotransmitter transporters. *Nature* 437, 215-223.

Zhao, Y., Terry, D., Shi, L., Weinstein, H., Blanchard, S.C., and Javitch, J.A. (2010). Single-molecule dynamics of gating in a neurotransmitter transporter homologue. *Nature* 465, 188-193.

Zhou, Z., Zhen, J., Karpowich, N.K., Goetz, R.M., Law, C.J., Reith, M.E., and Wang, D.N. (2007). LeuT-desipramine structure reveals how antidepressants block neurotransmitter reuptake. *Science* (New York, N.Y.) 317, 1390-1393.

**AN N-TERMINAL THREONINE MUTATION PRODUCES AN EFFLUX FAVORABLE,
Chapter 3
SODIUM-PRIMED CONFORMATION OF THE HUMAN DOPAMINE
TRANSPORTER**

Abstract

The dopamine transporter (DAT), a protein integral for clearing extracellular dopamine (DA), translocates DA between extracellular and intracellular environments through a series of conformational transitions. Mutagenesis of Thr 62, a residue adjacent to transmembrane 1a, to alanine (T62A) or aspartate (T62D) revealed that T62D-hDAT partitions in a predominately inward facing conformation, while T62A-hDAT functions more similarly to wild type (WT)-hDAT. Compared to WT, T62D-hDAT exhibited reduced [³H]DA uptake, enhanced baseline DA efflux and no efflux in response to amphetamine (AMPH). Here, we further investigate the basis of the mutants' altered function with respect to substrate uptake, membrane conductance and Na⁺ requirements. Confocal microscopy experiments reveal identical intracellular accumulation of the fluorescent DAT substrate, ASP⁺, in WT-, T62A- and T62D-hDAT-HEK293 cells. In the absence of substrate, identical membrane polarization was demonstrated in *Xenopus* oocytes expressing the T62 mutants. However, substrate-induced inward currents were present in oocytes transfected with WT and T62A-, but not T62D-hDAT. Replacement of extracellular sodium (Na⁺_e) was used to evaluate shifts in the sodium gradient facilitation of DAT transport functions. The EC₅₀ for Na⁺_e stimulation of [³H] DA uptake was identical in all

three constructs expressed in HEK-293 cells. As expected, decreasing $[Na^+]_e$ stimulated $[^3H]DA$ efflux in WT and T62A-hDAT cells. Conversely, the enhanced $[^3H]DA$ efflux in T62D-hDAT cells was independent of Na^+_e and was commensurate with $[^3H]DA$ efflux induced in WT cells either by removal of Na^+_e or by AMPH. We conclude that Thr-62 is important for conformational stability of DAT, and that T62D-hDAT represents an efflux willing, Na^+ -primed orientation. Possibly, T62D-hDAT represents an experimental model of the conformational impact of AMPH exposure to hDAT.

Introduction

The dopamine transporter (DAT) has a critical role in the regulation of dopamine (DA) neurotransmission due to its primary function of taking up released DA from the extracellular space back into the presynaptic nerve terminal. DAT is also the site of action for therapeutic and abused psychostimulants such as amphetamine (AMPH) (Levi and Raiteri, 1993; Leviel, 2011). AMPH is a competitive DAT substrate that, upon translocation into the terminal, is capable of inducing reverse transport and subsequently increasing extracellular DA (Sulzer et al., 2005).

The DAT is a member of the SLC6 family of transporters that require sodium and chloride ions for substrate translocation. The electrochemical gradient of Na^+ provides the energy required to move substrate through the transporter, against its concentration gradient (Chen et al., 2004b; Hahn and Blakely, 2007). The alternate access model is the common paradigm for the translocation of neurotransmitter and co-transported ions (Jardetzky, 1966), where the transporter transitions between outward to inward facing orientations to move substrate from outside to

inside the cell. Crystallization of the leucine transporter (LeuT), a bacterial SLC6 homologue (Krishnamurthy and Gouaux, 2012; Yamashita et al., 2005), has provided vast information about the transporter structure and translocation mechanism that further validate the alternate access model. Elegant molecular modeling comparisons to hDAT have identified fundamental transmembrane domains (TM) and amino acid residues involved in ligand binding and the extracellular to intracellular translocation of substrate (Shan et al., 2011; Zhao et al., 2012; Zhao et al., 2010). However, the mechanisms regulating the binding of DA and co-transported ions during reverse transport are not fully understood.

The DAT N-terminus contains various serine and threonine residues that are important for the regulation of transporter activity (Foster et al., 2002) and AMPH-induced DA efflux (Foster et al., 2012; Khoshbouei et al., 2004). We were interested in studying the threonine residue within the highly conserved, RETW sequence of the DAT N-terminus to gain further insight into the mechanisms of AMPH action. The RETW sequence is juxtaposed to the TM1a segment (Yamashita et al., 2005), which is within a DAT region identified as the intracellular gating network (Kniazeff et al., 2008). To study this site, the Thr 62 residue of DAT was mutated to an alanine (T62A) or aspartate (T62D) to mimic a non-phosphorylated and a phosphorylated state, respectively (Guptaroy et al., 2009). Based upon previous findings, we have determined that the T62D mutation shifts the orientation of hDAT from a primarily outward to inward facing conformation. Our initial studies showed a reduction in the uptake of [³H]DA and a loss of AMPH-stimulated DA efflux in T62D-hDAT compared to WT hDAT HEK cells (Guptaroy et al., 2009). These functions were rescued when measured in the presence of zinc, which has been

used to correct dysfunctions of other inward facing hDAT mutants (Loland et al., 2002; Meinild et al., 2004). Other major differences from WT observed in T62D-hDAT cells were the increase in basal, unstimulated DA release, a faster rate of DA efflux, and a significantly reduced K_m for [3 H]DA efflux (Guptaroy et al., 2009). Additional studies revealed an enhanced affinity for other substrates (norepinephrine, AMPH) in the Thr62 hDAT mutants cells (Guptaroy et al., 2011), especially in the predominately inward facing T62D-hDAT HEK cells. Enhanced substrate affinity is likely when the transition of substrate-bound transporter from the inward to outward orientation is kinetically favored, as deemed with inward-facing mutant transporters (Chen et al., 2004a; Guptaroy et al., 2011; Guptaroy et al., 2009).

In this study we used the T62D-hDAT as a model to further investigate the influence of transporter orientation on the membrane potential and the requirements of Na^+ for DAT functions. We hypothesized whether the elevated basal DA efflux measured in T62D-hDAT HEK cells could be attributed to 1) poor intracellular accumulation of substrate; 2) an intrinsic depolarized membrane; or 3) a modification in Na^+ gradient. These hypotheses were tested using a combination of electrophysiology measurements in *Xenopus* oocytes, and radioligand and fluorescent microscopy techniques in heterologous cells. The results from these experiments strengthened the conclusion that T62D-hDAT partitions in a predominantly inward-facing state and, moreover, that the conformation represents an inward ' Na^+ -primed' state able to maximize DA efflux.

Materials and Methods

Cell culture

Wildtype, T62A, and T62D mutant human dopamine transporter (hDAT) were cloned and stably expressed in human embryonic kidney 293-T cells as previously described (Guptaroy et al., 2009). Cells were maintained in high glucose Dulbecco's modified Eagle's medium supplemented with 10% fetal bovine serum and 1% penicillin/streptomycin at 37° C and 5% CO₂. All experiments utilizing hDAT HEK cells were performed with intact, attached cells at room temperature.

Confocal Microscopy and Image Analysis

Accumulation of the fluorescent substrate ASP⁺ [4-(4-(Dimethylamino)styryl)-N-methylpyridinium] (Molecular Probes, Eugene, OR) was measured with confocal imaging in live WT and Thr mutant hDAT HEK cells. Cells were plated on poly-D-lysine (PDL) coated, 35 mm glass bottom MatTek culture dishes (MatTek, Ashland, MA) at a density of 500-750,000 cells per dish 1 day prior to imaging. The culture media was aspirated and cells were washed twice in normal Krebs Ringer's HEPES (KRH) buffer, pH 7.4 [in mM: 125 NaCl, 4.8 KCl, 1.2 KH₂PO₄, 1.3 CaCl₂•2H₂O, 1.2 MgSO₄•7H₂O, 5.6 glucose, and 25 HEPES] containing 50 μM of pargyline (MAO inhibitor), 1 mM tropolone (COMT inhibitor), and 50 μM ascorbic acid (DA antioxidant) (Sigma, St. Louis, MO). Cells were incubated at 37° C in 2 ml of 5 μg/ml Hoechst nuclear stain (Molecular Probes) for 30 min. Then cells were washed twice quickly and then twice more for 5 min each with gentle rocking and light protection. Plates were mounted on an Olympus

FluoView 500 confocal microscope and focused in 100 μ l KRH to take the differential interference contrast (DIC) image. The center of the cell plane was determined with the nuclear stain. A test plate of WT-hDAT HEK cells was used to set the levels for intensity, brightness, and contrast for minimal saturation of the fluorescent signal of each laser channel. These microscope settings were not adjusted during the image acquisition of experiment plates. The Hoechst stain was excited with a UV laser at 405 nm and passed through a BA430-460 bandpass filter. ASP⁺ was excited using the Hene-green laser with excitation at 543 nm and a BA610IF bandpass filter. Images were acquired at room temperature with a time scan every 10 sec for 3 min. ASP⁺ (2 μ M, 2 ml) was carefully added to the cells after the first 10 sec acquisition. The average fluorescence intensity (AFI) within whole cell regions was identified and quantified with MetaMorph image acquisition software v. 7.71 (Molecular Devices, Sunnyvale, CA). By the end of image acquisition (3 min), the background fluorescence in parental HEK cells was around 80% of the ASP⁺ fluorescent signal in cells expressing WT or Thr 62 mutant hDAT.

ASP⁺ Competition of Radiolabeled Dopamine and WIN 35, 428

Cells were seeded onto 24-well plates at a density of 200,000 cells per well 1 day before the experiment. Uptake of 10 nM [³H]DA (specific activity 46 Ci/mmol) for 3 min or binding displacement of [³H] WIN 35,438 (specific activity 85 Ci/mmol) for 30 min (Perkin Elmer Waltham, MA) were measured at room temperature in ASP⁺ concentrations ranging from 0 to 1 mM prepared in KRH buffer containing 10 % DMSO. Non-specific uptake or binding was determined in the presence of 100 μ M cocaine or 5 μ M GBR-12935, respectively, following a 10

minute preincubation with the inhibitor alone. At the end of the assay, cells were washed 4 times in ice cold PBS then lysed in 0.25 ml 1% SDS. Radioactivity was measured in 5 ml of Scintiverse cocktail (Fisher Scientific, Waltham, MA) using a Beckman LS5801 scintillation counter (Fullerton, CA).

Extracellular Sodium Substitution

For extracellular sodium substitution experiments, the NaCl in the KRH buffer was replaced with N-methyl-D-glucamine chloride (NMDG-Cl). [³H]DA uptake was measured as stated above, while varying the levels of Na⁺. Assay buffer with 0, 10, 30, 50, 100 and 125 mM NaCl contained 125, 115, 95, 75, 25, and 0 mM of NMDG-Cl, respectively. Maximum uptake was obtained in the normal, 125 mM NaCl condition for all constructs.

For efflux experiments, cells were preloaded with 0.5 μM DA (containing 15 nM [³H] DA) in normal KRH. After washing, 0.25 ml of fresh Na⁺ substituted KRH was collected and replaced for 15 min to evaluate the baseline DA efflux. The Na⁺ effect of AMPH-induced DA release was determined after a 5 min application of 10 μM AMPH, followed by collection of an additional 5 min aliquot at 20 min. At the end of the assay, cells were solubilized to measure the final amount of DA remaining inside of the cells after efflux. Total [³H]DA after preloading was estimated as the sum of radioactivity in all efflux fractions and final intracellular DA. Basal DA efflux was taken as a percentage of the estimated total [³H]DA. AMPH-induced [³H]DA efflux was calculated as a percentage of the total [³H]DA inside the cell prior to the AMPH treatment.

Molecular Biology of hDAT Expression and Electrophysiology Measurements in Xenopus

Oocytes

Restriction enzyme sites for 5' NotI and 3' XbaI were added to the flag-tagged WT and Thr62 hDAT mutant DNA constructs (Guptaroy et al., 2009) and subcloned into the pSGEM *Xenopus* oocyte expression vector. After linearization of the plasmid with SbfHI-HF digestion (New England BioLabs Inc., Ipswich, MA), capped RNA (cRNA) was prepared according to protocol with the mMessage mMachine T7 kit (Ambion Inc., Ausin, TX). Stage V oocytes were microinjected with 23 ng of water or 1ng/nl hDAT cRNA and incubated at 18° C in SuperBarth's solution, pH 7.4 [in mM: 88 NaCl, 1 KCl, 0.33 Ca(NO₃)₂·4H₂O, 0.41 CaCl₂ ·2H₂O, 1 MgSO₄·7H₂O 2.4 NaHCO₃, 10 HEPES, 1 Na-Pyruvate, and 50 mg/ml gentamicin] for 4-8 days before electrophysiology recordings. Unless otherwise noted, oocytes were voltage clamped at -60 mV. Current was recorded continuously with perfusion of DA or AMPH. The perfusion solution contained (in mM) 93.5 NaCl, 2.0 KCl, 1.8 CaCl₂, 2.0 MgCl₂, 5.0 HEPES, pH 7.5. Recording electrodes had 1-5 MΩ resistance and were filled with 3M KCl. Current measurements were analyzed with ORIGIN 6.0 software. The electrophysiology experiments with oocytes were performed by Dr. Yongyue Chen in the laboratory of Dr. Louis DeFelice at the Virginia Commonwealth University, Richmond, VA.

Statistical Analysis

Dose-response curves were analyzed with GraphPad Prism 6 software (San Diego, CA) to determine the IC₅₀ and EC₅₀ values for [³H]DA uptake competition by nonlinear regression

analyses. Statistical differences were compared between constructs testing the null hypothesis of the parameter being the same between all data sets. A rejection of the null hypothesis indicated a statistical difference between the comparisons, where the p value was below 0.05. Values are provided \pm standard error of the mean (s.e.m) along with the 95% confidence intervals.

Results

Affinity and Accumulation of the Fluorescent Substrate, ASP⁺ in WT and Thr hDAT

Mutant HEK Cells. The uptake and binding properties of the ASP⁺ substrate to hDAT were confirmed with radioligand competition assays. The dose response curves for ASP⁺ competition of [³H]DA uptake (Figure 3-1A) and displacement of the cocaine analog [³H]WIN 35, 428 (Figure 3-1B) did not differ between WT and Thr 62 hDAT mutant cell lines. The IC₅₀ values (μ M) [with 95% confidence intervals] for ASP⁺ competition of [³H]DA uptake (Figure 3-1A) were 11.95 [8.87-16.1] in WT-, 17.60 [10.6-29.2] in T62A-, and 12.08 [10.3-14.1] in T62D-hDAT HEK cells. ASP⁺ inhibited [³H]WIN 35,428 binding with IC₅₀ (μ M) values of 11.95 [8.87-16.1] in WT-, 18.6 [10.6-29.2] in T62A-, and 12.1 [10.3-14.1] in T62D-hDAT HEK cells (Figure 3-1B).

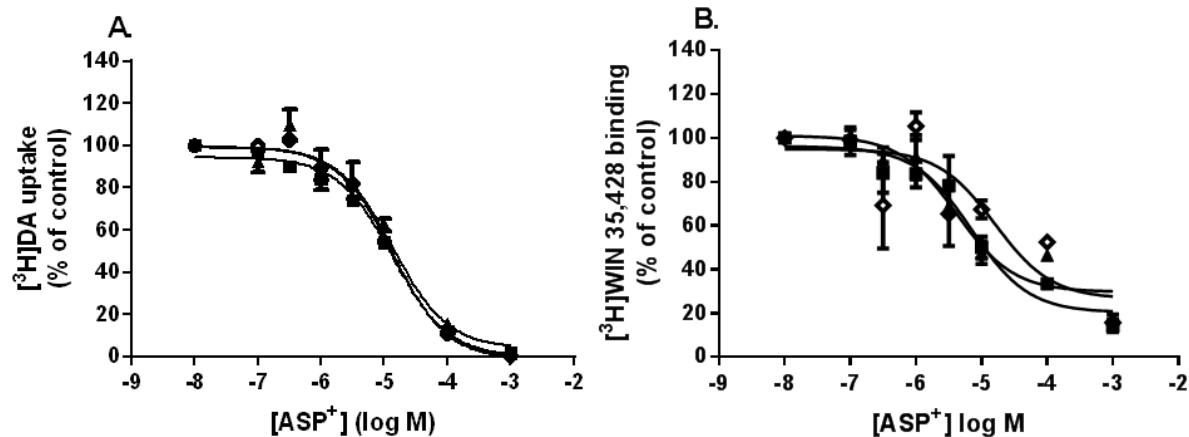


Figure 3-1. Affinity of the fluorescent substrate, ASP⁺ is unaffected by the T62A or T62D hDAT mutations. As detailed under Materials and Methods, **A.** uptake of 10 nM [³H]JDA for 3 min or **B.** binding of [³H]WIN35,428 for 30 min in WT- (■), T62A- (▲), and T62D-(◇) hDAT HEK cells was measured as a function of varying ASP⁺ concentrations. Data are expressed as the percent of the control without ASP⁺; and are shown as the mean ± s.e.m, n = 2 experiments performed in triplicate. The IC₅₀ (μM) values with 95% confidence intervals are reported in the text of the Results.

In previous studies (Guptaroy et al., 2009), we found that T62D-hDAT demonstrated high affinity, but very low V_{max} [³H]JDA uptake with high basal efflux. We postulated that substrate would not accumulate intracellularly due to accelerated outward transport. K_m and V_{max} values for [³H]JDA uptake for T62A-hDAT were intermediate between T62D-hDAT and WT (Guptaroy et al., 2009). We measured uptake of the fluorescent substrate 4-(4-(dimethylamino)styryl)-N-methylpyridinium (ASP⁺), which has been often studied as a substrate for DAT (Bolan et al., 2007; Schwartz et al., 2003; Zapata et al., 2007). ASP⁺ is structurally similar to the dopaminergic neurotoxin, 1-methyl-4-phenylpyridinium (MPP⁺). Because ASP⁺ is bound to mitochondria, it is not subject to rapid outward transport (Schwartz et al., 2003), which allows more accurate measurement of influx in the T62D-hDAT mutant. There was a small amount of background fluorescence prior to the addition of ASP⁺; however the fluorescence intensity

increased with time after cells were exposed to 2 μM of ASP^+ . The full range of intracellular ASP^+ accumulation at each time point is shown in Figure 3-2E. Although the average fluorescence intensity in cells with transporter is approximately 20% greater, the accumulation in parental HEK cells lacking DAT was on average 70% of WT-, 84% of T62A-, and 80% in T62D-hDAT HEK cells. The reason for high background fluorescence in empty HEK cells is not clear and is under investigation. The time dependent increase of ASP^+ fluorescence in T62A- and T62D-hDAT HEK cells were comparable to levels of WT-hDAT HEK cells. It should be noted, however, that by biotinylation measuring surface DAT, T62D-hDAT is expressed to only 50% of the level as hDAT (Guptaroy et al., 2009), thus there are 50% fewer transporters on the surface to take up ASP^+ . Despite the diminished number of transporters, the rate of uptake of ASP^+ into T62D-hDAT cells was equal to that of hDAT.

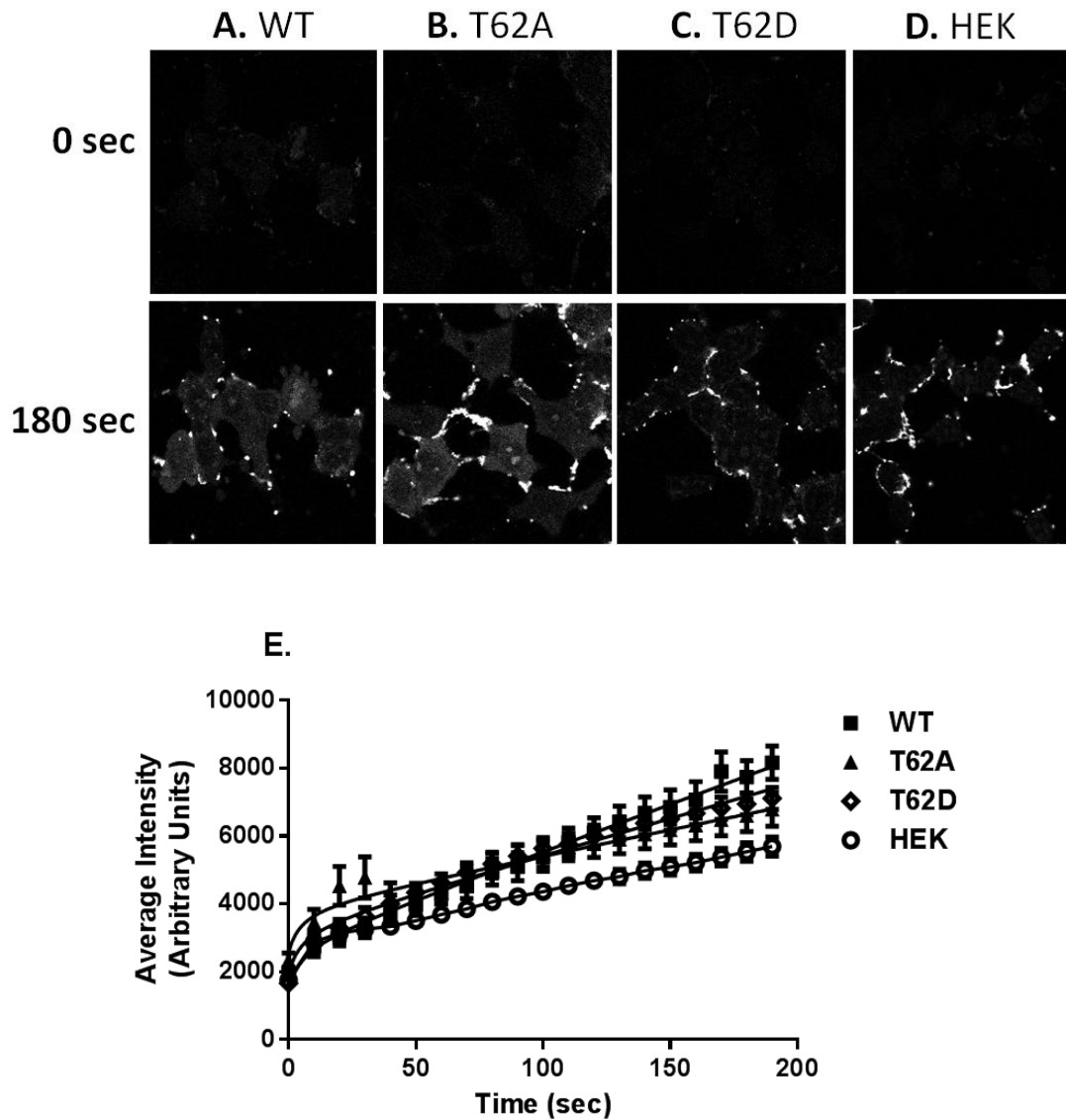


Figure 3-2. Accumulation of fluorescent substrate, ASP⁺ in T62A- and T62D-hDAT HEK cells. Representative confocal images of time dependent ASP⁺ accumulation are displayed in columns **A.** WT-, **B.** T62A-, and **C.** T62D-hDAT, and **D.** parental HEK cells. Acquired representative images at time 0 and 180 sec after exposure to 2 μ M ASP⁺. **E.** The average fluorescence intensity was quantified in intracellular regions of WT- (■), T62A- (▲), and T62D-(◇) hDAT HEK cells using Metamorph Imaging software. Data are plotted for the full 3 min image acquisition of 10 sec intervals, n = 3 imaging 20-40 total cells.

Current Measurements in *Xenopus* oocytes. Depolarization of the membrane is known to favor efflux or reverse transport of monoamine substrates (Rutledge, 1978; Zhen et al., 2005). We next tested whether elevated efflux in T62D-hDAT HEK cells was the result of an intrinsic depolarization of the membrane by the T62D conformation utilizing the *Xenopus* oocyte expression system. Oocytes were injected with equal concentrations of cRNA and DAT expression was confirmed by [³H]DA uptake assays in 5 individual oocytes. DA uptake in hDAT-expressing oocytes was approximately 40% greater than in control, water injected oocytes 4 days after cRNA injections (data not shown).

The resting membrane potential (RMP) was first measured in oocytes expressing the transporters. The RMP in control oocytes injected with water was around -40 mV. Expression of WT-, T62A-, or T62D-hDAT depolarized the recorded RMP to -25 mV (Figure 3-3). The level of depolarization induced by T62A- or T62D-hDAT expression in the oocytes was the same as WT-hDAT. The well characterized leak current present in DAT in the absence of substrate (Sonders et al., 1997) is likely accountable for the depolarization of the oocyte. The RMP recordings suggest the baseline current passing through the transporter in the absence of substrate is not affected by the Thr 62 mutations.

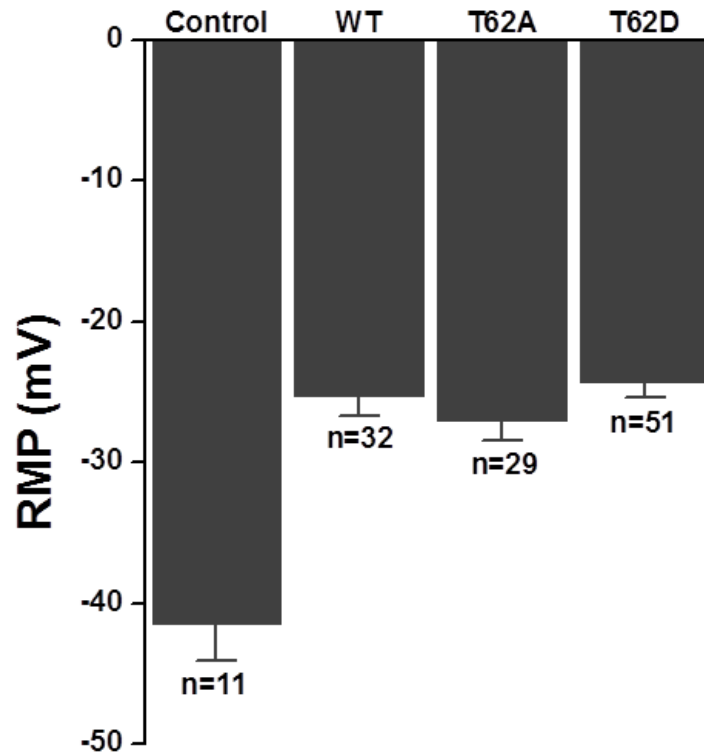


Figure 3-3. Expression of WT-, T62A-, and T62D-hDAT mutants causes similar membrane depolarization in *Xenopus* oocytes. *X.* oocytes were injected with 23 ng of cRNA for WT, T62A or T62D hDAT. Expression of hDAT reduces the recorded resting membrane potential of oocytes when compared to control oocytes injected with 23nl or water.

Substrate translocation via DAT is an electrogenic process that produces measureable currents. Substrates like AMPH and DA are known to induce inward currents that are primarily attributed to an inward flux of Na^+ ions (Sonders et al., 1997). We next measured the substrate-induced currents in WT-, T62A- and T62D-hDAT oocytes. Representative trace recordings from oocytes voltage clamped at -60 mV are shown in Figure 3-4A. Currents were measured after the application of 10 μM DA for 1 minute. DA rapidly produced inward currents in oocytes

expressing WT-hDAT that were absent in control oocytes lacking the transporter. T62A-hDAT oocytes also produced DA-induced inward currents, although the current magnitude was nearly half that measured in WT-hDAT oocytes. This finding corresponds with our previous reporting of a near 50% reduction in the V_{\max} for [^3H]DA uptake in T62A-hDAT HEK293 cells as compared to WT-hDAT HEK293 cells (Guptaroy et al., 2009). No current was detected in T62D-hDAT oocytes (Figure 3-4). Zinc has been used in numerous studies to reverse the defective translocation of T62D-hDAT HEK293 cells (Guptaroy et al., 2011; Guptaroy et al., 2009) and other inward facing DAT mutant transporters (Chen et al., 2004a; Loland et al., 2002). Binding of zinc stabilizes the outward facing conformation of DAT via an increase in chloride conductance (Loland et al., 2002; Meinild et al., 2004). We utilized zinc to determine if substrate-induced currents could be measured in T62D-hDAT oocytes. While Zn^{2+} alone produced a small current in T62D-hDAT oocytes, the co-application of 2 μM ZnCl_2 and DA revealed a measureable current (Figure 3-4). The current traces recorded with AMPH (20 μM) for each oocyte construct matched those measured using DA (data not shown). The DA induced accumulated changes in current in oocytes held at -60 mV are plotted in Figure 4B.

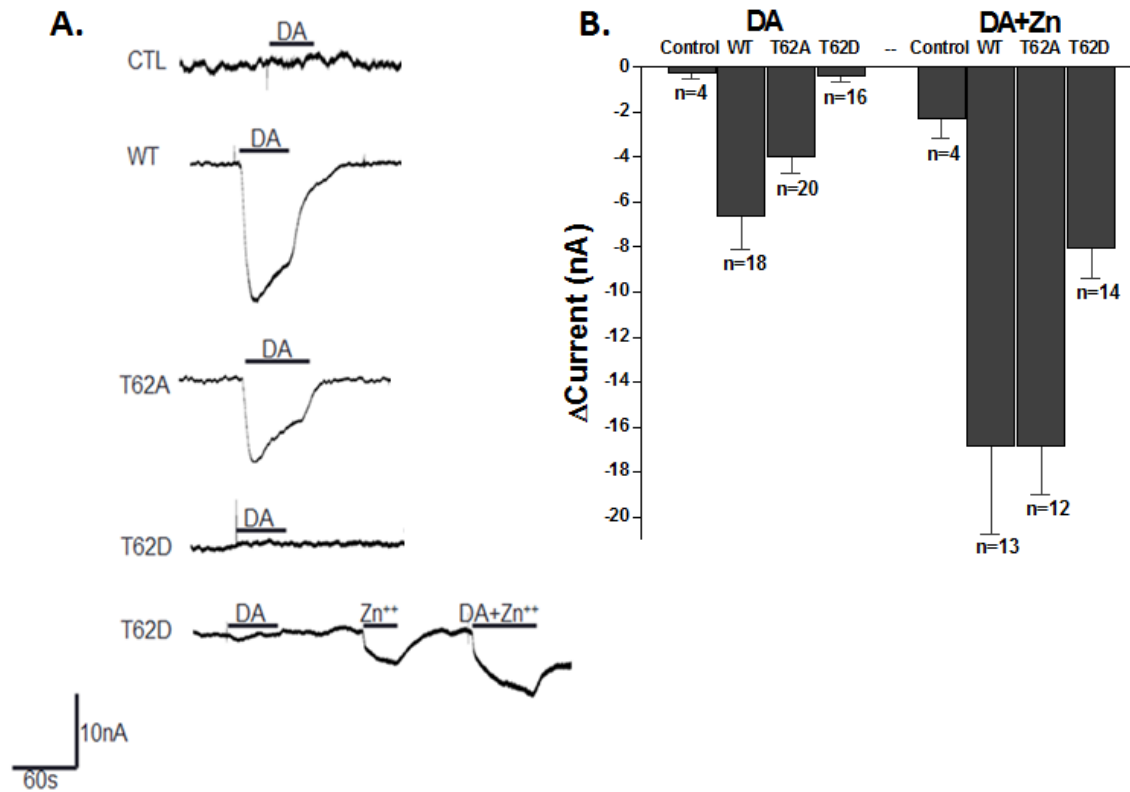


Figure 3-4. Dopamine-induced inward currents in T62D-hDAT oocytes are partially rescued by zinc. **A.** Representative continuous traces of currents measured in oocytes clamped at -60 mV are shown. Inward currents are observed in WT- and T62A-hDAT oocytes after application of 10 μ M dopamine (DA). Co-application of 2 μ M ZnCl₂ partially restored a measurable inward current in T62D-hDAT oocytes. **B.** Shows the change in accumulated current in WT-, T62A-, and T62D-hDAT oocytes held at -60 mV. The data are expressed as the average \pm s.e.m with numbers of oocytes for each condition given. The effects of zinc alone in all constructs can be seen in Figure 3-5.

The currents in WT-, T62A-, and T62D-hDAT oocytes were measured over a range of membrane potentials from -150 to 30 mV. The current-voltage (I-V) relationships are shown in Figure 3-5. DA-induced inward currents were detected at hyperpolarizing potentials (Ingram et al., 2002; Sonders et al., 1997) in oocytes expressing WT- (Figure 3-5A) or T62A-hDAT (Figure 3-5B). Smaller currents were measured in oocytes with zinc alone. However, the co-application

of zinc and DA resulted in a potentiation of the substrate-induced current in all three constructs. In T62D-hDAT oocytes (Figure 3-5C), DA-induced currents were only measurable in the presence of zinc.

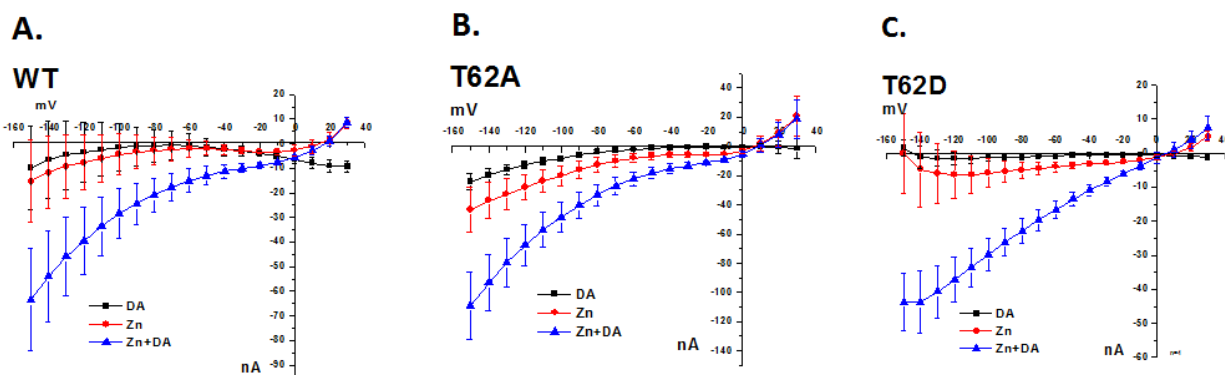


Figure 3-5. Current-voltage relationships in hDAT expressing *Xenopus* oocytes. A step voltage clamp protocol was used from -150 to 30 mV at a holding potential of -60 mV and 10 mV step increments for 30 sec duration. Oocytes were challenged with 10 μ M DA \pm 2 μ M ZnCl₂. At hyperpolarizing potentials, DA (black squares) induces an inward current in **A.** WT- and **B.** T62A-hDAT oocytes. Co-application with zinc (blue triangles) potentiates DA induced inward currents. **C.** In T62D-hDAT oocytes, DA inward currents are only measurable in the presence of zinc. Application of zinc alone (red circles) produced a small current in all constructs. Each I-V plot was generated from 4-6 oocytes expressing the indicated hDAT construct.

The absence of net current measured in response to substrate in the T62D-hDAT mutant suggested that there was an equal flow of ions in both directions. Because the inward current is likely a Na⁺ current, we were led to explore the effect of Na⁺ on the function of T62D-hDAT as compared to the other constructs. This was addressed with studies measuring uptake and efflux functions under NaCl replacement conditions.

Extracellular Sodium Substitution Experiments. To determine whether the T62A or T62D mutations would alter the Na^+ requirements for hDAT function, we measured [^3H]DA uptake and efflux in WT-, T62A-, and T62D-hDAT HEK cells while varying the extracellular concentrations of Na^+ (Na^+_e). NaCl was replaced with NMDG-Cl to maintain osmolarity of the cells. In all cell lines, there was very little uptake of [^3H]DA with complete NMDG-Cl substitution (0 mM Na^+_e). There was no statistical difference between the EC_{50} (mM) [95% CI] values for Na^+ stimulation of [^3H]DA uptake in WT- 39.6 [26.7-58.5], T62A- 40.5 [29.7-55.1], or T62D- 58.7 [39.4-87.6] (Figure 3-6).

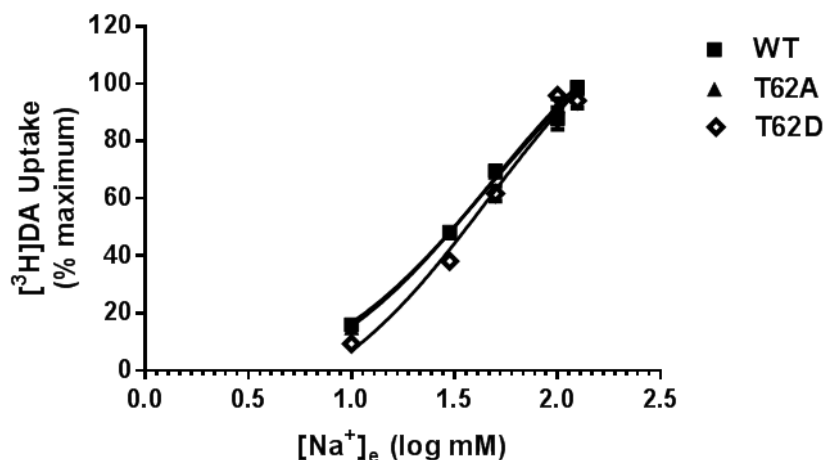


Figure 3-6. The reliance for extracellular Na^+ to promote DA uptake is not altered by the Thr62 hDAT mutations. Extracellular sodium (Na^+_e) stimulation of [^3H]DA uptake in WT- and T62 mutant hDAT HEK cells. Uptake of 10 nM [^3H]DA was conducted for 3 min at room temperature. Na^+ in the uptake buffer was replaced with NMDG-Cl to maintain osmolarity. The IC_{50} (mM) for Na^+_e in WT, T62A, and T62D was 39.6, 40.5, and 58.7, respectively. Data are from $n = 4$ experiments done in triplicate and reported as a percentage of the maximum uptake achieved at the normal, highest [Na^+_e] tested.

Outward transport through DAT demonstrates an inverse dependence on Na^+_e as compared to inward transport. Removal or lowering of extracellular Na^+ stimulates substrate efflux in cells expressing monoamine transporters (Piffl et al., 1997; Piffl and Singer, 1999) or brain tissue preparations (Liang and Rutledge, 1982; Raiteri et al., 1979) by shifting the internal Na^+ gradient to favor reversal of the transporter. Khoshbouei et al. (2003) demonstrated that the concentration of intracellular Na^+ drives the ability of AMPH to induce DA release through DAT. Previously we reported that T62D-hDAT had an elevated basal leak of [^3H]DA which exceeded that of WT at physiological levels of Na^+_e (Guptaroy et al., 2009). Here, the behavior of the basal efflux as a function of Na^+_e was examined.

WT-hDAT HEK cells showed the expected elevation in basal [^3H]DA efflux upon removal of Na^+_e and the elevation was maintained throughout the 15 min incubation period (Figure 3-7, open bars). The baseline efflux significantly decreases as [Na^+_e] progresses from 0 mM, 10 mM, 50 mM to 125 mM (Figure 3-7, white, checkered, gray, and black bars); indicating a return of the transporter from a predominantly inward-facing to an outward-facing conformation. This same pattern recurred at the 10 min and 15 min time points (Figure 3-7, checkered, gray, and black bars). In a 2-way ANOVA, there was a main effect of time ($p < 0.01$ ($F_{(3, 56)} = 5.755$)) and a significant interaction between [Na^+_e] and time ($p < 0.0001$ ($F_{(9, 56)} = 11.07$)) with no main effect of [Na^+_e] ($p = 0.059$, $F_{(3, 56)} = 2.625$). Significant stimulation of efflux by AMPH is only seen above the corresponding baseline at 50 mM Na^+_e ($p < 0.05$, $n = 3$, *post hoc* Tukey's) and 125 mM Na^+_e ($p < 0.0001$, $n = 3$, *post hoc* Tukey's) (Figure 3-7A, 20 min).

The pattern was similar in T62A-hDAT HEK cells even though the degree of [³H]DA efflux was lower than in WT (Figure 3-7B). By 2-way ANOVA, there was a significant effect of time ($p < 0.01$, $F_{(3, 46)} = 5.554$), and interaction of [Na^+_e] and time ($p < 0.001$, $F_{(9, 46)} = 4.175$), but no significant effect of [Na^+_e] ($p = 0.1528$, $F_{(3, 46)} = 1.842$). As shown in Figure 3-7, addition of AMPH prevents [³H]DA efflux in WT-hDAT (Figure 3-7A, D) and T62A-hDAT (Figure 3-7B) cells under conditions of absent, 0 mM or low, 10 mM Na^+_e . When the Na^+ gradient favoring intracellular Na^+ is less pronounced, that is, when [Na^+_e] is 50 mM or 125 mM, AMPH instead stimulates efflux in WT-hDAT and T62A-hDAT mutants (Figure 3-7A and B).

In T62D-hDAT HEK cells, there was a significant effect of time by 2-way ANOVA ($F_{(3, 51)} = 25.07$) but no interaction with time and [Na^+_e] and no main effect of [Na^+_e]. The basal [³H]DA efflux declined during the incubation period but was independent of Na^+_e (see legend Figure 3-7D). The decline in [³H]DA efflux was not due to a loss of intracellular [³H]DA since 70% - 80% of the [³H]DA originally taken up was still inside the cell after 20 min. AMPH does not induce [³H]DA efflux at any [Na^+_e] in the T62D-hDAT mutant, which remains inward-facing independent of Na^+_e (Figure 3-7C). All values at the 20 min time point, which contained AMPH, were significantly different from values for 0 mM Na^+_e at 5 min.

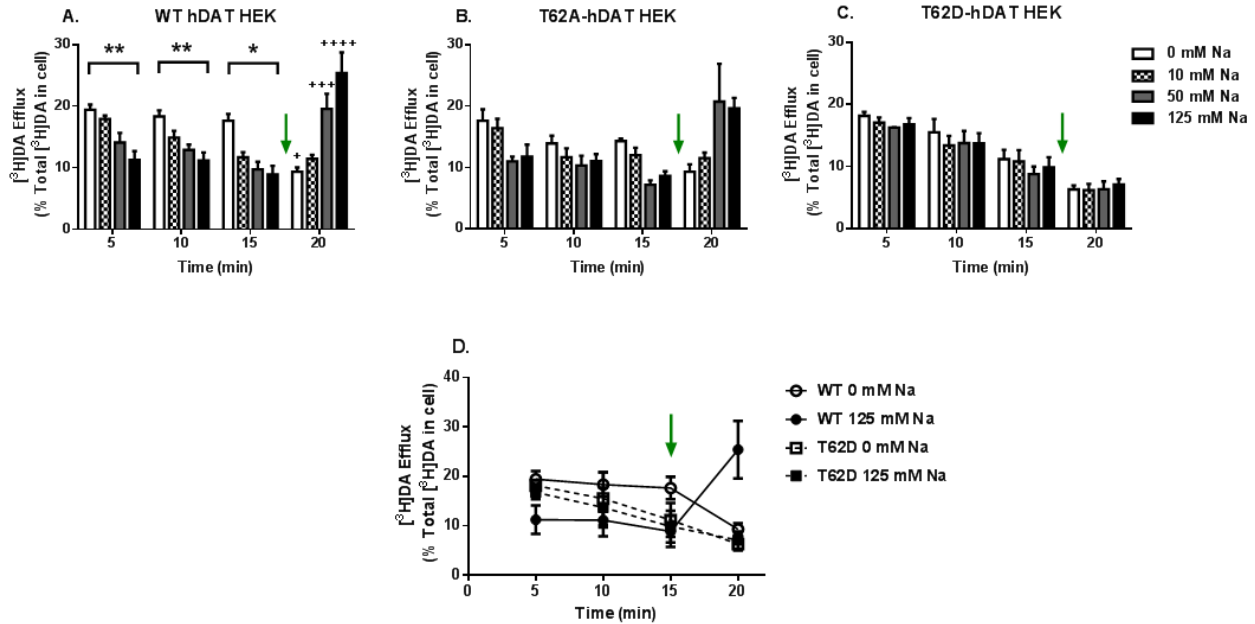


Figure 3-7. Initial $[^3\text{H}]\text{DA}$ efflux in T62D-hDAT is Na^+ independent and resembles inducible DA efflux of WT-hDAT HEK cells. A. WT-hDAT, B. T62A- and C. T62D-hDAT HEK cells were preloaded with $0.5 \mu\text{M}$ $[^3\text{H}]\text{DA}$ (in normal buffer) for 20 min. Basal and AMPH-induced DA efflux were determined while varying $[\text{Na}^+_e]$. After 15 min (green arrow), cells were stimulated with AMPH ($10 \mu\text{M}$) in varying $[\text{Na}^+_e]$ for 5 min. In WT (A), ** $p < 0.01$, * $p < 0.05$ for 0 versus 125 mM at times 5, 10, and 15 min; ++++ $p < 0.0001$, +++ $p < 0.001$, + $p < 0.05$ for 20 min (after AMPH) compared to 15 min (before AMPH) at each corresponding $[\text{Na}^+_e]$ D. Comparisons of basal and AMPH (green arrow) DA efflux in WT- (circles) and T62D- (squares) at 0 mM (open symbols) and 125 mM (closed symbols) Na^+_e . To account for variation in DA uptake, the data are represented as a percentage of the total $[^3\text{H}]\text{DA}$ inside of the cell after DA preloading. Data are from 3 experiments performed in triplicate. Analyses of the 3-way interaction ($time \cdot [\text{Na}^+_e] \cdot cell\ type$) is not significantly different between WT and T62D at 0 mM Na^+ (with the exception of 15 min, $p = 0.005$) or at 125 mM Na^+ (except the slight difference at 5 min, $p = 0.054$). DA efflux after AMPH (20 min) is significantly greater in WT compared to T62D at 125 mM Na^+ ($p < 0.0001$), with no difference between cell types at 0 mM Na^+ ($p = 0.23$). The effect of Na^+_e on DA efflux was significant in WT but not in T62D ($p < 0.001$, $time \cdot cell\ type \cdot [\text{Na}^+_e]$). Analyses of $cell\ type \cdot [\text{Na}^+_e] \cdot time$ shows a significant change after the addition of AMPH (15 min versus 20 min) in WT at both 0 mM ($p = 0.002$) and 125 mM Na^+ ($p < 0.0001$); and in T62D at 0 mM Na^+ ($p = 0.03$), but not 125 mM ($p = 0.235$).

In order to better visualize the similarities or differences between T62D hDAT and the inward (no Na^+_e) and outward (normal Na^+_e)-facing conformations of WT hDAT, data for only these two constructs at 0 mM and 125 mM Na^+_e were graphed (Figure 3-7D). In a general linear

model 3-way ANOVA, there was a significant effect of time x cell type ($F=10.277$, $df=3$, $p=0.0001$), a significant time x sodium interaction ($F=14.951$, $df=3$, $p=0.0001$) and a significant time x cell type x sodium interaction ($F=10.190$, $df=3$, $p=0.0001$). There was no significant cell type x sodium interaction ($p=0.5$). At the initial time point of 5 min, the rate of [^3H]DA efflux is identical for T62D hDAT at 0 and 125 mM Na^+_e ($p = 0.647$) and for WT at 0 mM Na^+_e ($p = 0.612$). It would appear that removal of Na^+_e constrained WT hDAT in an inward-facing position that is mimicked by T62D-hDAT independently of Na^+_e . Regardless of [Na^+_e], the rate of [^3H]DA efflux significantly declines between the 5 min and 20 min points for the T62D hDAT mutant (Figure 3-7D). However, efflux in WT-hDAT remained stable between 5 and 15 min whether at 0 mM Na^+_e or 125 mM Na^+_e . At the 20 min time point where AMPH is present, rates of [^3H]DA efflux from WT-hDAT at 0 mM Na^+_e are equal to those of T62D-hDAT at any concentration of Na^+_e (Figure 3-7D, 20 min open circle, open & closed squares). The rate of efflux of [^3H]DA elicited by AMPH at the more physiological 125 mM Na^+_e or by 0 mM Na^+_e in WT-hDAT and was comparable to T62D hDAT, demonstrating the reversal back to the inward-facing state. We therefore reasoned the T62D hDAT mutation produces a Na^+ -primed state of the transporter that readily releases DA. Another significant finding is the decrease in basal efflux elicited by AMPH in WT in the absence of Na^+_e .

[^3H]DA efflux was sensitive to inhibition by 100 μM cocaine in all three DAT constructs. The fractional efflux of [^3H]DA in the presence of 100 μM cocaine was constant within each construct independent of time and [Na^+_e]. Fractional [^3H]DA release in the presence of 100 μM

cocaine is 6.4 ± 0.1 for WT, 7.3 ± 0.6 for T62A-hDAT, and 4.9 ± 0.2 for T62D-hDAT (n=4 each cell type, for 4 $[\text{Na}^+_{\text{e}}]$).

Discussion

In this study, we delineate key characteristics of T62 DAT mutants that contribute to our understanding of DAT conformation regulation. Our previous experiments led us to conclude that T62D-hDAT was predominantly partitioned in an inward-facing conformation (Guptaroy et al., 2009) and we postulated, but did not prove, that the extremely low V_{max} of this mutant for $[\text{}^3\text{H}]\text{DA}$ uptake was due to rapid cycling of the transporter between inward- and outward-facing conformations. In this study we confirm that hypothesis by demonstrating that T62D-hDAT can take up a non-effluxing substrate normally as compared to WT. Moreover, we demonstrate that the mutation of Thr-62 to Asp-62 results in a conformation that represents the Na^+ -sensitive state of the inward gate. In spite of having an orientation representing maximal responsiveness to internal Na^+ with an unregulated, inwardly-open gate, T62D-hDAT is able to normally bind substrate in the outward-facing conformation and transition to inward-facing. The outward-facing conformation of T62D-hDAT retained Na^+ sensitivity equal to that of WT demonstrating the independence of Na^+ -dependent inward and outward-facing conformations.

The use of the fluorescent substrate, ASP^+ , permitted interrogation of whether the Thr62 hDAT mutations truly disrupt the influx of substrate and, by inference, its intracellular retention. ASP^+ has been well characterized as a substrate for both DAT and NET (Schwartz et al., 2003). ASP^+ has unique utility for our purpose because it is readily measured by fluorescence in heterologous

cells and not subject to efflux. Once inside the cell, ASP⁺ sequesters within mitochondria (Schwartz et al., 2003) and, as a non-catechol substrate, will not bind to the inward-facing gate and be subject to outward transport (Liang et al., 2009). The fact that ASP⁺ accumulation was identical in T62D-hDAT and WT-hDAT demonstrates normal (outward to inward) translocation in T62D. Therefore, the extremely low V_{\max} of [³H]DA in T62D-hDAT cells (Guptaroy et al., 2009) was due to continuous intracellular rebinding [³H]DA and its outward transport. This finding distinguishes T62D-hDAT from other DAT mutants that have been characterized as being inward facing. A DAT mutant with similar, but not identical characteristics to T62D-hDAT is A559V-hDAT, a variant isolated from 2 male siblings with ADHD (Mazei-Robison et al., 2008). Like T62D, A559V exhibits a baseline leak of DA but unlike T62D has normal [³H]DA uptake. This difference may be because T62 lies near the permeation pathway and within the intracellular gating network while A559 appears to lie within TM 12 (Yamashita et al., 2005).

Substrate movement and transporter conformations are driven by a network of molecular interactions. Thr 62 is within a prime location to affect transporter orientation due to its proximity to TM 1a, which forms part of the permeation pathway (Shan et al., 2011; Yamashita et al., 2005). This segment of the transmembrane domain is within an intracellular gating network (Kniazeff et al., 2008) that regulates conformational transitions in DAT (Shan et al., 2011). Previous *in silico* modeling of T62D-hDAT, in comparison to WT-hDAT, indicated a disruption of a functionally important microenvironment involving binding of T62 to other residues (Guptaroy et al., 2009). The T62D conversion disrupted binding of the residue to Y335

in intracellular loop (IL) 3 and K260 within IL2 resulting in a significant conformational change in which the cytoplasmic end of TM1 moves away from junctions with IL2 and IL3. In the T62A-hDAT mutant, only the interaction with Y335 is lost which would account for its milder effects on DAT function (Guptaroy et al., 2009). Notably, the Y335 and K260 residues have been implicated in the DAT intracellular gating network (Kniazeff et al., 2008).

Other predominantly inward-facing DAT mutants, such as D345N (Chen et al., 2004a) and Y335A (Loland et al., 2002) have extremely low measureable rates of DA uptake, but baseline DA efflux had not been measured. D345N appears to exist in an inward-facing conformation that cannot readily adopt an outward-facing conformation (Chen et al., 2004a). In the bacterial Na⁺-dependent leucine transporter (LeuT), an R30A mutation affected the conformation of the intracellular network leaving the extracellular network largely unchanged (Zhao et al., 2010). This demonstrates, as do our data, that conformations in the transporter are flexible and that a mutation near one gate need not severely curtail function at the other gate.

The DAT is electrogenic in that it carries Na⁺ and Cl⁻ across the membrane. Measurement of DAT currents demonstrated that a greater quantity of ions travel across the membrane than predicted (Sonders et al., 1997) by the 1:2:1 stoichiometric ratio of DA:Na⁺:Cl⁻ (Rudnick, 1998). Because DA efflux through DAT is enhanced at depolarized potentials (Khoshbouei et al., 2003) we proposed that expression of T62D could result in a higher resting membrane potential, as demonstrated in *Xenopus* oocytes for the inward-facing mutant Y335A-hDAT (Meinild et al., 2004). However, expression of each hDAT construct depolarized the oocyte membrane to the

same extent which is likely the result of a common, substrate-independent leak current (Sonders et al., 1997). Conversely, profound differences in current conductance in *Xenopus* oocytes expressing WT- and T62D-hDAT were found when measured in the absence versus presence of substrate. No net current was detected in response to either DA or AMPH in T62D-hDAT. This may imply that when T62D-hDAT is exposed to either DA or AMPH substrates the transporter more readily adopts a mode where the inward and outward flow of ions is equivalent. A net flux of ions was restored in T62D-hDAT by the addition of Zn^{2+} , which modifies transport through DAT by altering membrane potential through stimulating a chloride conductance (Meinild et al., 2004; Pifl et al., 2009). In heterologous HEK-293 cells or *Xenopus* oocytes, Zn^{2+} appears to stabilize an outward facing form of DAT, which results in a reduced influx of DA in WT, but enhanced influx in conformationally inward-facing mutants (Loland et al., 2002; Meinild et al., 2004). We previously demonstrated that addition of Zn^{2+} rescued [3H]DA influx and AMPH-induced DA efflux in T62D-hDAT-HEK cells (Guptaroy et al., 2009). Zn^{2+} partially restored a substrate-induced current in T62D-hDAT-expressing *Xenopus* oocytes and enhanced DA currents in those expressing WT and T62A-hDAT. However, with the accompaniment of Zn^{2+} , DA (and AMPH) can induce an inward current in T62D-hDAT because the outward facing state is somewhat stabilized. This allows an unequal shift in the direction of ion flow within T62D-hDAT oocytes that involves more Na^+ influx capable of provoking inward currents normally associated with substrate uptake (Sonders et al., 1997). Under voltage-clamped conditions, substrate alone did not induce a detectable current in *Xenopus* oocytes containing the inward-facing mutant Y335A-hDAT (Meinild et al., 2004). However, unlike T62D-hDAT, application

of Zn^{2+} alone induced a voltage-dependent current that was not further enhanced upon addition of substrate. Substrate-induced inward currents in voltage-clamped T62A-hDAT oocytes were approximately half the magnitude of WT-hDAT oocytes. This is in keeping with a half maximal reduction in the V_{max} for [^3H]DA uptake observed in T62A-hDAT cells, and our conclusion of the T62A mutation producing a transporter that is slower to transition between the outward and inward conformations (Guptaroy et al., 2009). Even though oocytes were injected with equal concentrations of cRNA, we did not directly measure hDAT surface expression in the oocytes. Therefore, it cannot be ruled out that the reduction in the substrate-induced currents of T62A-hDAT oocytes is due to fewer transporters expressed than in WT oocytes. This possibility may, however, be unlikely since transfection of equivalent DNA construct concentrations in HEK 293T cells showed similar levels of surface and total T62A and WT hDAT expression (Guptaroy et al., 2009) and we found similar amounts of [^3H]DA uptake in WT- and T62A-hDAT expressing oocytes. The discovery of varying current phenotypes in T62D-hDAT oocytes with and without substrate encouraged investigations into how the Thr 62 hDAT mutations would alter the extracellular and intracellular Na^+ gradients required for DA uptake and efflux, respectively.

Reduction of the transmembrane Na^+ electrochemical gradient by increasing intracellular Na^+ levels or reducing extracellular Na^+ concentration inhibits neurotransmitter uptake and simultaneously promotes reverse transport (Erreger et al., 2008; Khoshbouei et al., 2003; Liang and Rutledge, 1982; Raiteri et al., 1979; Zhen et al., 2005). As a substrate, AMPH increases the inward transport of both DA and Na^+ . Evidence suggests that the build-up of Na^+ at the

cytosolic face of the transporter underlies the ability of DAT to adopt an inward-facing conformation (Liang and Rutledge, 1982; Raiteri et al., 1979). Khoshbouei et al. (2003) demonstrated that direct increases in intracellular Na^+ stimulates carrier-mediated DA efflux and proposed that an AMPH-induced inward current increases intracellular Na^+ availability to DAT. Our data demonstrated that DA efflux in T62D-hDAT was insensitive to changes in the Na^+ electrochemical gradient, suggesting that the T62D-hDAT conformation is already in a Na^+ -receptive orientation. The fact that accumulation of the ASP⁺ substrate that is not subject to reverse transport, in T62D-hDAT is equivalent to WT hDAT suggests that the Na^+ -primed conformation of the inward-facing mutant does not preclude adoption of the outward-facing form which binds substrate. We have previously demonstrated that the K_m for [³H]DA at the inward-face in T62D hDAT is significantly less than that of WT (Guptaroy et al., 2009). Therefore, the Na^+ -primed conformation of DAT is able to readily rebind DA, such that it is unlikely that empty transporter returns to the surface.

The Na^+ -sensitivity of other inward-facing DAT mutants has not routinely been measured. The A559V DAT variant demonstrated normal DA uptake in the face of greater DA efflux that was due to an enhanced sensitivity to intracellular Na^+ (Mazei-Robison et al., 2008). A key difference between A559V hDAT and T62D-hDAT is that A559V hDAT was responsive to increased intracellular [Na^+] while T62D-hDAT was unresponsive to even partial changes in the transmembrane Na^+ gradient. Nonetheless, the similarities underscore the importance of the sodium gradient in maintaining the conformational states of DAT. Another similarity between A559V- and T62D-hDAT was the apparent inhibition of outward efflux by AMPH. Mazei-

Robison et al. (2008) measured this inhibition in cells containing A559V hDAT but not in WT, likely because their efflux measurements were conducted with high intracellular $[Na^+]$ conditions. However, AMPH will inhibit transporter-stimulated DA efflux in WT when Na_e^+ is zero. The diminution of DA efflux in WT hDAT under low Na_e^+ conditions was also noted by Piffl et al. (1997). Therefore, even though AMPH appears to bind to an inward-facing form of DAT (T62D-hDAT), as we demonstrated previously (Guptaroy et al., 2011; Guptaroy et al., 2009), it acts as an inhibitor rather than a substrate.

This study has uncovered novel attributes between the T62A and T62D-hDAT mutations. T62A-hDAT cells maintain a need for the Na^+ gradient to induce basal and AMPH-stimulated DA release that is not observed in T62D-hDAT HEK cells. Strikingly, the high level of basal DA efflux initially observed in T62D-hDAT at any Na_e^+ concentration is comparable to the DA efflux states of WT-hDAT induced either by removal of Na_e^+ or AMPH stimulation at 125 mM Na_e^+ . It is therefore plausible that the inward facing orientation of T62D-hDAT represents a Na^+ -primed conformational state in which reverse transport is favored. Taken together, our data place importance on the molecular interactions between residues differentially influencing the efflux properties of the transporter. The T62D-hDAT and other transporter mutants can serve as informational experimental models for changes that occur to the transporter after exposure to AMPH.

Acknowledgments

We would like thank Dr. Asim Beg (University of Michigan) for the pSGEM oocyte construct and initial help with *Xenopus* oocyte studies. We are grateful to Dr. Samuel Straight at the Center for Live Cell Imaging for consultation and assistance with MetaMorph Imaging Software. We also appreciate the statistical analyses of 3-way interactions provided by Felicia R. Webb at the University of Michigan. Lastly, we would like to acknowledge the University of Michigan Pharmacology Department confocal microscopy facility. This work was supported by the following NIH grants: DA011679 (MEG), 5T32DA007281 (RF), DA028112 and DA026947 (LJD).

References

Bolan, E.A., Kivell, B., Jaligam, V., Oz, M., Jayanthi, L.D., Han, Y., Sen, N., Urizar, E., Gomes, I., Devi, L.A., *et al.* (2007). D2 receptors regulate dopamine transporter function via an extracellular signal-regulated kinases 1 and 2-dependent and phosphoinositide 3 kinase-independent mechanism. *Molecular pharmacology* 71, 1222-1232.

Chen, N., Rickey, J., Berfield, J.L., and Reith, M.E. (2004a). Aspartate 345 of the dopamine transporter is critical for conformational changes in substrate translocation and cocaine binding. *The Journal of biological chemistry* 279, 5508-5519.

Chen, N.H., Reith, M.E., and Quick, M.W. (2004b). Synaptic uptake and beyond: the sodium- and chloride-dependent neurotransmitter transporter family SLC6. *Pflugers Archiv : European journal of physiology* 447, 519-531.

Erreger, K., Grewer, C., Javitch, J.A., and Galli, A. (2008). Currents in response to rapid concentration jumps of amphetamine uncover novel aspects of human dopamine transporter function. *J Neurosci* 28, 976-989.

Foster, J.D., Pananusorn, B., and Vaughan, R.A. (2002). Dopamine transporters are phosphorylated on N-terminal serines in rat striatum. *The Journal of biological chemistry* 277, 25178-25186.

Foster, J.D., Yang, J.W., Moritz, A.E., Challasivakanaka, S., Smith, M.A., Holy, M., Wilebski, K., Sitte, H.H., and Vaughan, R.A. (2012). Dopamine transporter phosphorylation site threonine 53 regulates substrate reuptake and amphetamine-stimulated efflux. *The Journal of biological chemistry* 287, 29702-29712.

Guptaroy, B., Fraser, R., Desai, A., Zhang, M., and Gnegy, M.E. (2011). Site-Directed Mutations near Transmembrane Domain 1 Alter Conformation and Function of Norepinephrine and Dopamine Transporters. *Molecular pharmacology* 79, 520-532.

Guptaroy, B., Zhang, M., Bowton, E., Binda, F., Shi, L., Weinstein, H., Galli, A., Javitch, J.A., Neubig, R.R., and Gnegy, M.E. (2009). A juxtamembrane mutation in the N terminus of the dopamine transporter induces preference for an inward-facing conformation. *Molecular pharmacology* 75, 514-524.

Hahn, M.K., and Blakely, R.D. (2007). The functional impact of SLC6 transporter genetic variation. *Annual review of pharmacology and toxicology* 47, 401-441.

Ingram, S.L., Prasad, B.M., and Amara, S.G. (2002). Dopamine transporter-mediated conductances increase excitability of midbrain dopamine neurons. *Nature neuroscience* 5, 971-978.

Jardetzky, O. (1966). Simple allosteric model for membrane pumps. *Nature* 211, 969-970.

Khoshbouei, H., Sen, N., Guptaroy, B., Johnson, L., Lund, D., Gnegy, M.E., Galli, A., and Javitch, J.A. (2004). N-terminal phosphorylation of the dopamine transporter is required for amphetamine-induced efflux. *PLoS Biol* 2, E78.

Khoshbouei, H., Wang, H., Lechleiter, J.D., Javitch, J.A., and Galli, A. (2003). Amphetamine-induced dopamine efflux. A voltage-sensitive and intracellular Na⁺-dependent mechanism. *The Journal of biological chemistry* 278, 12070-12077.

Kniazeff, J., Shi, L., Loland, C.J., Javitch, J.A., Weinstein, H., and Gether, U. (2008). An intracellular interaction network regulates conformational transitions in the dopamine transporter. *The Journal of biological chemistry* 283, 17691-17701.

Krishnamurthy, H., and Gouaux, E. (2012). X-ray structures of LeuT in substrate-free outward-open and apo inward-open states. *Nature* 481, 469-474.

Levi, G., and Raiteri, M. (1993). Carrier-mediated release of neurotransmitters. *Trends in neurosciences* 16, 415-419.

Leviel, V. (2011). Dopamine release mediated by the dopamine transporter, facts and consequences. *Journal of neurochemistry* 118, 475-489.

Liang, N.Y., and Rutledge, C.O. (1982). Evidence for carrier-mediated efflux of dopamine from corpus striatum. *Biochem Pharmacol* 31, 2479-2484.

Liang, Y.J., Zhen, J., Chen, N., and Reith, M.E. (2009). Interaction of catechol and non-catechol substrates with externally or internally facing dopamine transporters. *Journal of neurochemistry* 109, 981-994.

Loland, C.J., Norregaard, L., Litman, T., and Gether, U. (2002). Generation of an activating Zn(2+) switch in the dopamine transporter: mutation of an intracellular tyrosine constitutively alters the conformational equilibrium of the transport cycle. *Proceedings of the National Academy of Sciences of the United States of America* 99, 1683-1688.

Mazei-Robison, M.S., Bowton, E., Holy, M., Schmudermaier, M., Freissmuth, M., Sitte, H.H., Galli, A., and Blakely, R.D. (2008). Anomalous dopamine release associated with a human dopamine transporter coding variant. *J Neurosci* 28, 7040-7046.

Meinild, A.K., Sitte, H.H., and Gether, U. (2004). Zinc potentiates an uncoupled anion conductance associated with the dopamine transporter. *The Journal of biological chemistry* 279, 49671-49679.

Piffl, C., Agneter, E., Drobny, H., Reither, H., and Singer, E.A. (1997). Induction by low Na⁺ or Cl⁻ of cocaine sensitive carrier-mediated efflux of amines from cells transfected with the cloned human catecholamine transporters. *British journal of pharmacology* 121, 205-212.

Piffl, C., and Singer, E.A. (1999). Ion dependence of carrier-mediated release in dopamine or norepinephrine transporter-transfected cells questions the hypothesis of facilitated exchange diffusion. *Molecular pharmacology* 56, 1047-1054.

Piffl, C., Wolf, A., Rebernik, P., Reither, H., and Berger, M.L. (2009). Zinc regulates the dopamine transporter in a membrane potential and chloride dependent manner. *Neuropharmacology* 56, 531-540.

Raiteri, M., Cerrito, F., Cervoni, A.M., and Levi, G. (1979). Dopamine can be released by two mechanisms differentially affected by the dopamine transport inhibitor nomifensine. *The Journal of pharmacology and experimental therapeutics* 208, 195-202.

Rudnick, G. (1998). Ion-coupled neurotransmitter transport: thermodynamic vs. kinetic determinations of stoichiometry. *Methods in enzymology* 296, 233-247.

Rutledge, C.O. (1978). Effect of metabolic inhibitors and ouabain on amphetamine- and potassium-induced release of biogenic amines from isolated brain tissue. *Biochem Pharmacol* 27, 511-516.

Schwartz, J.W., Blakely, R.D., and DeFelice, L.J. (2003). Binding and transport in norepinephrine transporters. Real-time, spatially resolved analysis in single cells using a fluorescent substrate. *The Journal of biological chemistry* 278, 9768-9777.

Shan, J., Javitch, J.A., Shi, L., and Weinstein, H. (2011). The substrate-driven transition to an inward-facing conformation in the functional mechanism of the dopamine transporter. *PloS one* 6, e16350.

Sonders, M.S., Zhu, S.J., Zahniser, N.R., Kavanaugh, M.P., and Amara, S.G. (1997). Multiple ionic conductances of the human dopamine transporter: the actions of dopamine and psychostimulants. *J Neurosci* 17, 960-974.

Sulzer, D., Sonders, M.S., Poulsen, N.W., and Galli, A. (2005). Mechanisms of neurotransmitter release by amphetamines: a review. *Prog Neurobiol* 75, 406-433.

Yamashita, A., Singh, S.K., Kawate, T., Jin, Y., and Gouaux, E. (2005). Crystal structure of a bacterial homologue of Na⁺/Cl⁻-dependent neurotransmitter transporters. *Nature* 437, 215-223.

Zapata, A., Kivell, B., Han, Y., Javitch, J.A., Bolan, E.A., Kuraguntla, D., Jaligam, V., Oz, M., Jayanthi, L.D., Samuvel, D.J., *et al.* (2007). Regulation of dopamine transporter function and cell surface expression by D3 dopamine receptors. *The Journal of biological chemistry* 282, 35842-35854.

Zhao, C., Stolzenberg, S., Gracia, L., Weinstein, H., Noskov, S., and Shi, L. (2012). Ion-controlled conformational dynamics in the outward-open transition from an occluded state of LeuT. *Biophysical journal* 103, 878-888.

Zhao, Y., Terry, D., Shi, L., Weinstein, H., Blanchard, S.C., and Javitch, J.A. (2010). Single-molecule dynamics of gating in a neurotransmitter transporter homologue. *Nature* 465, 188-193.

Zhen, J., Chen, N., and Reith, M.E. (2005). Differences in interactions with the dopamine transporter as revealed by diminishment of Na(+) gradient and membrane potential: dopamine versus other substrates. *Neuropharmacology* 49, 769-779.

DISCUSSION

Chapter 4

A recurring theme of the work in this dissertation is the influence of conformation on transporter activity. Transporter orientation is driven by formation, stabilization, and disruption of molecular interactions to facilitate substrate translocation. Understanding the mechanism of AMPH action on transporter reversal has clinical relevance. As a substrate of DAT & NET, the end result of AMPH transport is the ‘reverse’ transport of DA and NE into the extracellular space. This action involves transition of inward- to outward-facing conformations. My characterization of NET and DAT mutants discussed in preceding chapters adds to our knowledge on the relation of conformational shifts to alterations in activity, and improves understanding on the molecular basis of transporter function and potential drug action. In this final dissertation chapter additional points of investigation will be discussed for the N-terminal Thr NET and/or DAT mutants.

Intracellular Gating and Reverse Transport

Mutation of the Proposed DAT Y335 Binding Partner

Molecular simulation studies in the literature have provided much insight on the outward to inward translocation of substrate. However, less is known about details of the reverse, inward to outward motions. Our analysis showed that the T62D-hDAT inward facing mutant has profoundly altered transporter activity and function as exemplified by the enhanced DA affinity and efflux rate (Guptaroy et al., 2009) and enhanced affinity for DAT substrates (Chapter 2)

(Guptaroy et al., 2011). The T62D-hDAT mutant displays elevated basal (unstimulated) DA efflux and is insensitive to further DA release by AMPH (Guptaroy et al., 2009). My data suggest the preferred conformation of the T62D mutation is an efflux-favored, Na⁺ primed state of the transporter (Chapter 3).

Through molecular modeling of the DAT intracellular gating network, it is proposed that binding of the N-terminal Thr 62 residue with Tyr 335 of TM 6 enables opening of the intracellular gate and assumption of the inward facing orientation (Shan et al., 2011). The T62D mutation results in a loss of the connection of Y335 with T62, along with disruption of other interactions with residues at or near the intracellular gating network (Guptaroy et al., 2009). The Y335A-hDAT mutant developed by the Gether laboratory Loland et al. (2002) has also been deemed an inward facing transporter due to the impaired DA uptake and changed binding profile for substrates ($\downarrow K_i$) and inhibitors ($\uparrow K_i$) in [³H]DA uptake competitions. However, an effect of the Y335A mutation on DA efflux was not reported (Loland et al., 2002). The impact of the Tyr 335 residue and its interaction with Thr 62 on reverse transport is worth exploring. This was approached by creating the Y335F-hDAT mutant. The phenylalanine substitution of tyrosine is a relatively subtle amino acid change that should disturb the T62 and Y335 intracellular connection. This mutant was stably expressed in HEK-293 cells for analysis of [³H]DA uptake and efflux.

DA Uptake and Efflux in the Y335F-hDAT Mutant

Preliminary results from [³H]DA saturation assays revealed an approximate 50% reduction in the V_{\max} ($p = 0.0002$) and unchanged K_m ($p = 0.6098$) for DA uptake in Y335F-hDAT HEK cells compared to WT.

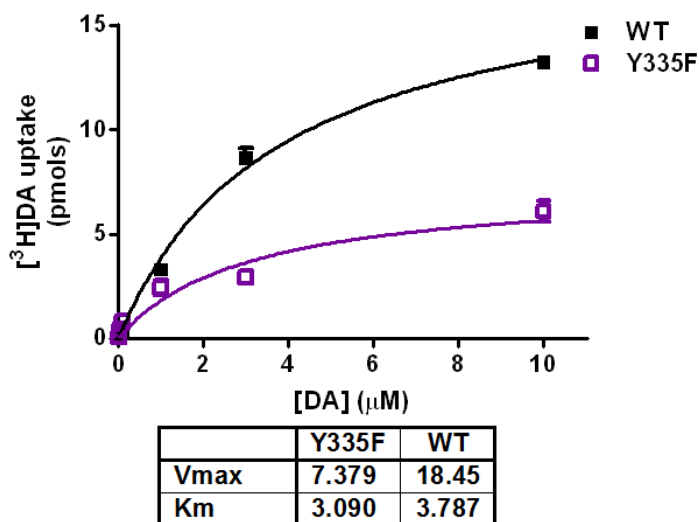


Figure 4-1. [³H]DA uptake saturation in WT- and Y335F-hDAT HEK cells. Uptake of 10 nM [³H]DA was measured in the presence of increasing unlabeled DA concentrations. The assay was conducted for 3 min at RT, and non-specific uptake was measured in the presence of 100 µM cocaine after a 10 min preincubation. V_{\max} (pmols) and K_m (µM) values were determined from the nonlinear regression curve fit analysis using GraphPad Prism 6 software. Data are from 1 (WT) or 2 (Y335F) experiment performed in triplicate.

I also performed pilot studies measuring the effects of extracellular Na^+ on basal and AMPH-induced DA efflux. The plated [³H]DA efflux assay (detailed in Chapter 3) was used to measure basal DA efflux at 10 and 20 min, followed by DA efflux after a 5 min AMPH (10 µM) stimulation. [³H]DA efflux was determined in normal (125 mM) and complete substitution (0 mM) of extracellular Na^+ . After preloading cells with 0.5 µM [³H]DA, DA efflux was measured

in aliquots of assay buffer that were collected and replaced at the indicated time points. For 0 mM Na⁺, NaCl in the assay buffer was replaced with 125 mM NMDG-Cl.

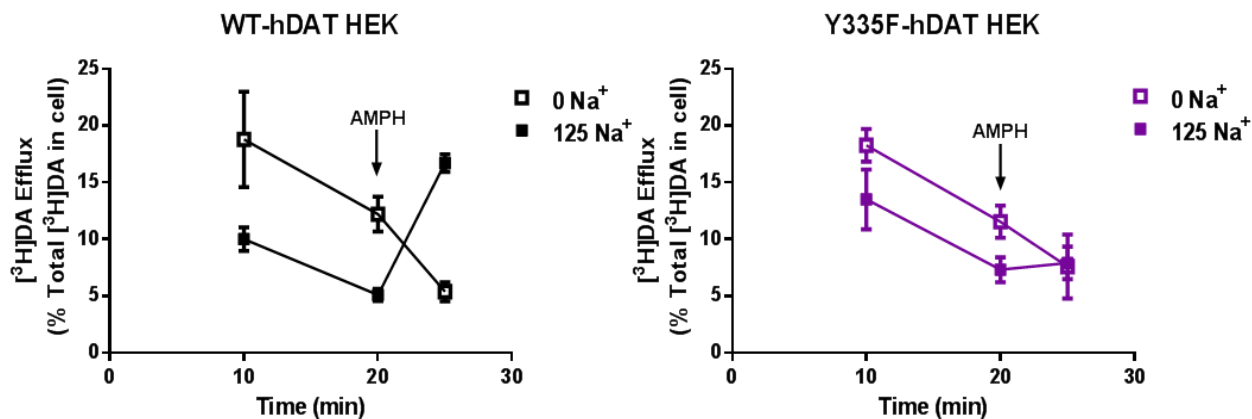


Figure 4-2. Effects of extracellular Na⁺ replacement on basal and AMPH-induced [³H]DA efflux. (left) WT- and (right) Y335F-hDAT HEK cells were preloaded with 0.5 μM [³H]DA for 20 min at RT. DA efflux was measured at normal, 125 mM Na⁺ (closed symbols) and 0 mM Na⁺ (open symbols). WT data are from a single experiment performed in quadruplicate. Y335F data are from 1 or 2 experiments performed in 3-8 replicates.

[³H]DA efflux data are expressed as a percent of the total DA within the cell. However, there was a 45% reduction in the amount of total DA taken up by Y335F-hDAT cells compared to WT (average total radioactive cpm in WT = 30796 and Y335F = 14004). This is in line with the observed change in V_{max} for DA uptake (Figure 4-1). Fitting with the lower measured [³H]DA uptake, baseline DA release appeared higher in Y335F- than WT-hDAT cells. Nonetheless, removal of extracellular Na⁺ increased baseline DA efflux in both cell types. This differed from the Na⁺ independence of elevated basal DA efflux observed in T62D-hDAT cells (Chapter 3). While inhibition of DA efflux with AMPH treatment at 0 mM Na⁺ was expected (Figure 3-7),

AMPH-stimulation of DA efflux at 125 mM Na⁺_e was negligible in Y335F-hDAT versus WT cells (Figure 4-2).

The Brandel superfusion assay is useful to further validate AMPH's effect (at normal Na⁺) in the Y335F-hDAT mutant cell line. Reuptake is less of a factor in the superfusion assay, which offers improved resolution for measuring carrier-mediated release. In this technique cells preloaded with DA are placed into superfusion chambers. KRH buffer is perfused over the cells for 30 min to establish a steady baseline. Afterward, five 1-min fractions of perfusate are collected (flow rate 0.8 ml/min), followed by 2 fractions of 10 μM AMPH stimulation, then 6 additional KRH fractions. The amount of DA within each fraction is measured using HPLC with electrochemical detection by comparison to a standard DA curve. The data are represented as the pmol of DA per mg of protein per 1 min and normalized to the total DA. Cells are maintained at 37°C throughout the entire assay.

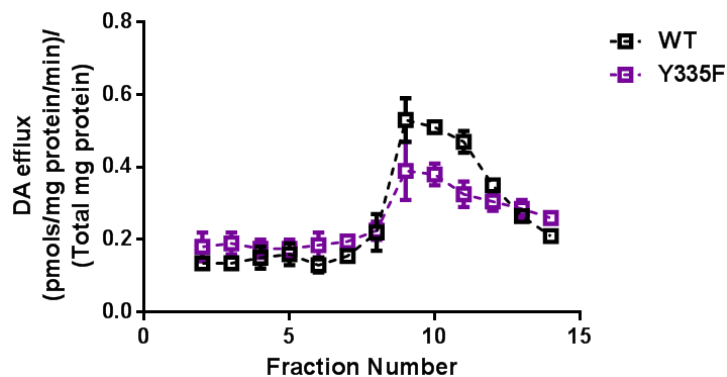


Figure 4-3. Brandel superfusion to measure AMPH-induced DA efflux in WT- and Y335F-hDAT HEK cells preloaded with 15 μM DA for 30 min at 37°C. After equilibration, the first fraction is discarded and 5 min baseline fractions are collected. Cells are perfused with 10 μM AMPH at fractions 7 & 8 then changed back to KRH buffer for the remaining collection period. Data are from a single experiment performed in duplicate.

The total DA was nearly 40% less in Y335F- versus WT-hDAT cells (WT = 319.7 and Y335F = 123 pmol/mg protein). After normalization to the total DA, DA efflux induced by AMPH appeared lower in Y335F-hDAT cells (Figure 4-3).

In the final pilot experiment total DA loading in Y335F- to WT-hDAT cells was standardized. This was done by incubating cells with a lower DA concentration (5 μ M) for a longer time period (3 hr). AMPH-induced DA efflux was measured as stated above.

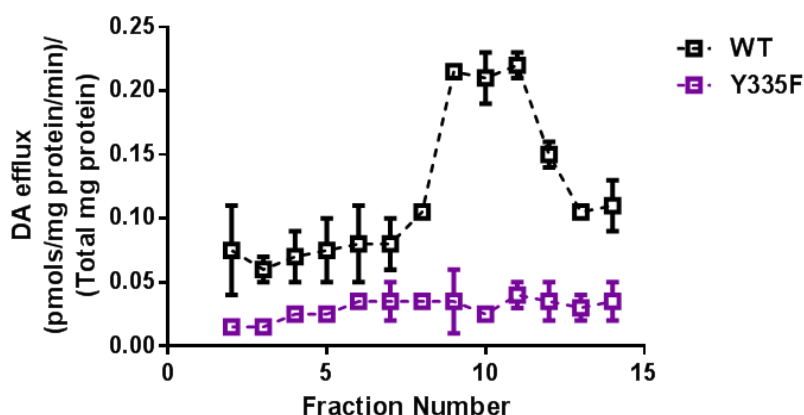


Figure 4-4. AMPH-induced DA efflux in WT- and Y335F-hDAT HEK cells preloaded with 5 μ M DA for 180 min at 37°C. Superfusion was conducted as stated in Figure 4-3. Data are from a single experiment performed in duplicate.

With these preloading conditions, the total DA in Y335F- was more comparable to WT-hDAT HEK cells (WT = 136 and Y335F = 121 pmol DA/mg protein). Despite the elevated baseline DA efflux in WT cells, there was a clear loss of AMPH-induced DA efflux in the Y335F-hDAT mutant cells (Figure 4-4).

My preliminary data characterizing the Y335F-hDAT mutant points to the importance of this residue in AMPH-induced reverse transport of DA. The pattern of DA efflux seen with Y335F thus far differs from that seen in either T62A or T62D-hDAT mutants. In a certain sense, the Y335F mutation seems to be a hybrid of the functional effects elicited by the Thr 62 mutations but shares more characteristics with T62A- than T62D-hDAT. The reduced DA uptake in Y335F and influence of the Na⁺ gradient on DA efflux in Y335F were similar to T62A-hDAT. The ability of AMPH to elicit efflux in Y335F-hDAT was severely compromised but the data in Figure 4-3 suggest that loading with a high concentration of DA (15 μM) might permit stimulated efflux. The Y335F mutation is posited to yield a mutant with normal DA intake, but have defective AMPH-stimulated DA output through the transporter. This could likely occur through the conservation of interactions involved in extracellular gating with modest disruption of intracellular connections that mediate reverse transport. On the contrary, the T62D mutation perturbs the intracellular network to a greater extent, impacting both basal and AMPH-induced reverse transport.

Additional repetitions of these Y335F-hDAT pilot studies as well as analyses of DA uptake with Na⁺ replacement would be needed to strengthen this hypothesis. Furthermore, in order to rule out variations in transporter expression, surface expression of the Y335F hDAT mutant using biotinylation or binding of WIN 35,428 would need to be evaluated. This should be performed in the absence and presence of substrate to address constitutive and stimulated DAT trafficking.

Proposed Alteration of Transport Schematic in T62D-hDAT

Though they tend to oversimplify the many intricacies of the transport process, schematics are useful to depict the transitions involved in the transport cycle under normal and modified conditions (Gnegy, 2003; Shi et al., 2008). The kinetics of transporter current measurements have been effectively correlated to the steps of the alternating access model of transport, further validating schematic representations (Bulling et al., 2012; Erreger et al., 2008). The conformational shifts from the T62D and Y335F hDAT mutations lead to changes in the transport cycle. These proposed changes are highlighted in Figure 4-5 to explain the functional differences of the DAT mutants.

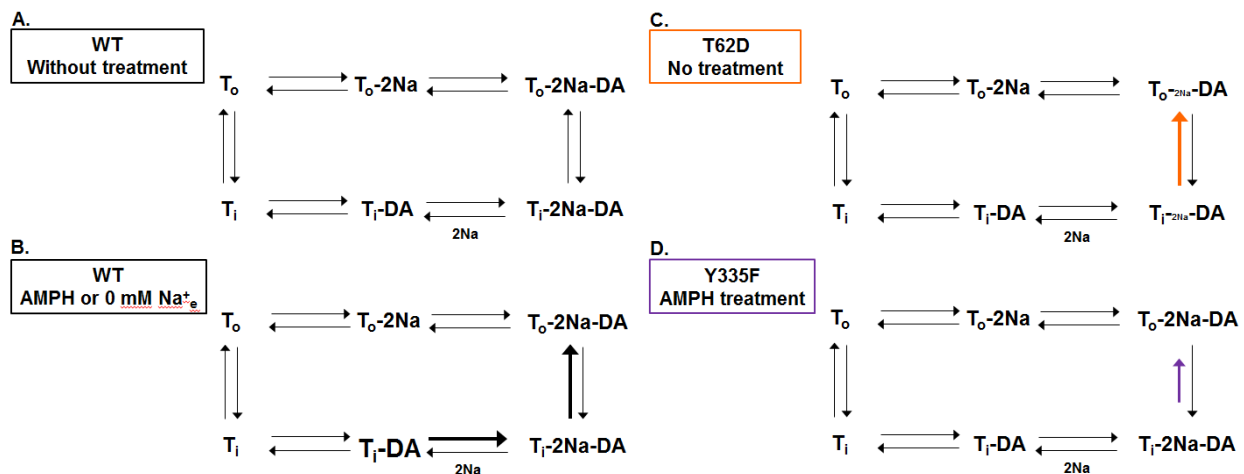


Figure 4-5. Schematic of transport cycle in WT-, T62D- and Y335F hDAT. Normal transport cycle in WT (A), carrier mediated reverse transport in WT with high intracellular Na⁺ (B), Na⁺ independent DA efflux in T62D (C), and reduced AMPH-induced DA release in Y335F (D). T_o = outward transporter, T_i = inward transporter, Substrates = 2 sodium ions and 1 dopamine molecule.

Under normal conditions, empty WT transporter oscillates between binding co-transported ions and substrate that stimulates a rapid transition to the inward facing orientation where transporter contents are released before return of the empty inward transporter to the outward orientation (Figure 4-5A). As depicted in Figure 4-5B, carrier-mediated DA efflux occurs in WT-hDAT when AMPH (or low Na^+) stimulates an increase of intracellular Na^+ levels, and “places DAT in Na^+ -exchange mode—where occupied carrier rearranges to outward facing more rapidly than empty carrier” (Erreger et al., 2008). T62D-hDAT is depicted as existing in a Na^+ -primed mode with pronounced inward to outward rearrangement of occupied carrier in a manner that is not driven by intracellular Na^+ (small font Na^+ ions) (Figure 4-5C). The Y335F-hDAT mutation may result in a reduction of DA occupied DAT cycling to the outward facing orientation in response to AMPH. However, high intracellular Na^+ (e.g. during removal of Na^+) still stimulates release in the absence of AMPH (Figure 4-5D).

Though not included on the schematic above, Cl^- is important for substrate transport substrate binding and unbinding (Zomot et al., 2007), DA uptake and inward currents (Ingram et al., 2002), and DA efflux (Diliberto et al., 1989). I have performed preliminary experiments examining the importance of extracellular Cl^- . Reducing extracellular Cl^- modestly increased basal DA efflux in both WT and T62D-hDAT. Therefore, DA efflux in T62D-hDAT did not appear to be insensitive to Cl^- as it was to Na^+ . Additionally, manipulating the extracellular Cl^- did not restore the ability of AMPH to elicit DA efflux in T62D-hDAT. Further studies comparing Y335F-, T62A-, and T62D-hDAT mutants should incorporate effects Cl^- substitution on DAT functions.

Future Directions

DAT Phosphorylation

Multiple studies have implicated phosphorylation in the regulation of transporter functions. The highly conserved DAT Thr 62 residue and NET Thr 58 are a putative phosphorylation sites for protein kinases such as PKA and PKC (Giros and Caron, 1993; Vaughan, 2004; Volz and Schenk, 2005). Because the RETW sequence is conserved in monoamine transporters in which AMPH is a substrate, and because the Thr within the sequence is a putative phosphorylation site, we mutated Thr to Asp to give a phosphorylation-mimicking state and to Ala to represent a non-phosphorylatable state. It is not currently known whether direct phosphorylation occurs at Thr 62 in DAT or Thr 58 in NET. Phosphorylation of DAT has been demonstrated to occur within N-terminal serines, up through ser53 (Vaughan, 2004). Although this phosphorylation may be important for regulation of DAT function, these serines do not exist in NET, and would not play a role in AMPH function in that transporter. Our data would suggest that if Thr 62 or Thr 58 were phosphorylated in response to AMPH or a change in the electrochemical gradient to Na⁺, that it would be a fleeting phosphorylation. Although it is important to discern whether this residue is actually phosphorylated during the transport cycle, the T→D mutation has proven highly useful as a means to help us elucidate the DAT and NET functions and transport cycle.

It is possible that phosphorylation at the Thr within the RETW sequence could contribute to AMPH function. Phosphorylation has been associated with DAT- and NET-mediated DA efflux in several studies. AMPH increases PKC activity in brain (Giambalvo, 2003) and heterologous

cells (Park et al., 2003). Moreover, AMPH-induced DA release through both DAT (Kantor and Gnegy, 1998) and NET (Kantor et al., 2001) requires PKC, particularly PKC β as seen in cell systems and striatal preparations (Johnson et al., 2005; Kantor and Gnegy, 1998; Kantor et al., 2001). The DAT N-terminus influences AMPH-induced DA efflux as indicated by a significant reduction in DA release in DAT lacking the first 22 amino acids (Δ N22-DAT) (Khoshbouei et al., 2004), in which phosphorylation by PMA-stimulated PKC activation is reduced (Granás et al., 2003). Despite evidence for the first 22 DAT amino acids taking part in PKC regulation of AMPH-induced DA efflux, other N-terminal residues can play role as well. Recently, loss of direct phosphorylation at rat DAT (rDAT) Thr 53 (T53-rDAT) has been associated with reduced DA uptake and MPP⁺ efflux (Foster et al., 2012). Determining the phosphorylation state at T62-hDAT and T58-hNET sites would help elucidate whether increased efflux observed in the inward facing T62D-hDAT is solely an attribute of conformational disruptions in the mutant or if actual Thr 62 phosphorylation is a component as well, which could have direct effects or indirect effects on transporter activity, for instance via alterations in trafficking or binding of regulatory proteins.

Trafficking and Inward Transport

Although PKC activation influences DAT uptake and surface expression in some instances (Chen et al., 2009; Furman et al., 2009; Vaughan et al., 1997), evidence also suggests DAT internalization occurs independently of PKC phosphorylation (Granas et al., 2003). The first 22 amino acids have been implicated in DAT internalization effects. However the involvement of other N-terminal residues may depend on the conformational state of the transporter. A mix of mutations (that included the R60 and W63 of RETW sequence) that was reported to disrupt the outward-facing orientation resulted in increased endocytosis, suggesting single mutations alone may not be disruptive to the transporter endocytic signals (Sorkina et al., 2009). However, in an investigation of phosphoacceptor sites important for transporter regulation, Lin et al. (2003) showed the single T62A mutation or a combination of other mutated hDAT sites can differentially affect kinase effectors like PI3K versus PKC. There was no difference in the percentage of transporter expressed at the surface between the T62→A or T62→D mutants in either hNET or hDAT (Guptaroy et al., 2011; Guptaroy et al., 2009), which may imply constitutive trafficking is unaffected by the Thr mutations. Further experiments could investigate whether the mutations effect the endocytic signal with other factors like time course (acute versus long term) and drug treatment (PMA or AMPH stimulation).

Protein interactions

The investigations within my dissertation have dealt with transporters expressed in cell-based systems. Though this widely used approach is advantageous to study transporters in isolation, it

is also crucial to think about transporters in the context of their physiological environment. DAT interacts with a variety of proteins (Torres, 2006) and mutations in Thr 62 hDAT and Thr 58 hNET could alter function by altering requisite protein-protein interactions. Two proteins in particular which bind to the N-terminus of DAT and significantly alter DAT function are syntaxin 1A and the D2 DA autoreceptor. Another protein which binds to the N-terminus of DAT and thus provides a means to significantly alter DAT function is RACK1 (Lee et al., 2004; Ron et al., 1994), which is a docking protein for PKC β , especially PKC β II (Ron et al., 1999).

Syntaxin 1A and Dopamine Autoreceptor

Syntaxin is a presynaptic SNARE protein well known for its function in docking of synaptic vesicles for neurotransmitter release (Sudhof, 2004). However syntaxin1A appears to play a more general role in docking of small vesicles, such as those containing NET and DAT, as well as synaptic vesicles (Quick, 2006). Syntaxin 1A directly interacts with the first 42 residues of NET (Sung et al., 2003) and 33 residues of DAT (Binda et al., 2008). Syntaxin 1A alters both surface expression and function of DAT and NET but its actions are complex. Overexpression of syntaxin 1A and NET increases surface NET yet limits NET function (Sung et al., 2003); while overexpression of syntaxin 1A with DAT decreases surface DAT yet enhances AMPH-induced DA efflux. Since phosphorylation and transporter functions and protein-protein interactions are intertwined to some degree, it would be instructive to probe the effect of transporter conformation on binding of the T62-DAT or T58-NET mutants to syntaxin.

Along with DAT, the dopamine D2-like autoreceptor (D2R) is a key protein for controlling extracellular DA levels, and DAT coupling to D2R increases DAT activity. Similar to syntaxin 1A, a direct interaction has been established between residues 1-26 of the DAT N-terminus and residues 311-344 of D2 autoreceptor 3rd extracellular loop (Lee et al., 2007). Coupling of DAT/D2R in co-transfected HEK 293 cells increased surface DAT expression (Lee et al., 2007). PKC β is needed for D2R activation of DAT trafficking (Chen et al., 2013). It is very likely the conformation of DAT would change the coupling of DAT to D2Rs, and warrants exploration in the Thr62 hDAT mutants. The A559V hDAT variant, which has intact DA uptake but irregular DA efflux (Mazei-Robison et al., 2008) shares similar features with our T62D-hDAT mutant (as discussed in Chapter 3), and may also exist in an inward-facing conformation. Recently the efflux state of A559V hDAT was found to be dependent on N-terminal phosphorylation via CaMKII, and was inhibited by the D2-like receptor antagonist raclopride (Bowton et al., 2010). Such studies surveying protein-protein interactions in the NET and DAT N-terminal Thr mutants would aid in determining if orientation influences the association of transporter proteins and their resulting functional effects.

An Experimental Behavioral Model of T62D-hDAT

Use of transgenic mouse models, usually of specific gene knockouts, has been a staple method of studying the action and behaviors of addictive drugs (Sora et al., 2010). Our understanding of psychostimulant action on monoamine transporters (DAT, NET, and SERT) and their link to disease states has been greatly advanced by the use of mice with genetic deletions of the transporter (Gainetdinov and Caron, 2003; Sora et al., 2010). The DAT knockout mouse shares

phenotypes like reduced DA clearance and hyperactivity (Giros and Caron, 1993) that bear similarity to ADHD symptoms. The DAT knockout mouse has been proposed as a model for ADHD, but global deletion and dysfunction of DAT is an unlikely attribute to the disease (Gainetdinov and Caron, 2003). This is exemplified by the normal DA uptake function but enhanced DA reverse transport expressed by the rare A559V genetic variant of DAT found in two siblings with ADHD (Mazei-Robison et al., 2008). Therefore, it is important to develop additional animal models that better represent impairments of transporter functions.

A relatively new behavioral assay for AMPH action was discovered in *Caenorhabditis elegans* called swim induced paralysis (SWIP). Excessive synaptic DA results in paralysis of *C. elegans* when it is placed in water. AMPH-induced SWIP in WT *C. elegans* requires dopamine receptors and DA efflux through the *C. elegans* DA transporter (DAT-1) (Carvelli et al., 2010). The *C. elegans* system could be used to develop a behavioral phenotype for the T62D-hDAT mutant with the SWIP assay. This would require expression of fluorescently tagged T62D-hDAT in DAT-1 knockout (*dat-1*) *C. elegans* to identify organisms containing the hDAT mutant. The enhanced constitutive DA efflux in T62D should induce SWIP without further stimulation of paralysis by AMPH. SWIP in T62D *C. elegans* would resemble the behavior of AMPH treated WT *C. elegans* or the intrinsic SWIP in *dat-1 C. elegans*. Positive results would confirm the notion of the T62D-hDAT serving as a conformational representation of AMPH induced changes to DAT.

The T62D-hDAT has potential application as a mouse model of diseases involving enhanced DA overflow in the synapse. The proposed elements discussed earlier such as protein interactions and trafficking can be studied in a native environment. More importantly such an animal model may be useful in a variety of physiological relevant studies such as AMPH sensitization, development of tolerance to psychostimulants, preferences for additional drugs of abuse (e.g. alcohol, nicotine, opioids), or cognitive impairments.

Conclusions

The N-terminal Thr 62 and Thr 58 residues of hDAT and hNET respectively, are important regulatory sites of transporter orientation. Transporter conformational shifts are instrumental to carrying out the movement of neurotransmitter from one side of the membrane to the next. This is especially important for clearance of neurotransmitter from the extracellular space. Yet on the other hand, is also a key part of intracellular transporter-mediated neurotransmitter release to maintain neuronal tone or in response to drug action.

Alanine or aspartate substitutions of the Thr sites affect the equilibrium of transporter conformation and consequently impacts function. The T→D mutant NET and DAT preferred the inward facing conformation that enhanced basal DA reverse transport, abrogated [³H]DA uptake and AMPH's effect of efflux stimulation. The work of this dissertation further analyzed alterations in hNET and hDAT properties elicited by the Thr mutations. Findings of variations in ligand interactions were presented in chapter 2. Substrate affinity was significantly enhanced in T→A, and chiefly so in T→D hNET and hDAT mutants. Interactions of inhibitors were

unaffected in hNET mutants, but altered in hDAT mutants in a manner influenced by the inhibitor structure. Functional characterization of the T62 hDAT mutants was continued in chapter 3. Significant discoveries were 1) normal transporter intake, seen by accumulation of fluorescent substrate ASP⁺; and 2) a Na⁺-independence of the elevated DA efflux in T62D-hDAT. My results emphasize the variety of consequences conformational change can have on transporter functions. The preliminary results and ideas presented in the final chapter extend the investigations of T62D-hDAT inward facing mutant towards an additional amino acid binding partner, protein-protein interactions, and application to behavior model. The use of transporter mutants will continue to improve knowledge of transporter mechanisms and the amino acids involved in regulation of their activity both on a homeostatic basis and when targeted by drugs.

References

- Binda, F., Dipace, C., Bowton, E., Robertson, S.D., Lute, B.J., Fog, J.U., Zhang, M., Sen, N., Colbran, R.J., Gnegy, M.E., *et al.* (2008). Syntaxin 1A interaction with the dopamine transporter promotes amphetamine-induced dopamine efflux. *Molecular pharmacology* 74, 1101-1108.
- Bowton, E., Saunders, C., Erreger, K., Sakrikar, D., Matthies, H.J., Sen, N., Jessen, T., Colbran, R.J., Caron, M.G., Javitch, J.A., *et al.* (2010). Dysregulation of dopamine transporters via dopamine D2 autoreceptors triggers anomalous dopamine efflux associated with attention-deficit hyperactivity disorder. *J Neurosci* 30, 6048-6057.
- Bulling, S., Schicker, K., Zhang, Y.W., Steinkellner, T., Stockner, T., Gruber, C.W., Boehm, S., Freissmuth, M., Rudnick, G., Sitte, H.H., *et al.* (2012). The mechanistic basis for noncompetitive ibogaine inhibition of serotonin and dopamine transporters. *The Journal of biological chemistry* 287, 18524-18534.
- Carvelli, L., Matthies, D.S., and Galli, A. (2010). Molecular mechanisms of amphetamine actions in *Caenorhabditis elegans*. *Molecular pharmacology* 78, 151-156.
- Chen, R., Daining, C.P., Sun, H., Fraser, R., Stokes, S.L., Leitges, M., and Gnegy, M.E. (2013). Protein kinase Cbeta is a modulator of the dopamine D2 autoreceptor-activated trafficking of the dopamine transporter. *Journal of neurochemistry* 125, 663-672.
- Chen, R., Furman, C.A., Zhang, M., Kim, M.N., Gereau, R.W.t., Leitges, M., and Gnegy, M.E. (2009). Protein kinase Cbeta is a critical regulator of dopamine transporter trafficking and regulates the behavioral response to amphetamine in mice. *The Journal of pharmacology and experimental therapeutics* 328, 912-920.
- Diliberto, P.A., Jeffs, R.A., and Cubeddu, L.X. (1989). Effects of low extracellular chloride on dopamine release and the dopamine transporter. *The Journal of pharmacology and experimental therapeutics* 248, 644-653.
- Erreger, K., Grewer, C., Javitch, J.A., and Galli, A. (2008). Currents in response to rapid concentration jumps of amphetamine uncover novel aspects of human dopamine transporter function. *J Neurosci* 28, 976-989.

Foster, J.D., Yang, J.W., Moritz, A.E., Challasivakanaka, S., Smith, M.A., Holy, M., Wilebski, K., Sitte, H.H., and Vaughan, R.A. (2012). Dopamine transporter phosphorylation site threonine 53 regulates substrate reuptake and amphetamine-stimulated efflux. *The Journal of biological chemistry* 287, 29702-29712.

Furman, C.A., Chen, R., Guptaroy, B., Zhang, M., Holz, R.W., and Gnegy, M. (2009). Dopamine and amphetamine rapidly increase dopamine transporter trafficking to the surface: live-cell imaging using total internal reflection fluorescence microscopy. *J Neurosci* 29, 3328-3336.

Gainetdinov, R.R., and Caron, M.G. (2003). Monoamine transporters: from genes to behavior. *Annual review of pharmacology and toxicology* 43, 261-284.

Giambalvo, C.T. (2003). Differential effects of amphetamine transport vs. dopamine reverse transport on particulate PKC activity in striatal synaptoneurosomes. *Synapse* 49, 125-133.

Giros, B., and Caron, M.G. (1993). Molecular characterization of the dopamine transporter. *Trends in pharmacological sciences* 14, 43-49.

Gnegy, M.E. (2003). The effect of phosphorylation on amphetamine-mediated outward transport. *European journal of pharmacology* 479, 83-91.

Granas, C., Ferrer, J., Loland, C.J., Javitch, J.A., and Gether, U. (2003). N-terminal truncation of the dopamine transporter abolishes phorbol ester- and substance P receptor-stimulated phosphorylation without impairing transporter internalization. *The Journal of biological chemistry* 278, 4990-5000.

Guptaroy, B., Fraser, R., Desai, A., Zhang, M., and Gnegy, M.E. (2011). Site-Directed Mutations near Transmembrane Domain 1 Alter Conformation and Function of Norepinephrine and Dopamine Transporters. *Molecular pharmacology* 79, 520-532.

Guptaroy, B., Zhang, M., Bowton, E., Binda, F., Shi, L., Weinstein, H., Galli, A., Javitch, J.A., Neubig, R.R., and Gnegy, M.E. (2009). A juxtamembrane mutation in the N terminus of the dopamine transporter induces preference for an inward-facing conformation. *Molecular pharmacology* 75, 514-524.

Ingram, S.L., Prasad, B.M., and Amara, S.G. (2002). Dopamine transporter-mediated conductances increase excitability of midbrain dopamine neurons. *Nature neuroscience* 5, 971-978.

Johnson, L.A., Guptaroy, B., Lund, D., Shamban, S., and Gnegy, M.E. (2005). Regulation of amphetamine-stimulated dopamine efflux by protein kinase C beta. *The Journal of biological chemistry* 280, 10914-10919.

Kantor, L., and Gnegy, M.E. (1998). Protein kinase C inhibitors block amphetamine-mediated dopamine release in rat striatal slices. *The Journal of pharmacology and experimental therapeutics* 284, 592-598.

Kantor, L., Hewlett, G.H., Park, Y.H., Richardson-Burns, S.M., Mellon, M.J., and Gnegy, M.E. (2001). Protein kinase C and intracellular calcium are required for amphetamine-mediated dopamine release via the norepinephrine transporter in undifferentiated PC12 cells. *The Journal of pharmacology and experimental therapeutics* 297, 1016-1024.

Khoshbouei, H., Sen, N., Guptaroy, B., Johnson, L., Lund, D., Gnegy, M.E., Galli, A., and Javitch, J.A. (2004). N-terminal phosphorylation of the dopamine transporter is required for amphetamine-induced efflux. *PLoS Biol* 2, E78.

Lee, F.J., Pei, L., Moszczynska, A., Vukusic, B., Fletcher, P.J., and Liu, F. (2007). Dopamine transporter cell surface localization facilitated by a direct interaction with the dopamine D2 receptor. *The EMBO journal* 26, 2127-2136.

Lee, K.H., Kim, M.Y., Kim, D.H., and Lee, Y.S. (2004). Syntaxin 1A and receptor for activated C kinase interact with the N-terminal region of human dopamine transporter. *Neurochemical research* 29, 1405-1409.

Lin, Z., Zhang, P.W., Zhu, X., Melgari, J.M., Huff, R., Spieldoch, R.L., and Uhl, G.R. (2003). Phosphatidylinositol 3-kinase, protein kinase C, and MEK1/2 kinase regulation of dopamine transporters (DAT) require N-terminal DAT phosphoacceptor sites. *The Journal of biological chemistry* 278, 20162-20170.

Loland, C.J., Norregaard, L., Litman, T., and Gether, U. (2002). Generation of an activating Zn(2+) switch in the dopamine transporter: mutation of an intracellular tyrosine constitutively alters the conformational equilibrium of the transport cycle. *Proceedings of the National Academy of Sciences of the United States of America* 99, 1683-1688.

Mazei-Robison, M.S., Bowton, E., Holy, M., Schmudermaier, M., Freissmuth, M., Sitte, H.H., Galli, A., and Blakely, R.D. (2008). Anomalous dopamine release associated with a human dopamine transporter coding variant. *J Neurosci* 28, 7040-7046.

Park, Y.H., Kantor, L., Guptaroy, B., Zhang, M., Wang, K.K., and Gnegy, M.E. (2003). Repeated amphetamine treatment induces neurite outgrowth and enhanced amphetamine-stimulated dopamine release in rat pheochromocytoma cells (PC12 cells) via a protein kinase C- and mitogen activated protein kinase-dependent mechanism. *Journal of neurochemistry* 87, 1546-1557.

Quick, M.W. (2006). The role of SNARE proteins in trafficking and function of neurotransmitter transporters. *Handbook of experimental pharmacology*, 181-196.

Ron, D., Chen, C.H., Caldwell, J., Jamieson, L., Orr, E., and Mochly-Rosen, D. (1994). Cloning of an intracellular receptor for protein kinase C: a homolog of the beta subunit of G proteins. *Proceedings of the National Academy of Sciences of the United States of America* 91, 839-843.

Ron, D., Jiang, Z., Yao, L., Vagts, A., Diamond, I., and Gordon, A. (1999). Coordinated movement of RACK1 with activated betaIIIPKC. *The Journal of biological chemistry* 274, 27039-27046.

Shan, J., Javitch, J.A., Shi, L., and Weinstein, H. (2011). The substrate-driven transition to an inward-facing conformation in the functional mechanism of the dopamine transporter. *PloS one* 6, e16350.

Shi, L., Quick, M., Zhao, Y., Weinstein, H., and Javitch, J.A. (2008). The mechanism of a neurotransmitter:sodium symporter--inward release of Na⁺ and substrate is triggered by substrate in a second binding site. *Molecular cell* 30, 667-677.

Sora, I., Li, B., Igari, M., Hall, F.S., and Ikeda, K. (2010). Transgenic mice in the study of drug addiction and the effects of psychostimulant drugs. *Ann N Y Acad Sci* 1187, 218-246.

Sorkina, T., Richards, T.L., Rao, A., Zahniser, N.R., and Sorkin, A. (2009). Negative regulation of dopamine transporter endocytosis by membrane-proximal N-terminal residues. *J Neurosci* 29, 1361-1374.

Sudhof, T.C. (2004). The synaptic vesicle cycle. *Annu Rev Neurosci* 27, 509-547.

Sung, U., Apparsundaram, S., Galli, A., Kahlig, K.M., Savchenko, V., Schroeter, S., Quick, M.W., and Blakely, R.D. (2003). A regulated interaction of syntaxin 1A with the antidepressant-sensitive norepinephrine transporter establishes catecholamine clearance capacity. *J Neurosci* 23, 1697-1709.

Torres, G.E. (2006). The dopamine transporter proteome. *Journal of neurochemistry* 97 *Suppl 1*, 3-10.

Vaughan, R.A. (2004). Phosphorylation and regulation of psychostimulant-sensitive neurotransmitter transporters. *The Journal of pharmacology and experimental therapeutics* 310, 1-7.

Vaughan, R.A., Huff, R.A., Uhl, G.R., and Kuhar, M.J. (1997). Protein kinase C-mediated phosphorylation and functional regulation of dopamine transporters in striatal synaptosomes. *The Journal of biological chemistry* 272, 15541-15546.

Volz, T.J., and Schenk, J.O. (2005). A comprehensive atlas of the topography of functional groups of the dopamine transporter. *Synapse* 58, 72-94.

Zomot, E., Bendahan, A., Quick, M., Zhao, Y., Javitch, J.A., and Kanner, B.I. (2007). Mechanism of chloride interaction with neurotransmitter:sodium symporters. *Nature* 449, 726-730.

